Fakultät für Medizin

der Technischen Universität München

Chirurgische Klinik und Poliklinik

Molecular Characterization of Metastasis-associated Signaling Pathways and their Interactions in Colon Cancer

Dr. med. Ulrich Peter Nitsche

Vollständiger Abdruck der von der Fakultät für Medizin der Technischen Universität München zur Erlangung des akademischen Grades eines

Doctor of Philosophy (Ph.D.)

genehmigten Dissertation.

Vorsitzender: apl. Prof. Dr. rer. nat. Helmuth Adelsberger

Prüfer der Dissertation: 1. Univ.-Prof. Dr. med. Bernhard Holzmann

2. Priv.-Doz. Dr. med. Anne Krug

Die Dissertation wurde am 17.09.2012 bei der Fakultät für Medizin der Technischen Universität München eingereicht und durch die Fakultät für Medizin am 19.12.2012 angenommen.

“Pathogenesis of human neoplasia is a puzzle

that might prove solvable in the coming decades.”

Eric R. Fearon and Bert Vogelstein
A Genetic Model for Colorectal Tumorigenesis
Cell, 1990[32]

Index

Abbreviations

*S	Serine phosphorylation site
*Y	Threonine phosphorylation site
°C	Degree Celsius
µg	microgram
µl	microliter
µM	micromolar
5-FU	5-Fluorouracil
a	Adenine (if sequential)
AI	Allelic imbalance
AJCC	American Joint Committee on Cancer
Akt	Protein Kinase B
APC	Adenomatous polyposis coli
ARE	AU-rich element
AUC	Area under the curve
AUF1	AU-rich element RNA-binding protein 1 (HNRNPD)
BAX	B-cell lymphoma 2–associated X protein
Bcl-9	B-cell CLL/lymphoma 9 protein
BES	N,N-Bis(2-hydroxyethyl)taurine
BIC	Bayesian Information Criterion
BRAF	v-raf murine sarcoma viral oncogene homolog B1
BSA	Bovine serum albumin
c	Cytosine (if sequential)
$CaCl_2$	Calcium chloride
CC	Coiled coil
CCDC92	Coiled-coil domain containing 92
CD	Cluster of differentiation
CDC5L	Cell division cycle 5-like protein
cFOS	FBJ murine osteosarcoma viral oncogene homolog
ChIP	Chromatin immune precipitation
CI	Confidence interval
CIMP	c post g island methylator phenotype
CIN	Chromosomal instability
CKI	Cyclin-dependent kinase inhibitor
cMET	hepatocyte growth factor receptor
cMYC	gene similar to myelocytomatosis viral oncogene
CRC	Colorectal cancer
C_t	Cycle threshold
CTNNB1	β-Catenin
ctrl	Control
DAPI	4',6-diamidino-2-phenylindole
dATP	Deoxyadenosine triphosphate
DCC	Deleted in Colorectal Carcinoma
dCTP	Deoxycytidine triphosphate
DD	Death domain
DEPC	Diethylpyrocarbonate
dGTP	Deoxyguanosine triphosphate
DMEM	Dulbecco's modified Eagle's medium
DMSO	Dimethyl sulfoxide
(c)DNA	(complementary) Deoxyribonucleic acid
dNTP	Deoxynucleoside triphosphate
DPF	Adaptor protein 2α binding site
dTTP	Deoxythymidine triphosphate
DUSP18	Dual specificity phosphatase 18
E. coli	Escherichia coli
EDTA	Ethylenediaminetetraacetic acid
EGFR	Epidermal growth factor receptor
Erb	Estrogen receptor beta
ERK1/2	Extracellular signal-regulated kinases 1/2
ESA	European Surgical Association
FACS	Fluorescence-activated cell sorting
FAP	Familial adenomatous polyposis
FCS	Fetal calf serum
FDR	False discovery rate
FSC	Forward Scatter
fwd	Forward
FZD10	Frizzled homolog drosophila 10 (drosophila)
g	gram / G-force (gravity) / Guanine (if sequential)
G	Grading / Gap (phase of cell cycle)
G418	Geneticin
GDP	Guanosine diphosphate
GFP	Green fluorescent protein

GMCSF	Granulocyte macrophage colony-stimulating factor
GSK	Glycogen synthase kinase 3 beta
GTP	Guanosine triphosphate
h	hour(s) / human
H_2O	Water
H_2O_2	Hydrogen peroxide
HCl	Hydrogen chloride
Hek	Human embryonic kidney (cell line)
HER	Human epidermal growth factor receptor 2
HGF	Hepatocyte growth factor
HNPCC	Hereditary Nonpolyposis Colorectal Cancer
HNRNPD	Heterogeneous nuclear ribonucleoprotein D0 (AUF1)
HPLC	High-performance liquid chromatography
HPRT	Hypoxanthine-guanine phosphoribosyltransferase
HR	Hazard ratio
HRM	High resolution melting
ICD-O	International Classification of Diseases for Oncology
IF	Immunofluorescence
IGF2R	Insulin-like growth factor 2 receptor
IGFBP7	Insulin-like growth factor-binding protein 7
IgG	Immunoglobulin G
IP	Immunoprecipitation
KCl	Potassium chloride
kDa	kilodalton
l	liter(s)
L	Lymphatic invasion
LB	Lysogeny broth (medium)
LEF	Lymphoid enhancer-binding factor
LGR5	Leucine-rich repeat-containing G-protein coupled receptor 5
(18q)LOH	Loss of heterozygosity (of chromosome 18q)
LRP	Lipoprotein receptor-related protein
M	molar
MACC1	Metastasis-associated in colon cancer-1
MAPK	Mitogen-activated protein kinase (additional K: -kinase)
MEK	MAP/ERK kinase (MAPKK)
mg	milligram
$MgCl_2$	Magnesium chloride
MGMT	O-6-methylguanine-DNA methyltransferase
$MgSO_4$	Magnesium sulfate
min	minute/minutes
miRNA	Micro RNA
ml	milliliter
MLH1	MutL homolog 1
MLH3	MutL homolog 3
(d/p)MMR	(deficient/proficient) mismatch repair
MOPS	3-(N-morpholino) propanesulfonic acid
MSH2	MutS homolog 2
MSH6	MutS homolog 6
MSI	Microsatellite instable (-H: high, -L: low)
MSS	Microsatellite stable
MTT	3-(4,5-Dimethylthiazol-2-yl)-2,5-diphenyltetrazolium bromide
mut	Mutated
n	Number
Na	Sodium
Na_2HPO_4	Sodium phosphate dibasic
Na_3VO_4	Sodium orthovanadate
NaAc	Sodium acetate
NaCl	Sodium chloride
NaF	Sodium fluoride
NaOH	Sodium hydroxide
ng	nanogram
NH_4Cl	Ammonium chloride
NLS	Nuclear localization signal
nm	nanometer
NP-40	Nonylphenoxypolyethoxyl-ethanol
NPF	Epsin15 homology domain
NPV	Negative predictive value
OPN	Osteopontin
P	Phosphate/phospho-
p(-value)	Probability (value)
p16	Cyclin-dependent kinase inhibitor 2A, multiple tumor suppressor 1
p53/TP53	tumor protein 53

PAGE	Polyacrylamide gel electrophoresis
PAK4	Serine/threonine-protein kinase PAK 4
PBS(T)	Phosphate buffered saline (including Tween)
PCP	Planar cell polarity
(rt)PCR	(real time) Polymerase chain reaction
PFA	Paraformaldehyde
pH	potentia/pondus hydrogenii
PI3K(CA)	Phosphatidyl Inositol 3-kinase (catalytic subunit)
PIC	Protease inhibitor cocktail
PIP3	Phosphatidylinositol (3,4,5)-triphosphate
PMS1	postmeiotic segregation increased 1
PMS2	postmeiotic segregation increased 2
PMSF	Phenylmethylsulfonyl fluoride
PPP	Proline rich
PPV	Positive predictive value
PTEN	Phosphatase and tensin homolog
R0	complete surgical resection
RALGDS	Ral guanine nucleotide dissociation stimulator
RAP1A	Ras-related protein Rap-1A
(K)RAS	(Kirsten) rat sarcoma viral oncogene homolog
rev	Reverse
RIPA	Radioimmunoprecipitation assay
RISC	RNA-inducing silencing complex
(m)RNA	(messenger) Ribonucleic acid
RNF170	Ring finger protein 170
ROC	Receiver operating-characteristic
rpm	Revolutions per minute
rRNA	ribosomal RNA
S	Svedberg
SAM	Sterile alpha motif
SAMD12	Sterile alpha motif domain containing 12
SASH1	SAM- and SH3-domain containing 1
SDS	Sodium dodecyl sulfate
sec	second(s)
SH3	Proto-oncogene tyrosine-protein kinase Src homology 3
SH3BP4	Sarcoma (Src) homology 3 domain-binding protein 4
shRNA	Small hairpin RNA
siRNA	Small interfering / short interfering / silencing RNA
SLY	SH3 protein expressed in lymphocytes
SMAD	Mothers against decapentaplegic homolog
SNP	Single-nucleotide polymorphism
SOC	Super Optimal broth with Catabolite repression (medium)
SSC	Sideward Scatter
t	Thymine (if sequential)
TCF	Transcription factor 7-like 2 (T-cell specific, HMG-box)
TEMED	Tetramethylethylenediamine
TGFBR2	Transforming growth factor, beta receptor II
TGFβ	Transforming growth factor beta
TNFα	Tumor necrosis factor alpha
TNM	Tumor, node, metastasis
Tris	Tris(hydroxymethyl) aminomethane
TRITC	Tetramethyl Rhodamine Iso-Thiocyanate
TTP	Tristetraprolin
TYMS	Thimidylate synthase
u	Uracil (if sequential)
Ub	Ubiquitin
UICC	International Union Against Cancer
UPL	Universal Probe Library
UTR	Untranslated region
V	Angioinvasion / Volt
V5	Protein tag from paramyxovirus simian virus 5
V600E	Valin to Glycine exchange at codon 600
WB	Western Blot
Wnt	Portmanteau of Wg (wingless) in Drosophila and Int1 (integration 1)
wt	Wild type
XTT	2,3-bis-(2-methoxy-4-nitro-5-sulfophenyl)-2H-tetrazolium-5-carboxanilide
yr	year(s)
ZU5	ZO-1 and Unc5-like (protein domain)
ΔCter	construct lacking the C-terminal end

1 Introduction – Colorectal cancer

1.1 Global burden

With an annual incidence of 47.9 and a mortality of 17.6 cases per 100 000 people, colorectal cancer is the third most common malignancy in the western world.[56] The life-time risk for developing colorectal cancer is five percent. Depending on the tumor stage at the time of diagnosis, nearly 50% of colorectal cancer patients die due to cancer related causes, mainly associated with metastatic spread.[56, 82, 128]

In 80% of patients, colorectal cancer occurs sporadically, i.e., without obvious inheritance. Empirically identified risk factors are advanced age, male sex, inflammatory bowel disease (Crohn's disease, ulcerative colitis), and mucosal precursor lesions. Moreover, environmental or consumer risk factors have been identified, such as obesity, reduced physical activity, diabetes, smoking, alcohol, and a "western-style" diet, composed of low fiber but high fat and red meat intake.[23, 70] However, in 75% of all patients with sporadic colorectal cancer, no obvious specific risk factors could be identified, with the exception of advanced age.[23]

1.2 Clinical implications

The allocation of patients to specific groups regarding their individual tumor extent (staging) is pivotal for recommendation of further therapeutic procedures, as well as for individual prognosis estimates. An ideal classification system allows for early staging, is robust enough to be feasible in clinical routine, and yields precise prediction of prognosis. Currently, tumor entity and histological type are classified according to the „International Classification of Diseases for Oncology" (ICD-O), in accordance with the classification of tumors by the World Health Organization.[131] The

TNM classification system (tumor, node, metastasis) by the International Union Against Cancer (UICC) and American Joint Committee on Cancer (AJCC) is the current "gold standard", in being a worldwide recognized classification system.[82, 113, 129] It describes the invasion depth of the primary tumor (T1 to T4 for the colorectum) and tumor cell infiltrates into lymphatic nodes (N0 to N2) or distant organs (M0/M1; see Figure 1 and below). Depending on the stage at diagnosis and the presence of prognostic factors, therapeutic strategies and the resulting prognosis of colorectal cancer patients vary significantly.[3, 14, 23, 82] Like in the TNM classification, colon and rectal cancer are often described together.[113] However, there are clear differences of recurrence rates, which have led to the recommendation of intensified perioperative regimes for rectal cancer.[82, 106, 130] Ongoing research has revealed molecular differences between colon and rectal cancer, further supporting the existence of two separate entities.[23, 26, 70, 130]

Figure 1: Stages of colorectal cancer according to UICC / AJCC.[72] Stage I tumors are limited to the muscularis propria (T1/2), while tumors invading the subserosa and beyond (T3/4) are stage II. In stage III, local lymph nodes are involved (N+), whereas in stage IV, distant metastases are present.[113]

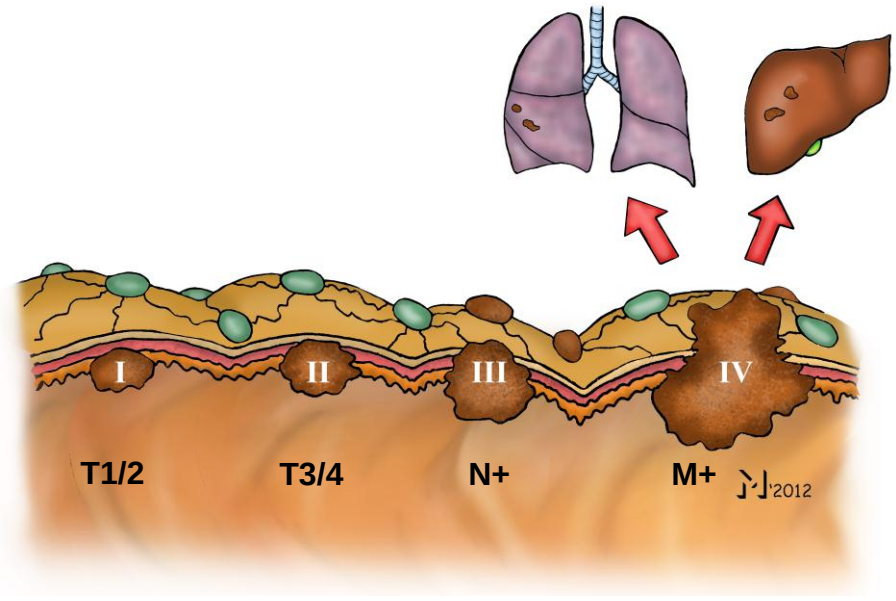

The subgroup of UICC stage I patients (T1-2 primary tumor without obvious tumor cell spread, 19% of patients[98]) have a very low recurrence risk after surgery, and an excellent prognosis. Precise identification of these patients allows local excision

without radical resection procedures. Characteristic for stage I low-risk patients are T1 tumors, high differentiation (low grading) and the absence of lymphatic vessel infiltration.[36]

About 30% of patients have localized advanced tumor disease at the time of diagnosis, without affected lymph nodes or distant metastases (UICC stage II, T3−4 N0 M0).[44, 98] These patients are considered to be cured after complete tumor resection. However, survival rates vary significantly within this group.[36] Approximately 20% of stage II patients develop recurrence of their disease[31, 36, 117, 134], and clinical evidence suggests that this group may benefit from systemic adjuvant chemotherapy.[14, 100, 102, 130] However, generalized adjuvant treatment of all stage II patients results in less than two percent reduction of global recurrence risk.[40] In order to avoid the toxicity and the financial burden of chemotherapy from which more than 95% of patients will not benefit, chemotherapy for stage II patients is not recommended routinely today.[106, 120, 130] However, data from clinical trials have led to the clinical definition of a stage II high-risk group, for whom adjuvant chemotherapy is recommended: T4 tumors with poor differentiation, lymphovascular invasion, perineural invasion, inadequate lymphadenectomy, emergency operation, tumor perforation, and comorbidities.[97, 106] Unfortunately, the definition of the high-risk stage II group according to these criteria is not accurate. Molecular genetic prognostic factors are hitherto not implemented in the classification so far.[34, 42, 92]

Five year survival rates of patients with UICC stage III (local lymph node involvement, N+, 29% of patients[98]) vary significantly between 89% and 36%.[82] At present, all patients receive the same recommended treatment in form of surgery and adjuvant chemotherapy, although it seems that stage III is quite heterogeneous, and comprises subgroups with different tumor biology. General administration of adjuvant chemotherapy reduces the recurrence risk in stage III from 40% to 20%, thus approximating stage II patients without adjuvant treatment.[40, 82, 120]

Median survival in stage IV (distant metastasis, M+, 22% of patients[98]) is generally poor but was improved from six to more than 20 months over the past decades by more advanced chemotherapeutic regimes and newly introduced small molecules.[77] Clinical as well as molecular markers allow selection of stage IV patients who profit from specific multimodal therapeutic approaches, possibly resulting in long term survival.[26, 81]

1.3 Clinical and molecular genetic risk estimation

The clinical behavior of colorectal cancer results from parallel and complex interaction, ranging from molecular to cellular and tissue levels. The challenge is to understand the molecular basis of an individual's tumor and to determine the factors that drive tumor progression, as well as its responsiveness or resistance to antitumor agents.[74] Reliable markers and precise definition of a patients' prognosis would allow a personalized therapy, e.g. by evidence-based application of specific inhibitors to certain mutated signaling pathways. While prognostic markers allow the estimation of survival or recurrence in the absence of treatment, predictive markers provide information about the assumed response to a specific therapy.[128] The aim is to identify and understand every patient's individual tumor genetics and signaling cascades deregulations. This should not only allow highly specific treatment of distinct patients, but also avoid toxic side effects by sparing patients a systemic treatment from which they would not benefit. Various approaches for risk estimation using clinical and genetic factors have been studied so far.[26, 34, 41, 61, 82, 128] Most studies focus on a single molecular marker, which inherently involves the risk of lacking robustness for large and heterogeneous patient groups. Therefore, an integrative approach would be desirable to identify and understand connections between single markers and underlying pathways. As our own analysis could show, risk determination based only on the TNM classification has reached its limits.[82] Based on current guidelines, further histopathological factors (e.g., lymphovascular invasion, resection margins, tumor grade, serum levels of carcinoembryonic antigen) are not generally accepted as prognostic and even less as predictive tools.[23, 26, 106, 120, 128, 130] Thus, current research aims to establish screening methods

and biomarkers that facilitate reliable estimation of prognosis and predict responses to individually tailored therapy, beyond the classical clinical factors.

Current technologies allow fast and cost-effective sequencing of the entire coding genome of a human cancer cell.[74] This, together with high-throughput expression arrays, has led to an explosive increase in the number of newly discovered markers, mainly DNA and RNA based, moving from hypothesis-driven targeted research to unbiased screening of the whole genetic spectrum.[128] However, only a limited number of promising markers are available so far.[8, 9, 14-16] The current literature on biomarkers is somewhat contradictory, and in most cases based on retrospective analyses without strict specifications.[26, 110] Findings were often reported only once and in relatively small series without further independent validation.[128] Until now, no molecular marker has made it into clinical practice, with the exception of KRAS in case of targeted anti-EGFR therapy (Epidermal growth factor receptor; see below). Early identification of high-risk patients remains difficult.[26, 34, 61, 68, 103] The main challenge is therefore to validate the initial findings in the clinical setting, and to translate the wealth of knowledge regarding colorectal cancer genomics into clinical application.[74]

1.4 Pathways of colorectal carcinogenesis

Since lesions of the large bowel are frequent and relatively easy to access via endoscopy, colorectal cancer has been well described both in histopathological, and molecular genetic terms for the past decades, making it a role model for carcinoma formation in general. In the following, established molecular pathways will be discussed whose deregulation has been described to drive colorectal cancer formation. This work focuses on the analysis of a combination of established and novel molecular genetic markers to achieve accurate metastasis risk prediction in sporadic colon cancer.

The individual markers and their relation to signaling cascades and clinical outcome will be reviewed. In addition to the large majority of sporadic carcinomas, 10-20% of colorectal cancers occur with a hereditary background.[70, 130] However, a distinct underlying genetic syndrome has yet been found only in six percent of cases.[128] The most frequent and relevant hereditary syndromes, Lynch Syndrome (HNPCC, Hereditary Nonpolyposis Colorectal Cancer) and Familial adenomatous polyposis (FAP), are described further below.

1.4.1 Chromosomal versus microsatellite instability

Mutational inactivation of tumor suppressor genes, activation of oncogenic pathways, epigenetic changes caused by mechanisms that do not involve the underlying DNA sequence, and loss of genomic stability all together play a role in driving the development of colorectal cancer.[74] Genomic instability in turn facilitates the acquisition of multiple tumor-associated mutations and can be categorized in two major groups, chromosomal instability and microsatellite instability.[55, 74, 86] Virtually every colorectal carcinoma is thought to display a form of genomic instability.

Chromosomal instability (CIN; the so-called tumor suppressor pathway) occurs in up to 85% of sporadic colon cancers and arises by aberrant expression or mutation of mitotic checkpoint genes, microtubule spindle defects, and telomere dysfunction.[1, 39, 94, 120] Aneuploidy may be caused by allelic imbalance, chromosomal amplification or translocation.[39, 128] In contrast, the residual 10-20% of sporadic colon cancers demonstrate a microsatellite instable (MSI) phenotype, also referred to as the mutator phenotype (see below).[3, 10] In general, MSI patients can be divided into those with sporadic microsatellite instability (mainly loss of function of MLH1 by methylation), and a smaller group with hereditary mutations in mismatch repair genes (HNPCC, see below).[17, 86]

Recently, epigenetic control of gene expression as alternative mechanism contributing to instability of the transcribed genome has come into focus, particularly by the analysis of CpG island methylation in the silencing of genes. This has led to the identification of the CpG island methylator phenotype (CIMP), which is associated with a strong and wide-spread methylation of CpG-residues in many gene loci throughout the genome. CIMP appears in 20% of all sporadic cases, with particular overlap to the MSI phenotype.[74, 120, 122, 128] However, some authors consider CIMP as a third alternative of independent elementary precondition to carcinogenesis.[26, 128, 132] Furthermore, combination of CIN and MSI may be present in about 5% of cases.[128] Up to 27% of patients may be categorized as "triple negative", neither showing CIN, nor MSI and CIMP.[86, 128]

1.4.2 From the "Vogelgram" to the era of whole genome sequencing

As early as 1990, Fearon and Vogelstein postulated the adenoma-carcinoma sequence, soon nicknamed "Vogelgram", and proposed a sequence of consecutive mutations leading to the development of colorectal cancer.[32] Until today, this work is assumed as landmark and role model for understanding cancer genetics. Colorectal cancer develops slowly over several years or even decades, and progresses through cytological distinct stages of growth ranging from single crypt lesions through benign adenoma to malignant carcinoma with the potential for invasion and metastasis (Figure 2).[26] Traditionally, APC (adenomatous polyposis coli) or CTNNB1 mutations (gene encoding the signaling molecule β-Catenin) with consecutive aberrant activation of canonical Wnt signaling are supposed to be the initial event, leading to formation of dysplastic crypts in the colon mucosa and early adenomas.[32, 66, 128] KRAS mutations are a likewise early event, and are sufficient to drive cancer formation in the absence of Wnt activation.[54] Alternatively, a BRAF gain-of-function mutation (V600E) may develop in microsatellite instable tumors.[32, 54, 128] Levels of chromosomal instability rise with the following steps that include allelic imbalance on chromosome 18q and resulting reduced expression of SMAD4 (Mothers against

decapentaplegic homolog 4), mutations affecting microsatellite sequences and leading to loss of function of Transforming growth factor, beta receptor II (TGFBR2), Insulin-like growth factor 2 receptor (IGF2R) and PTEN (PI3K signaling), and inactivating mutations in TP53 - or in the apoptosis inducer BAX (TP53 independent).[66, 74, 120, 128] Although genomic alterations which occur during the malignant transformation from normal epithelium to cancer cells are well described, specific events that lead to formation of metastasis are uncertain. Full-genome sequencing of primary colorectal cancer and distant metastases in the same patient showed no new mutations exclusive for the metastases,[58] implying that new mutations are not required to enable a tumor cell to leave the primary tumor and seed at a distant site.[63, 128]

Figure 2: Adenoma-carcinoma sequence for colorectal cancer.[32, 72, 74, 128] Successive molecular changes can promote normal epithelial cells to a single dysplastic crypt and finally to invasive cancer.

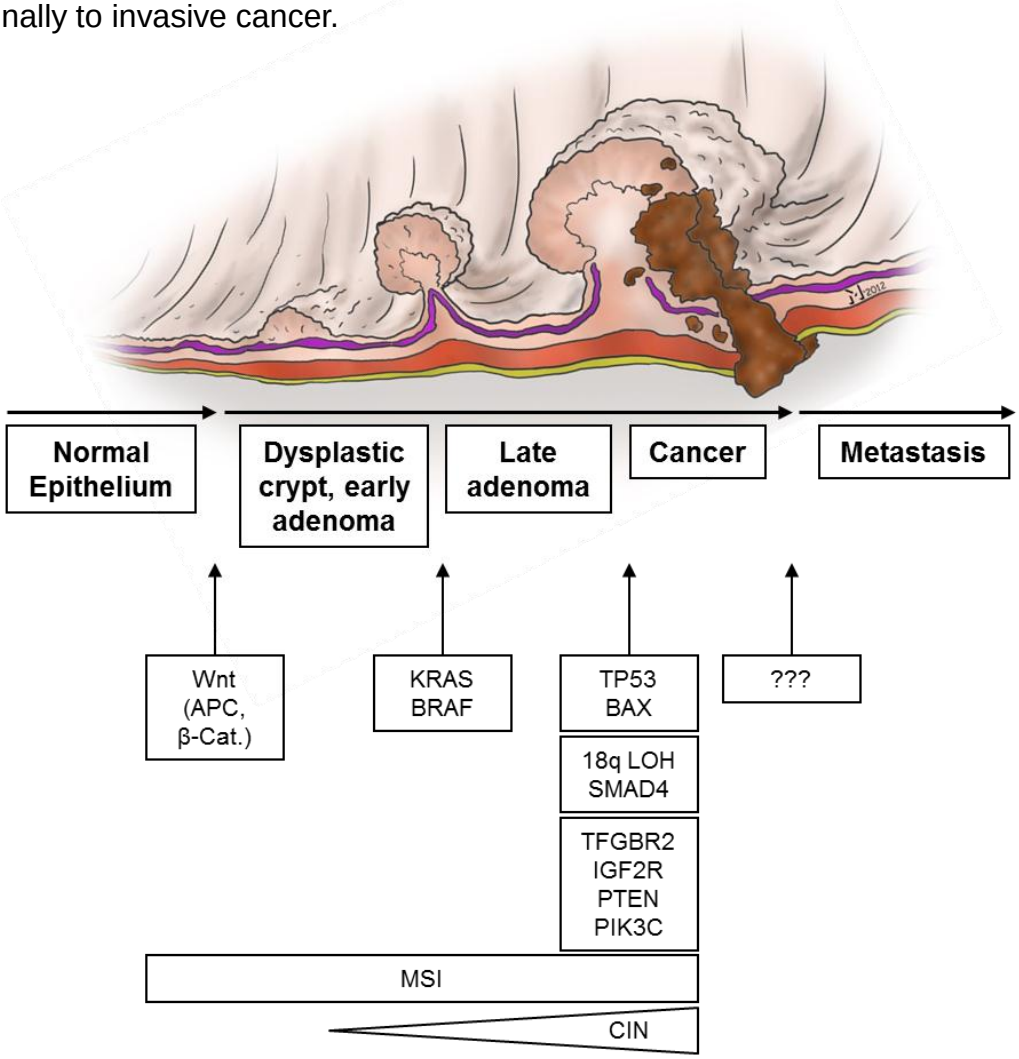

Anticipating two decades of molecular genetic research, Fearon and Vogelstein mentioned the possibility of parallel occurring mutations.[32] Taking into account recent advances, individual differences in tumor genetics are now considered to be crucial for prognosis and tumor progression. Microarray-based transcriptome studies have been investigated extensively and have underlined the genetic complexity as well as heterogeneity, leading to the current assumption of different mutational pathways in colorectal cancer that can occur in parallel.[26, 41, 61, 66, 103] Inflammation and immune control of tumors has gained considerable interest.[47] In addition to transcriptome profiling, new methods like “deep” or “next generation sequencing” allow insights into both mutations and expression levels, revealing a wealth of new information on colorectal carcinogenesis.[22] Among the key differentiators of sporadic colon cancer are microsatellite instability, specific mutations of the oncogenes KRAS and BRAF, and early activation of the canonical Wnt pathway.[17, 26, 51, 128]

1.4.3 From the linear adenoma-carcinoma sequence to three major pathways of colorectal cancer

Based on the postulated adenoma-carcinoma-sequence[32], at least three specific molecular pathways of colorectal cancer were described in the last years (Figure 3).[32, 36, 37] Allocation of tumors according to their underlying molecular changes has led to the definition of the so-called “Traditional pathway” of colorectal carcinogenesis, defined as microsatellite stable (MSS) but chromosomally instable tumors which do not harbor KRAS or BRAF mutations.[66] The “Serrated pathway” is characterized by BRAF mutation, subsequent development of the CpG island methylator phenotype, and high rates of mismatch repair (MMR) deficiency, resulting in microsatellite instability (MSI), and is associated with good prognosis. Tumors of the third or “Alternate pathway” are microsatellite stable, display KRAS mutations and may have worse prognosis.[66] Precursor lesions and colorectal cancers of the traditional, serrated, and alternate pathway show distinct histological, clinical and molecular features.[66] It is still unclear how these pathways and metastasis markers are related to individual risk, and which mutual connections and interactions exist between these pathways.

Figure 3: Different pathways of colorectal carcinogenesis based on the model of Leggett et al.[66] Depending on specific consecutive genetic alterations, colorectal cancer can be divided into the Traditional, Serrated, and Alternate pathway.

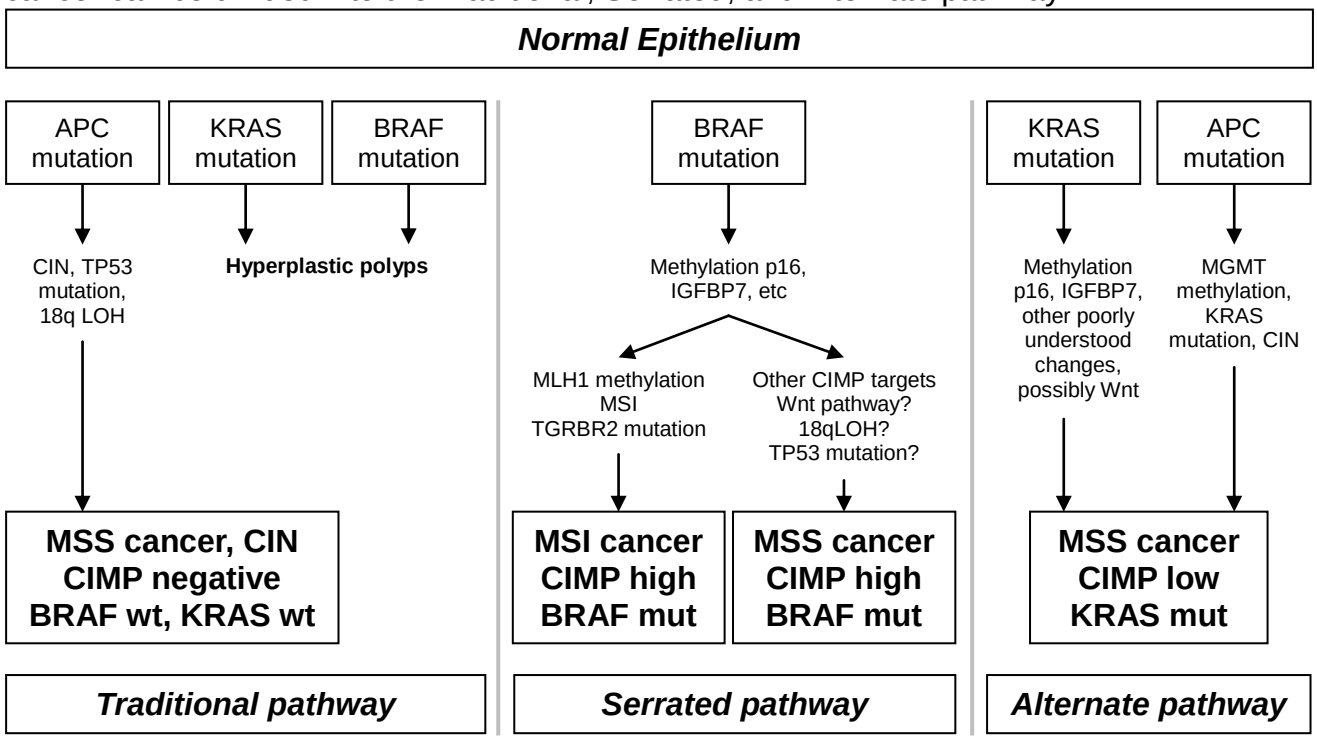

1.5 Biomarkers for colorectal cancer

A prognostic biomarker provides information about the patient's overall outcome regardless of therapy, whereas a predictive biomarker gives information about the effect of a particular therapeutic intervention.[120] However, in practice, the distinction between prognostic and predictive factors is not straightforward, and many factors are a mixture of both.[25, 26] Today, some distinct mutations in known oncogenes or tumor suppressor genes are regarded as the most powerful biomarkers, e.g. the single point mutation V600E for the BRAF kinase (see below). The reasons for preferably developing some distinct mutations are not always clear. Besides DNA mutation analysis, recent attention is focused increasingly on gene expression levels or gene expression profiles. Measurement of transcript levels may rather reflect biological effects than allow to identify underlying reasons; however, this method yields highly useful information which might correlate closely with clinical outcome.

1.5.1 KRAS and BRAF

These classical (proto-) oncogenes are not only causative drivers of carcinogenesis; they also constitute possible prognostic, respectively predictive biomarkers for colorectal cancer. Oncogenic mutations of the GTPase KRAS (Kirsten rat sarcoma viral oncogene homolog) and the serine/threonine kinase BRAF (v-raf murine sarcoma viral oncogene homolog B1) activate a downstream signaling cascade that mainly involves mitogen-activated protein kinases (MAPKs, Figure 4). Mutations occur in 30-50% (KRAS) and 5-15% (BRAF) of colorectal cancers.[26, 74, 120] Mutations are mainly found in KRAS (rather than HRAS or NRAS genes) and constitute an early event in the adenoma-carcinoma sequence (see above).[128] KRAS mutations are predominantly located in in exon 2 (codon 12 in 87%, codon 13 in 11%), and to a minor extent in exon 3 (codon 61 in 1%).[8] Other loci are possible but occur in less than 0.1% of cases, since they result in lower constitutive RAS signaling and therefore convey a lower selective advantage to cancer cells.[119, 128] Oncogenic RAS mutations inhibit the ability of GTPase activating proteins to effect the hydrolysis of RAS-bound GTP to GDP, which leads to a constitutively active conformation of the oncoprotein, and to further signaling directly to RAF kinases. The most prevalent and active BRAF mutation, from a valine to a glutamic acid at position 600 in exon 15 (V600E)[52] locks the BRAF serine-threonine protein kinase in the active state, which drives the MAPK signaling cascade.[74] Since both proto-oncogenes are affiliated to the same pathway, there is no selection pressure to acquire more than one mutation, and therefore, concomitant KRAS and BRAF mutations are extremely rare.[26, 93]

Figure 4: KRAS / BRAF signaling pathway.[9] Downstream signaling of the Epidermal growth factor receptor (EGFR) leads to activation of the Mitogen-activated protein kinase (MAPK) pathway, including KRAS and BRAF.

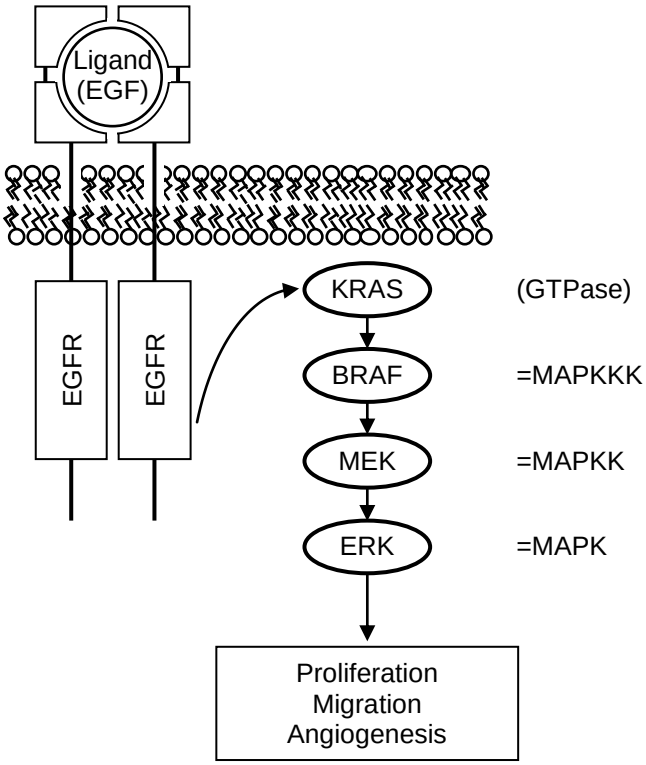

There is currently no clear evidence for a prognostic role of KRAS mutations in colorectal cancer.[128] Despite findings that KRAS mutations in general predict a worse prognosis[4], subsequent analyses proposed an association with poorer prognosis only for the glycine to valine substitution at codon 12, specifically in stage III patients.[28, 128] BRAF V600E mutation seems to have a negative prognostic effect. However, BRAF mutations are frequently associated with sporadic microsatellite instability, which, at least in part, seems to counteract the adverse effect of a BRAF mutation.[26, 85] Besides the uncertain prognostic value of KRAS mutations, there is clear evidence for a predictive role of KRAS and BRAF mutations, indicating the response of a given tumor to treatment with specific inhibitors of the growth factor receptor EGFR. Currently, there are two anti-EGFR antibodies available and approved for metastatic colorectal cancer, cetuximab (Erbitux, ImClone LLC, New York, NY, USA) and panitumumab (Vectibix, Amgen, Thousand Oaks, CA, USA). Specific BRAF inhibitors (Vemurafenib) are meanwhile available, but not used routinely for the treatment of colorectal cancer. Owing to the convergence of the EGFR and KRAS/BRAF

pathways, patients do not profit from pharmacological inhibition of the EGFR if their tumors constitutively upregulate this pathway by a downstream activating mutation of KRAS or BRAF.[27, 128] Today, KRAS status is the only predictive biomarker for colorectal cancer that is routinely used in clinical practice. In fact, the test for KRAS mutations constitutes the only compulsory molecular genetic test for colorectal cancer, based on the requirements of the health insurance authorities in Germany.

1.5.2 Microsatellite instability

Microsatellite instability can be found in about 10-20% of cases of sporadic colon cancer, with reduced rates diagnosed in higher disease stages.[120, 128] Underlying inability to repair strand slippage within repetitive DNA sequence elements leads to changes of the size of mononucleotide or dinucleotide repeats (microsatellites), which are scattered throughout the genome.[74] This epiphenomenon is caused by the loss of mismatch-repair function (Figure 5). Supposable mutations or causative gene silencing of DNA occur in control genes of the DNA replication system (MLH1, but also MSH2, MSH6, PMS2, PMS1, and MLH3).[23, 53, 67] Subsequently, tumor suppressor genes with mononucleotide or dinucleotide repeat sequences in functional regions or their protein-coding sequences are inactivated, such as the Transforming growth factor beta receptor II (TGFBR2), or BAX.[74]

Figure 5: Mismatch repair system.[17, 124] Slips in microsatellites (i.e., repetitive DNA sequences, represented by green arrowheads) can occur during DNA replication and lead to insertion or deletion of nucleotides. Thus, if factors of the mismatch repair system (represented in yellow) cannot restore the initial sequence due to mutations, microsatellite instability occurs.

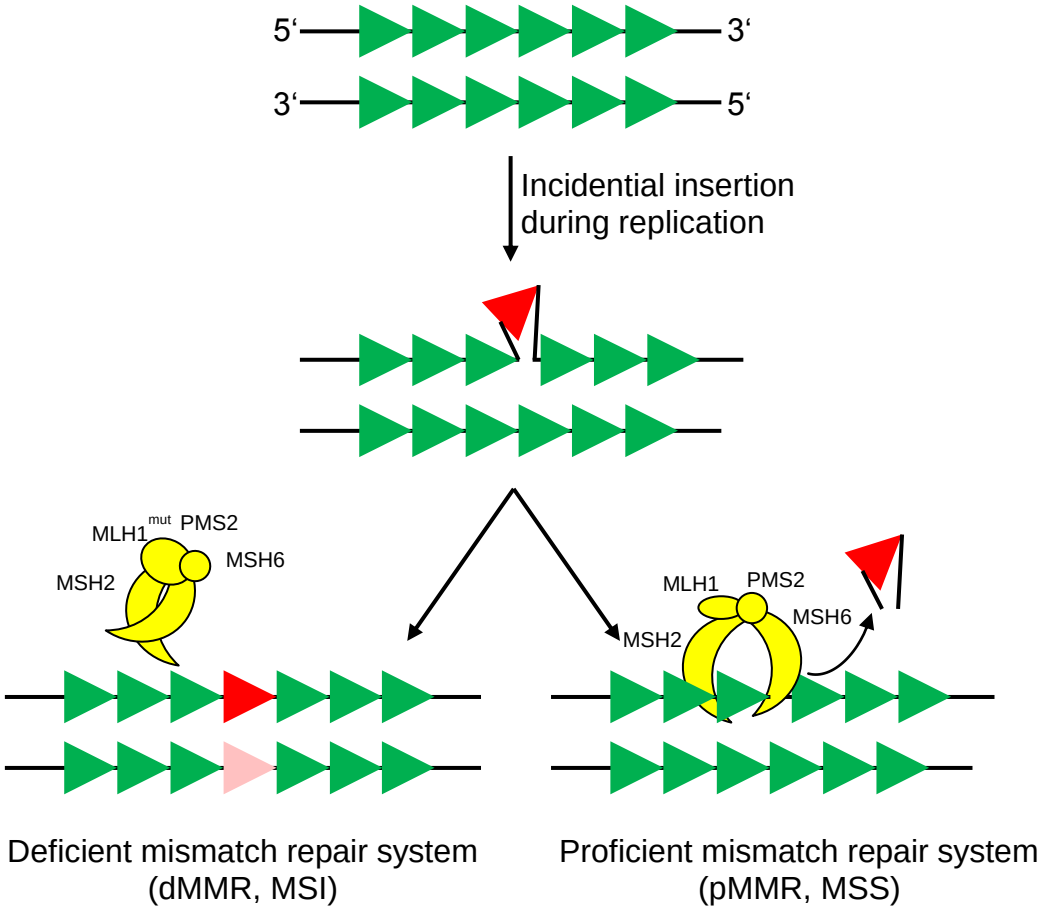

Germ line mutations in DNA repair genes occur infrequently, leading to malignant lesions, and are referred to as Lynch Syndrome.[70] Due to the colonic involvement in Lynch Syndrome, it has also been called Hereditary Nonpolyposis Colorectal Cancer (HNPCC). Lynch Syndrome is the most frequently identified type of familial colorectal cancer, being responsible for 3% of hereditary or 0.3% of all colorectal cancers.[23, 70] Patients with Lynch Syndrome have a specific phenotype, characterized by the Amsterdam criteria and its subsequent modification, the Bethesda criteria.[123, 126] Characteristics include high rates of right sided carcinomas (80% of cases proximal of the splenic flexure), accompanying extra-colonic malignancies (carcinoma of the endometrium, ovary, stomach, small bowel, pancreas, hepatobiliary tract, brain, and upper uroepithelial tract), early onset (mean age 45 years versus 63 years for non-

Lynch Syndrome patients), rapid progression from precursor lesions (2.3 years versus 10 years), poor differentiation, but also better postoperative long term outcome compared to stage corrected sporadic cancers.[70]

PCR amplification of a specific panel of five to 10 microsatellite repeats can be used to distinguish between microsatellite stability and low or high grade microsatellite instability (MSS, MSI-L, MSI-H). Typically, a tumor is defined as MSI-L when bearing instability in one out of five standard microsatellite markers and as MSI-H when bearing instability in at least two out of five markers.[17] Another common method is immunohistochemistry primarily using antibodies against the MLH1 protein,[120] which provides information about proficiency or deficiency (dMMR) of the mismatch repair system, in turn causing microsatellite instability.

A positive prognostic effect for patients with microsatellite instable tumors was confirmed repeatedly.[43, 128] Translation of novel proteins of various length and frameshift mutations according to varying microsatellite lengths may lead to increased antigen presentation on tumor cells, triggering adaptive host defense and leading to better survival.[17] The predictive role of microsatellite instability is less clear.[120] Benefit of 5-Fluorouracil (5-FU) based chemotherapy seems to be limited for microsatellite instable patients compared to microsatellite stable patients.[128] In vitro data suggest that a functioning mismatch repair system is required for cytotoxicity by incorporation of 5-FU into DNA.[57] Taken together, microsatellite instability is the most promising and clinically used prognostic biomarker in colorectal cancer.[120] The general use of adjuvant chemotherapy in stage II patients remains a matter of debate. However, MSI patients are supposed to have the most favorable outcome and no postoperative systemic treatment is recommended for this subgroup.[120]

1.5.3 Wnt pathway

According to the adenoma-carcinoma sequence, several independent genetic changes act together in colorectal cancer.[32] However, certain signaling pathways are clearly singled out as pivotal factors in tumor formation.[74] Overactivation of the canonical Wnt signaling pathway is considered as the key factor among these changes and initiating events in colorectal cancer.[74]

Soluble Wnt signaling molecules can trigger several different physiological reactions upon binding to target cells, regulating cell-to-cell interactions, such as tissue polarity and migration during embryogenesis ("Wnt / planar cell polarity (PCP) signaling pathway"). In the homeostasis of normal colonic epithelia, but also in colon cancer, the so-called "canonical Wnt pathway", which involves the signaling protein β-Catenin, is mainly affected. Physiological Wnt signaling occurs upon binding of Wnt proteins to their receptor Frizzled, leading to inhibition of the "destruction complex", which normally phosphorylates β-Catenin, thereby earmarking it for proteolytic destruction in the proteasome (the destruction complex contains APC and Axin2, amongst others, see Figure 6). Consequently, β-Catenin translocates and accumulates in the nucleus, where it binds to nuclear partners from the TCF/LEF family in order to form a transcription factor.[74, 108] Wnt pathway target genes like Cyclin D1, cMYC or Osteopontin are crucially important for proliferation and differentiation of colonic epithelial cells, and therefore also implicated in malignant transformation.

Figure 6: Wnt signaling pathway.[12] In the absence of Wnt, β-Catenin is phosphorylated by the APC/GSK complex, leading to ubiquitination and degradation. If Wnt signaling is present, the degradation complex is inhibited, β-Catenin accumulates in the nucleus and leads to enhanced expression of Wnt targets, e.g. Osteopontin. As identified recently, LGR5 homologues are facultative Wnt receptor components that mediate Wnt signal enhancement by soluble R-spondin proteins.[24]

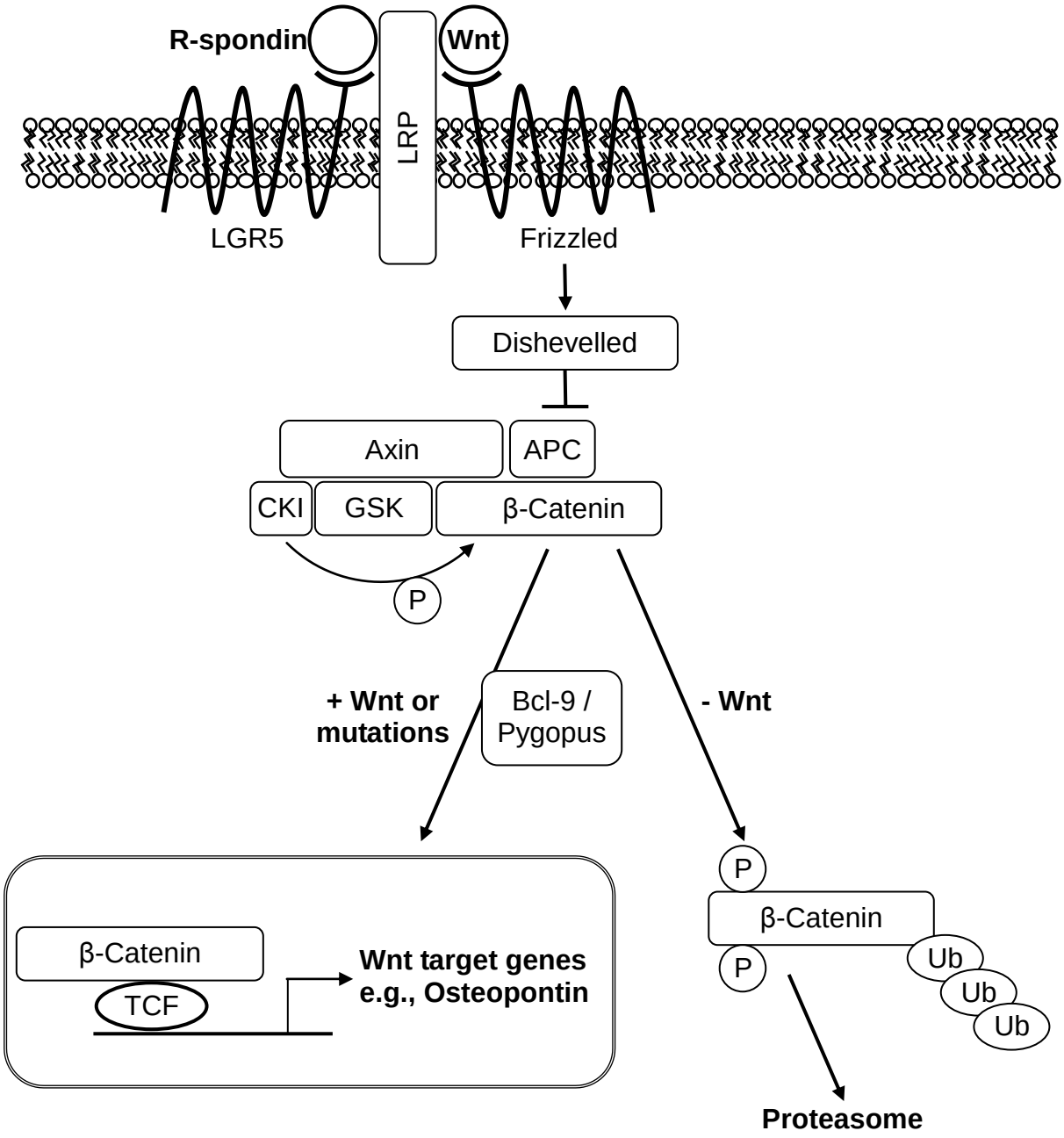

About 60% to 90% of colorectal carcinomas are thought to have alterations that affect the Wnt signaling pathway, leading to aberrant activation of Wnt signaling in the absence of soluble Wnt ligands. Mutations occur mainly in APC and lead to C-terminal protein truncation with resulting loss of function. Germ line mutations in APC are inherited in an autosomal dominant way and account for the second most

frequent genetic syndrome after Lynch, which is Familial adenomatous polyposis (FAP, 1% of hereditary and 0.1% of all colorectal cancers).[23] Colonic mucosal hyperproliferation and development of hundreds of adenomatous polyps with a risk of almost 100% of malignant transformation by the age of 40 years are the consequences.[46, 74] A minority of mutations affects the phosphorylation sites in exon 3 of β-Catenin (CTNNB1), causing protein stabilization, or involves mutations of the destruction complex scaffold protein Axin 2.[108, 128] Because of the high prevalence and large number of different described mutations in various genes, measurement of these factors is difficult and provides a prognostic marker only of restricted usefulness.[108, 128] However, our own previous results have shown that the expression levels of one particularly sensitive Wnt target gene, encoding the secreted phosphoprotein Osteopontin, provides robust and reliable information as to aberrant activation of the Wnt pathway, either by loss of function of APC, or by oncogenic mutation of β-Catenin. Thus, Osteopontin was identified to be a transcriptional target of aberrant Wnt signaling.[55, 96] Expression levels of Osteopontin provide a practical surrogate marker for quantification of canonical Wnt signaling activity.[96]

1.5.4 SASH1

Structure

The gene SASH1 (SAM- and SH3-domain containing 1) is a candidate tumor suppressor gene located on chromosome 6q24.3, a common site of allelic loss in cancer.[76, 135] Belonging to the evolutionarily conserved SLY-family[11], SASH1 protein (approximately 135 kDa) exhibits a bipartite nuclear localization signal (NLS), two different protein-protein interaction motifs (a SH3-domain and two SAM-domains), a proline rich domain which could be important for self-binding or the formation of homo-multimers, and a “coiled coil” domain (Figure 7).[75, 76] SH3 domains bind to proline-rich protein motifs and are involved in regulation of cell motility, growth and differentiation, protein transport and degradation, and immune response.[21, 75, 88] SAM domains facilitate interactions of signaling molecules and can be found in scaffold

proteins, regulators of transcription and translation, and in tyrosine or serine/threonine kinases. SAM domains can form homo- and heterodimers and are able to bind to RNA.[62, 75] Both, SH3 and SAM domains are frequently found in signal adapter or scaffolding proteins.[76] At least one (NLS1) of the two N-terminal NLS seems to be important for the active transport of SASH1 into the nucleus.[75] The “coiled coil” motif is frequently found in transcription factors or in proteins involved in vesicle trafficking.[38, 75]

Figure 7: Gene and protein structure of SASH1. The upper panel depicts the transcript with 7 685 base pairs and 20 exons, while the structure of the 1 247 amino acid containing protein with relevant domains is shown in the lower panel.[75]

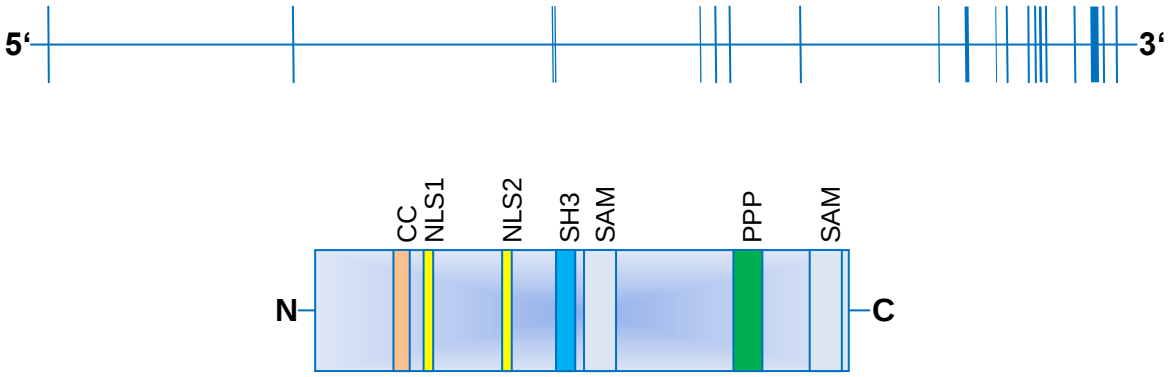

Function

SASH1 is widely expressed in juxta-membrane actin rich cytoplasmatic structures. However, the main fraction of SASH1 is found in the nucleus, sparing the nucleoli. No SASH1 is detectable in lymphocytes and dendritic cells.[95] With SH3 and SAM binding sites but without a predicted catalytic center, SASH1 is supposed to act mainly as signal adapter protein, e.g. by tyrosine kinase signaling.[75, 128] By direct interaction with the oncogenic protein Cortactin, it is involved in cell migration and cell-matrix adhesion, processes that are important for invasion and metastasis of tumor cells.[76] A further direct or indirect interaction partner of phosphorylated SASH1 is 14-3-3σ, a p53 effector protein with oncogenic characteristics in colon cancer.[15, 29, 75] SASH1 mRNA and protein levels are reduced in breast and colon

cancer and represent an independent negative prognostic factor regarding metachronous metastasis.[95, 135] SASH1 downregulation appears late in tumorigenesis, strengthening its putative role in tumor progression and metastasis.[95] Interactions of SASH1 with the cytoskeleton via Cortactin may support tumor cell motility and migration towards formation of metastases. Notably, physiologically high expressions of SASH1 were detected in the brain and gut. The only described human hereditary point mutation in the SASH1 locus leads to Multiple Lentiginosis ("Leopard Syndrome"), a dysfunctional pigment distribution of the skin.[87] Paternal deletion of the SASH1 region 6q24.3 leads to multiple congenital malformations.[75, 83] No tumor relevant mutations are described in the coding region of SASH1[22], suggesting that promoter methylation or other epigenetic factors may lead to downregulation of SASH1 transcripts in tumor cells. CpG islands for CIMP silencing are present in SASH1.[75, 121] Frequent LOH of the SASH1 region in human and murine tumor models supports this hypothesis.[75, 95] Taken together, direct DNA binding of SASH1 is unlikely due to the absence of specific domains. High levels of SASH1 and location in the nucleus may lead to tumor suppressing regulation of transcription by polymerization of SAM domains, to cell cycle arrest in the G0/G1 phase, and to apoptosis.[20, 75, 135] SASH1 located near to the cellular membrane may lead to migratory inhibiting effects by reorganization of the cytoskeleton.[20, 75] In this work, weight was specifically placed on SASH1 due to its role as putative metastasis markers in colorectal cancer.[95]

1.5.5 MACC1

Structure

In 2009, Stein et al. identified the gene MACC1 (metastasis-associated in colon cancer-1), which corresponds to *"Homo sapiens mRNA for putative binding protein 7a5"*.[117] MACC1 is located at chromosome 7p21.1. It contains seven exons, coding a cDNA of 2,559 nucleotides. MACC1 encodes a protein of 852 amino acids (97 kDa) and shows 49.3% identity of nucleotide sequence to human SH3 domain-binding

protein 4 (SH3BP4), respectively 43.7% identity of amino acids.[30, 117] There are five additional splice variants of MACC1, which are all predicted to be non-functional.[115] MACC1 contains a SH3 domain like SASH1, together with a proline-rich SH3 binding motif. Both domains were shown to be essential for the biological function of MACC1.[117] Further identified domains are an adaptor protein 2α binding site (DPF), two Epsin15 homology domains (NPF), a clathrin box, a ZU5 domain, and sites for putative post-translational modifications: central and C-terminal tyrosine phosphorylation sites and N-terminal serine/threonine phosphorylation sites (Figure 8).[95, 117] Two death domains are located C terminally, which are supposed to rather represent regulators of cell motility and proliferation than receptor triggered apoptosis.[95]

Figure 8: Gene and protein structure of MACC1. The upper panel depicts the transcript with 7 417 base pairs and 7 exons, while the structure of the 852 amino acid containing protein with relevant domains is shown in the lower panel.[115]

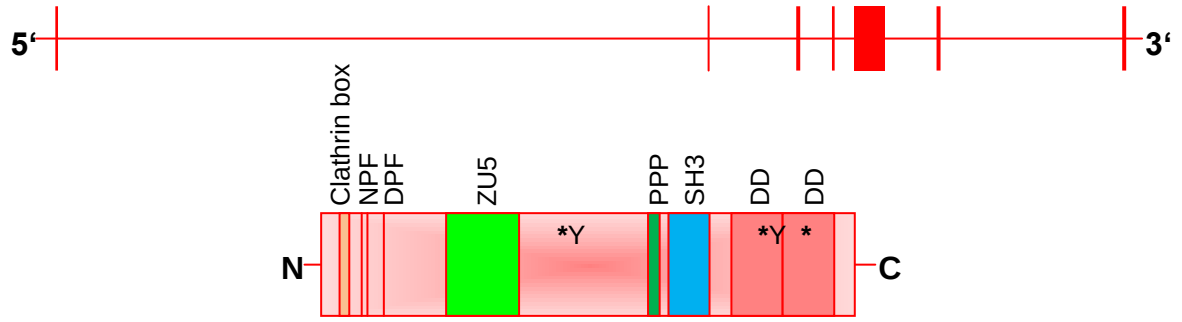

Function

Physiological MACC1 expression levels are highest in tissues arising from the endoderm, namely intestine and stomach. Therefore, it might have an important function during embryonic development in relation to endoderm-derived organogenesis.[95] Gain of chromosome 7, which contains MACC1, is one of the most frequently chromosomal aberrations in colorectal cancer.[115] HGF (Hepatocyte growth factor) leads to translocation of MACC1 from the cytoplasm into the nucleus, where it binds 50 to 230 base pairs upstream of the transcription start site to the promoter of

the receptor tyrosine kinase cMET. MACC1 thus leads to transcriptionally upregulation of cMET expression, further inducing cell proliferation, invasion, motility and HGF-triggered scattering, tumor growth and metastasis.[115, 117, 137] SNPs in the coding region were not found to play a relevant role.[65, 105] In non-small cell lung cancer, cMET dependent phosphorylation of Cortactin and SASH1 was described.[45, 75] MACC1 expression classifies subjects with low versus high risk of metachronous tumor metastasis independently of stage[117] and has been validated as prognostic factor several times.[16, 33, 65, 78, 91, 111, 112, 137, 138] MACC1 seems to have higher prognostic power than the identified downstream target cMET, suggesting effects additional to the HGF/cMET pathway.[33, 117] Analogous to SASH1, MACC1 does not comprise a kinase domain. The absence of protein function after deletion of the SH3 or proline-rich domains suggest a crucial role of MACC1 in signaling transduction cascades by direct protein-protein interactions.[89, 108, 117] MACC1 is among the 151 most frequently mutated genes in colorectal cancer.[22]

1.5.6 Further currently discussed biomarkers for risk prediction in colorectal cancer

The focus of this work is based on a number of selected markers which are associated with the occurrence of metastasis in colon cancer. Stratification into different risk groups should be facilitated by the marker selection. In addition to the markers discussed above, a plethora of potential biomarkers emerged during the last years. The currently most promising biomarkers for colorectal cancer will be briefly discussed in the following, even though this does not represent a comprehensive overview of all potential risk-predictors.[26, 74, 120]

TP53

As a tumor suppressor gene, the p53 gene encodes a transcription factor, which mainly regulates the cell cycle and cell survival. In 35-55%, it is mutated in colorectal cancer, generally leading to loss of function of the protein, or to the expression of

point-mutated variants.[120] Traditionally, p53 mutation was seen as the second key step in colorectal cancer after APC mutation.[74] Physiologically, TP53 initiates cell cycle arrest, DNA repair or apoptosis as response to cellular stresses like DNA damage. p53 mutations are often associated with the chromosomally instable phenotype (CIN) and inversely correlated with microsatellite instability (MSI). However, in MSI-H patients, inhibition of the p53 pathway may be facilitated by mutations in the BAX protein, another inducer of apoptosis. [74, 120] Similar to most of the markers discussed here, there are conflicting data, both claiming and refusing the prognostic and predictive character of p53. The inconsistency may at least in part arise from different methods of assessing the p53 status.

Chromosome 18q LOH/AI and DCC

Allelic imbalance (AI) or loss of heterozygosity (LOH) has been described to be prognostic in colorectal cancer.[120] However, 18q AI can be the consequence of a number of genetic events. It is currently not clear what is actually measured by 18q AI.[120] It might be a surrogate marker for the frequently occurring CIN phenotype or reflect several effects resulting from loss of function of genes located within the chromosomal region (DCC, SMAD4, see below).[120] The prognostic and predictive value of tumor 18q AI is currently examined in the E5202 adjuvant colon cancer trial[13], the first colon cancer study that uses prognostic and predictive markers prospectively.[26]

SMAD4

SMAD4 (Mothers against decapentaplegic homolog 4) together with the related proteins SMAD2 and SMAD3 plays a critical role downstream in the Transforming growth factor beta (TGFβ) signaling pathway for tumor suppression (see below). The gene is located on chromosome 18q, a frequent site of loss of heterozygosity in colorectal cancers (see above). In 10-35% of cases inactivation occurs, mainly by homozygous deletion (allelic imbalance), or mutation.[74]

TGFβ

In about one third of colorectal cancers, somatic mutations inactivate the Transforming growth factor beta receptor II (TGFBR2). In tumors of the microsatellite instability pathway, distinct frame shift mutations in a polyadenine repeat within the TGFBR2 coding sequence occur frequently. Moreover, inactivating missense mutations occur in microsatellite stable tumors and affect the TGFBR2 kinase domain. However, more frequently, mutations and deletions inactivate downstream TGFβ pathway components like SMAD4 (see above).[74] Mutations that inactivate the TGFβ pathway are detected late in the adenoma-carcinoma-sequence and show coincidence with the transition from adenoma to high-grade dysplasia or carcinoma.[74]

TYMS

The thymidylate synthase (TYMS) is essential for pyrimidine biosynthesis proceeding DNA synthesis. 5-FU (a pyrimidine analogon broadly used for chemotherapy) inhibits the TYMS protein. Thus, TYMS expression and activity is considered predictive for 5-FU response.[120] Data for the prognostic influence are conflicting. Surprisingly, patients who are treated with surgery alone may have poorer prognosis if TYMS protein levels are high, although the reasons for this remain unclear.[120]

EGFR

The Epidermal growth factor receptor (EGFR) is a member of the tyrosine kinase family known as the Erb or HER receptor family.[26] Main downstream signaling routes are the RAS-RAF-MAPK pathway (see above), and the Phosphatidyl inositol 3-kinase (PI3K) pathway with the downstream protein serine/threonine kinase Akt (see below).[26] Overexpression of EGFR occurs in 65-70% of colon cancers and results in poor prognosis.[26] Activating mutations in one of the factors mentioned above leads to

non-response to anti-EGFR therapy, further making it the currently most frequently used predictive marker (see above).[74]

PI3KCA, PTEN

One third of colorectal cancers bear activating somatic mutations in PI3KCA, which encodes the catalytic subunit of phosphatidylinositol 3-kinase (PI3K).[74] The regulatory subunit of PI3K binds proteins including KRAS, integrates various signals from membrane receptors, and activates PI3KCA. Activated PI3KCA phosphorylates the lipid PIP3 (Phosphatidyl-inositol (3,4,5)-trisphosphate), which localizes Akt to the cell membrane, where it becomes activated.[26] Enhanced downstream signaling of activated Akt leads to cell proliferation and survival and can be often detected in human malignancies. PI3KCA mutation might be correlated with response to anti-EGFR inhibitors (see above).[26] Other less common genetic alterations that may substitute for PI3KCA mutations are loss of the tumor suppressor and inhibitor of PI3K signaling PTEN (Phosphatase and tensin homolog), by mutation or promoter hypermethylation or co-amplification of Akt and PAK4, two downstream mediators of PI3K signaling.[26, 74] Although the prognostic role of PTEN is still under investigation, it shows promise as a predictive marker for wild-type KRAS patients treated with anti-EGFR therapy.[26]

Tumor-infiltrating lymphocytes

The positive or negative influence of the immune system on carcinogenesis is now widely recognized. With the invasion of malignant cells into the submucosa, various host immune responses can take place that potentially shape the outcome of the disease. A clear positive correlation between the number of tumor infiltration lymphocytes and longer patient survival in colorectal cancer has been shown repeatedly, may prognostic even outperform TNM classification stages[26], and could be a promising approach for clinical control of progression, metastasis and

recurrence in the near future. Pronounced lymphocyte infiltration is more marked in microsatellite instable tumors and may be due to the generation of a large number of abnormal peptides by frame shift mutations.[26] These novel epitopes may trigger a cellular immune response, e.g., by activating $CD4^+$ T-helper lymphocytes, which mainly produce cytokines like Interleukin-2 and Interferon-α.[26] $CD8^+$ T-effector cells produce perforin and Granzyme B, which are cytotoxic to their target cells, and have the capacity to directly kill colon cancer cells.[26] Natural killer cells from the innate immune system express several ligands of the tumor necrosis factor family and can induce apoptosis of malignant target cells.[26]

Genetic signatures, Micro RNAs

Gene expression studies, studies describing differentially expressed regulators, Micro RNAs (miRNAs), or genome-wide association studies have been emerging over the last years.[128] By this unbiased high-throughput screening approaches, huge amounts of data are collected. The main practical problem lies in the correct statistical analysis, interpretation and the performance of independent validation studies, rather than in the identification of a specific expression profile which allows prediction of prognosis or therapy response in a single study cohort. Today, no gene set or signature is used routinely in daily clinical practice.[110] However, within the next years, commercial approaches that are currently under clinical validation may be approved, with the most promising ones being OncotypeDX (Genomic Health Inc., Redwood City, CA, USA), and ColoPrint (Agendia NV, Amsterdam, The Netherlands) for colorectal cancer.[61, 103]

2 Aim of the work

The aim of this work was to evaluate the prognostic significance of described as well as newly identified signaling pathways in colon cancer in a comprehensive approach.

In the first part of the study, a patient cohort should be screened in order to derive clinical relevant marker correlations in a deductive manner. In particular, the clinical practicability, models of risk prediction, and allocation of patients into defined tumor groups was assessed. Further, marker variability during the course of metastasis formation was tracked by comparison of primary tumors and corresponding metastatic tissues.

In the second part, identified correlations between individual signaling pathways should be further evaluated by in vitro experiments in order to elucidate functional connections on the molecular level. Here, the focus should be on connections between the tumor suppressing gene SASH1 and the metastasis-associated gene MACC1.

3 Material

3.1 Chemicals	reference	Company, city
10X T4 DNA Ligase Buffer	B69	Thermo Scientific, Rockland, IL, USA
2-Mercaptoethanol C_2H_6OS	M3148	Sigma-Aldrich, Steinheim
3-Morholinopropanesulfonic acid $C_7H_{15}NO_4S$ (MOPS)	69947	Sigma-Aldrich, Steinheim
Acetic acid $C_2H_4O_2$	71251	Sigma-Aldrich, Steinheim
Acrylamide (30%) / Bis solution 37.5:1	161-0158	Bio-Rad, Hercules, CA, USA
Agarose (purified)	50004	SeaKem, FMC Bio Products, Rockland, ME, USA
Actinomycin D (Lyovac-Cosmegen)	NA	Lundbeck, Dublin, Ireland
Albumin, from bovine serum (BSA)	A7906	Sigma-Aldrich, Steinheim
Ammonium chloride NH_4Cl	1009245000	Merck, Darmstadt
Ammonium persulfate (APS, 10%)	A 3678	Sigma-Aldrich, Steinheim
Ampicillin	A0166	Sigma-Aldrich, Steinheim
Attractene Transfection Reagent	301005	Qiagen, Hilden
Bacto Yeast extract, Technical	288620	BD, Franklin Lakes, NJ, USA
Benzamidine	12072	Sigma-Aldrich, Steinheim
Blotting-Grade Blocker (Milk)	170-6404	Bio-Rad, Hercules, CA, USA
Bromphenol blue (saturated dilution)	B-5525	Sigma-Aldrich, Steinheim
Calcium chloride $CaCl_2$	C4901	Sigma-Aldrich, Steinheim
Cycloheximide	C4859	Sigma-Aldrich, Steinheim
D(+)-Glucose $C_6H_{12}O_6$	G-5400	Sigma-Aldrich, Steinheim
D(+)-Saccharose / Suchrose $C_{12}H_{22}O_{11}$	4621.1	Roth, Karlsruhe
Detection reagent 1 Peroxidase Solution	1859701	Thermo Scientific, Rockland, IL, USA
Detection reagent 2 Luminol Enhancer Solution	1859698	Thermo Scientific, Rockland, IL, USA
Diethylpyrocarbonate $C_6H_{10}O_5$ (DEPC)	D5758	Sigma-Aldrich, Steinheim
Dimethyl sulfoxide (DMSO) C_2H_6OS	D5879	Sigma-Aldrich, Steinheim
dNTP Set (10mM)	R0182	Thermo Scientific, Rockland, IL, USA
Endorphin neuromodulators	Not for sale	Bibi, Anne, Munich
Ethanol 70%, 96%, 100%	NA	Pharmacy Klinikum rechts der Isar
Ethidiumbromide dilution 1%	2218	Roth, Karlsruhe
Ethylenediaminetetraacetic acid (EDTA, pH8.0, 0.5M)	E-5134	Sigma-Aldrich, Steinheim
Eukitt	NA	Kindler, Freiburg
FastDigest BglII	FD0083	Thermo Scientific, Rockland, IL, USA
FastDigest XhoI	FD0694	Thermo Scientific, Rockland, IL, USA
FBS Superior (FCS)	S 0616	Biochrom, Berlin
Formaline (3.5-3.7%)	PZN 2652965	Fischar, Saarbrücken
Formaline (36.5-38%)	F-8775	Sigma-Aldrich, Steinheim
Formamide CH_3NO	F-7503	Sigma-Aldrich, Steinheim

FuGENE HD Transfection Reagent	E2311	Promega, Madison, WI, USA
G418 Sulfate	345810	Calbiochem, Merck, Darmstadt
Gelatine	G-9391	Sigma-Aldrich, Steinheim
Glycerol (Glyerine) $C_3H_8O_3$	G8898	Sigma-Aldrich, Steinheim
Hepes (4-(2-hydroxyethyl)-1-piperazineethanesulfonic acid)	H-3375	Sigma-Aldrich, Steinheim
Hydrochloric acid HCl	4625.1	Roth, Karlsruhe
Hydrogen peroxide H_2O_2	NA	Pharmacy Klinikum rechts der Isar
Isopropanol C_3H_8O	NA	Pharmacy Klinikum rechts der Isar
L-Glutamine	K 02833	Biochrom, Berlin
Lithium chloride LiCl	L-7026	Sigma-Aldrich, Steinheim
Magnesium chloride $MgCl_2$	M8266	Sigma-Aldrich, Steinheim
Magnesium sulfate $MgSO_4$	M-7506	Sigma-Aldrich, Steinheim
Mayer's Hemalaun (Romeis Nr 648, instead of Hematoxylin)	NA	Pharmacy Klinikum rechts der Isar
Medium DMEM (1X)	41965	Gibco, Life Technologies Corporation, Grand Island, NY, USA
Medium DMEM / Ham's F12 (1:1)	FG 4815	Biochrom, Berlin
Medium McCoy's 5A (1X) + GlutaMAX-I	36600	Gibco, Life Technologies Corporation, Grand Island, NY, USA
Methanol CH_4O	1060091000	Merck, Darmstadt
Mitomycin C	M4287	Sigma-Aldrich, Steinheim
N,N,N',N'-tetramethylenediamine (TEMED)	161-0800	Bio-Rad, Hercules, CA, USA
N,N-Bis(2-hydroxyethyl)taurine (BES)	B-6266	Sigma-Aldrich, Steinheim
Noniclet-P40 (NP 40)	N3550	US Biological, Swamscott, MA, USA
Nuclear fast red solution (instead of Eosin)	N3020	Sigma-Aldrich, Steinheim
Oligo(dT)18 Primer	SO132	Thermo Scientific, Rockland, IL, USA
Orange G Sodium Salt	O-1625	Sigma-Aldrich, Steinheim
Page Ruler Prestained Protein Ladder	SM0671	Thermo Scientific, Rockland, IL, USA
Paraformaldehyde	P6148	Sigma-Aldrich, Steinheim
PBS-Dulbecco (1x)	L 1825	Biochrom, Berlin
Penicillin / Streptomycin (Pen/Strep)	A 2213	Biochrom, Berlin
Pepstatin A	P4265	Sigma-Aldrich, Steinheim
Phenol:Chloroform:Isoamyl Alcohol 25:24:1	P3803	Sigma-Aldrich, Steinheim
Ponceau red RR	199761	Sigma-Aldrich, Steinheim
Potassium chloride KCl	529552	Merck, Darmstadt
Protease Inhibitors Set (PIC)	11 206 893 001	Roche, Mannheim
Random Hexamer Primer	SO142	Thermo Scientific, Rockland, IL, USA
Re-Blot Plus Mild Solution 10x	2502	Milipore, Temecula, CA, USA
Recombinant Human HGF	294-HG	R&D Systems, Minneapolis, MN, USA
RevertAid H Minus Reverse Transcriptase	EP0452	Thermo Scientific, Rockland, IL, USA
RiboLock RNase Inhibitor	EO0382	Thermo Scientific, Rockland, IL, USA
RT-Buffer (M-MulV RT, 5x)	EP0452	Thermo Scientific, Rockland, IL, USA
Sodium acetate (NaOAc, pH8.0, 3M)	S-2889	Sigma-Aldrich, Steinheim
Sodium chloride NaCl	3957.2	Roth, Karsruhe

Sodium deoxycholate	D6750	Sigma-Aldrich, Steinheim
Sodium dodecyl sulfate (SDS) Pellets	CN30.3	Roth, Karlsruhe
Sodium fluoride NaF	S7920	Sigma-Aldrich, Steinheim
Sodium hydrogen carbonate $NaHCO_3$	8551.1	Roth, Karlsruhe
Sodium hydroxide NaOH	1091371000	Merck, Darmstadt
Sodium orthovanadate Na_3VO_4	S-6508	Sigma-Aldrich, Steinheim
Sodium phosphate dibasic Na_2HPO_4	255793	Sigma-Aldrich, Steinheim
T4 DNA Ligase	EL0011	Thermo Scientific, Rockland, IL, USA
TRI Reagent	T9424	Sigma-Aldrich, Steinheim
Tris(hydroxymethyl)aminomethane (Tris)	37192	Serva Electrophoresis, Heidelberg
Tris(triphenylphosphine)rhodium(I) chloride (Tris-Cl)	205036	Sigma-Aldrich, Steinheim
Triton X-100	161-0407	Bio-Rad, Hercules, CA, USA
Trypsine-EDTA (1x)	L11-660	PAA Laboratories, Pasching, Austria
Trypton / Peptan from Casein	8952.1	Roth, Karlsruhe
TurboFect Transfection Reagent	R0541	Thermo Scientific, Rockland, IL, USA
Tween 20 Detergent	655205	Calbiochem, Merck, Darmstadt
Xylol (Xylene) C_8H_{10}	PZN 7475522	Heidinger, Stuttgart
β-Glycerol phosphate disodium salt pentahydrate (β-Glyc.phos)	50020	Sigma-Aldrich, Steinheim

3.2 Single-use devices	reference	Company, city
µ-Dish 25mm, low & Culture-Insert	80206	Ibidi, Martinsried
8-Strip tubes / Ind Caps	LW2510	Peske, Aindling-Arnhofen
96-well PCR microplate, Lightcycler-type, white (for LightCycler 480 II)	I1402-9909	Starlab, Hamburg
Amersham Hyperfilm MP	28-9068-42	GE Healthcare, Chalfont St Giles Buckinghamshire, UK
BD Falcon 15ml Polystyrene Conical Tube	352095	BD, Franklin Lakes, NJ, USA
Cell Culture Dish 10cm	353003	Falcon (Becton Dickinson), Le Pont De Claix, France
Cell Culture Dish 15cm	353025	Falcon (Becton Dickinson), Le Pont De Claix, France
Cell Culture Dish 6cm	353002	Falcon (Becton Dickinson), Le Pont De Claix, France
Cell Culture Dish 6-well	353934	Falcon (Becton Dickinson), Le Pont De Claix, France
Cell Culture Dish 96-well	353219	Falcon (Becton Dickinson), Le Pont De Claix, France
Conical Falcon Tubes 15ml	352097	BD, Franklin Lakes, NJ, USA
Conical Falcon Tubes 50ml	358206	BD, Franklin Lakes, NJ, USA
Cryo-Vial FS	LW3332	Alpha Laboratories, Eastleigh, UK
FACSClean (FACSafe)	340345	BD, Franklin Lakes, NJ, USA
FACSFlow	342003	BD, Franklin Lakes, NJ, USA
FACSRinse	340345	BD, Franklin Lakes, NJ, USA
Feather Disposable Scalpel No 10	02.001.30.010	Feather, Osaka, Japan
Filter tips 0.1-10µl	A300SX	Kisker Biotech, Steinfurt

Filter tips 2-20µl	A20S	Kisker Biotech, Steinfurt
Filter tips 2-200µl	A200S	Kisker Biotech, Steinfurt
Filter tips 50-1 000µl	A1000S	Kisker Biotech, Steinfurt
Gel Blotting Paper	10 426 994	Whatman, Dassel
LB-Ampi bacteria plates	NA	BD, Franklin Lakes, NJ, USA
Micro Amp Optical Adhesive Film	4311971	Applied Biosystems, Foster City, CA, USA
Microscope cover slides	0101000	Marienfeld superior, Marienfeld
Microtome blade	C 35	Feather, Osaka, Japan
p2 color victim nail polish	232 shockful	2 Kosmetik, Wiener Neudorf, Austria
Pasteur pipettes (glass)	7477 15	Brand, Wertheim
PCR 96-Well TW-MT-Platte, colorless (for 7300 Real-Time PCR System)	712410	Biozyme, Hess. Oldendorf
Pipette 2ml	86.1252.001	Sarstadt, Nümbrecht
Pipette 5ml	86.1253.001	Sarstadt, Nümbrecht
Pipette 10ml	86.1254.001	Sarstadt, Nümbrecht
Pipette 25ml	86.1685.001	Sarstadt, Nümbrecht
Protein G Sepharose	P3296	Sigma-Aldrich, Steinheim
Research plus pipette 0.1-2.5µl	3120 000.011	Eppendorf, Hamburg
Research plus pipette 0.5-10µl	3120 000.020	Eppendorf, Hamburg
Research plus pipette 2-20µl	3120 000.097	Eppendorf, Hamburg
Research plus pipette 10-100µl	3120 000.046	Eppendorf, Hamburg
Research plus pipette 20-200µl	3120 000.038	Eppendorf, Hamburg
Research plus pipette 100-1 000µl	3120 000.062	Eppendorf, Hamburg
Safe-Lock Tubes 0.5ml	0030 121.023	Eppendorf, Hamburg
Safe-Lock Tubes 1.5ml	0030 120.086	Eppendorf, Hamburg
Safe-Lock Tubes 2.0ml	0030 120.094	Eppendorf, Hamburg
Snap-cap Falcon Tubes 14ml	352051	BD, Franklin Lakes, NJ, USA
Stainless Steel Beads, 5 mm	69989	Qiagen, Hilden
Superfrost Plus Microscope slides	J1800AMNZ	Menzel, Braunschweig
Tissue-Tek O.C.T. Compound	4583	Sakura, Alphen aan den Rijn, Netherlands
Whatman Protran Nitrocellulose Transfer Membrane	10 401 196	Whatman, Dassel

3.3 Kits / Compositions	reference	Company, city
Cell Proliferation kit (XTT)	11 465 015 001	Roche, Mannheim
DNeasy Blood & Tissue Kit	69504	Qiagen, Hilden
LightCycler 480 High Resolution Melting Master (for HRM)	04 909 631 001	Roche, Mannheim
Power SYBR Green PCR Master Mix (for 7300 Real-Time PCR System)	4368577	Applied Biosystems, Foster City, CA, USA
QIAGEN Plasmid Plus Maxi Kit	12963	Qiagen, Hilden
QIAprep Spin Miniprep Kit	27104	Qiagen, Hilden
QIAquick Gel Extraction Kit	28704	Qiagen, Hilden

QIAshredder	79654	Qiagen, Hilden
RNase-Free DNase Set	79254	Qiagen, Hilden
RNeasy Mini Kit	74106	Qiagen, Hilden
TaqMan Gene Expression Master Mix (for UPL)	4369016	Applied Biosystems, Foster City, CA, USA
Therascreen BRAF Pyro Kit	971470	Qiagen, Hilden
Therascreen KRAS Pyro Kit	971460	Qiagen, Hilden
Type-it Microsatellite PCR Kit	206243	Qiagen, Hilden
Universal Probe Set, Mouse	04 683 641 091	Roche, Mannheim

3.4 Multi-use / Technical devices	reference	Company, city
7300 Real-Time PCR System	SDS 7300	Applied Biosystems, Darmstadt
Apotome	423667-9000-000	Zeiss, Göttingen
Autoclave Systec	D-65	Systec, Wettenberg
Axio Observer.Z1 microscope	Various components	Zeiss, Göttingen
Benchtop centrifuge PerfectSpin Mini	C1301B-230V	Peqlab, Erlangen
Biofuge 28RS (39 000g)	75003650	Heraeus Kendro, Osterode
Biometra Minigla Twin Komplett (Gel chamber for PAGE)	2509253	Biometra, Göttingen
Bioruptor Ultrasonic device	UCD-200	Diagenode, Liège, Belgium
Centrifuge (for Eppendorf tubes)	5415R	Eppendorf, Hamburg
Continuous motion platform for Western Blot incubation	1040	Heidolph Instruments, Schwabach
Corning Stripettor Plus Pipetting Controller for 2-25ml pipettes	4091	Corning, NY, USA
Cryostat	CM3050 S	Leica, Wetzlar
Dako Pen (Fat pen)	S2002	Dako, Glostrup, Denmark
EcoVac vacuum pump	07001	Schütt-biotech, Göttingen
FACS Calibur	4CS-E4923	BD, Franklin Lakes, NJ, USA
FACSFlow Supply System (waste cubitainer)	34014430	BD, Franklin Lakes, NJ, USA
Gel chambers	Various	Various
Glass ware (Beaker glass, Erlenmeyer flask, graduated cylinder)	Various	Schott Duran, Wertheim/Main
Heating Block	MBT250	Kleinfeld Labortechnik, Gehrden
Ice maker	ZBE 30-10	Ziega, Isernhagen
IML Dounce tissue grinder (tight)	357538	Wheaton, Millville, NL, USA
Incubator Heraeus	BBD6220	Heraeus Kendro, Osterode
Innova refrigerated incubator shaker for bacteria	4230	New Brunswick scientific, Edison, NJ, USA
Laminar airflow cabinet Hera safe	KS18	Heraeus Kendro, Osterode
LightCycler 480 II	05 015 278 001	Roche, Mannheim
Magnetic stir bars	Various	Various
Mithras Multimode Microplate Reader	LB940	Berthold Technologies, Wildbad
Mixing rotor Variospeed Variotim	3 50 33	Renner, Darmstadt

Molecular Imager Gel Doc XR System	170-8170	Bio-Rad, Hercules, CA, USA
Multifuge 3S-R (for Falcons and Plates)	75004371	Heraeus Kendro, Osterode
NanoDrop 1000 Spectrophotometer	ND-1000	Thermo Scientific, Rockland, IL, USA
Neubauer cell counting chamber	0640130	Marienfeld superior, Marienfeld
Optimax X-Ray Film Processor (Developing machine for Western Blot films)	1170-1-0000	Protec, Oberstenfeld
PCR System 9700 (for cDNA)	N805-0200	Applied Biosystems, Foster City, CA, USA
pH Level I (pH-meter)	E 163694	WTW inoLab, Weilheim
Power Pack (Power transformer for PAGE and Agarose gels)	P25T	Biometra, Göttingen
Purelab (for ddH_2O)	Ultra GE MK2	Elga, Marlow, Buckinghamshire, UK
PyroMark Q24	9001514	Qiagen, Hilden
TissueLyser II	85300	Qiagen, Hilden
Trans-Blot SD Semi Dry Transfer Cell	221BB47149	Bio-Rad, Hercules, CA, USA
Transformer (220V-117V) for FACS Calibur	34002910	BD, Franklin Lakes, NJ, USA
Vortex-Genie 2	G-560E	Scientific Industries, Bohemia, NY, USA

3.5 Software	reference	Company, city
7300 System Software	Version 1.4.0.25	Applied Biosystems, Foster City, CA, USA
Adobe Photoshop	Version CS3	Adobe, San Jose, CA, USA
ApE - A Plasmid Editor	Version 1.17	M. Wayne Davis, http:// biologylabs.utah.edu/ jorgensen/ wayned/ ape/
AxioVision	Version 4.8.2 SP1	Zeiss, Göttingen
CellQuest Pro	Version 6.0	BD, Franklin Lakes, NJ, USA
Excel	Version 2010	Microsoft Corp., Redmond, WA, USA
FlowJo Flow Cytometry Analysis Software	Version 8.8.2	Tree Star, Ashland, OR, USA
Gelsoftware Quantity one	Version 4.6.2	Bio-Rad, Hercules, CA, USA
GraphPad Prism	Version 5.00	Graph Pad Software, La Jolla, CA, USA
IBM SPSS Statistics	Version 19	SPSS Inc., IBM Corporation, Somers, NY, USA
ImageJ	Version 1.46	Research Service Branch, http://rsb.info.nih.gov
LightCycler® 480 Gene Scanning Software (for HRM)	NA (05 103 908 001)	Roche, Mannheim
LightCycler® 480 Software (for UPL)	Version 1.5.0.39 (04 994 884 001)	Roche, Mannheim
MikroWin 2000	Version 4.31	Berthold Technologies, Wildbad
Nanodrop	Version 2.5.4	Thermo Scientific, Rockland, IL, USA
PyroMark Q24 Software	Version 2.0	Qiagen, Hilden
R Software	Version 2.13.0	R Foundation for Statistical Computing, Vienna, Austria

3.6 Cells	reference	Company, city
DLD1	CCL-221 (ATCC)	Rockville, Maryland, USA
E. coli (MAX Efficiency DH5α Competent Cells)	18258-012	Invitrogen, Darmstadt
HCT116	CCL-247 (ATCC)	Rockville, MD, USA
Hek293	CRL-1573 (ATCC)	Rockville, MD, USA
HT29	HTB-38 (ATCC)	Rockville, MD, USA
SW480	CCL-228 (ATCC)	Rockville, MD, USA
SW620	CCL-227 (ATCC)	Dep. of Pathology, LMU, Prof. Dr. rer. nat. A. Jung

3.7 Antibodies, Reagents	reference	Company, city
4′,6-Diamidino-2-phenylindole (DAPI)	D9542	Sigma-Aldrich, Steinheim
Antibody Actin	A5316	Sigma-Aldrich, Steinheim
Antibody CDC5L	ab51320-100	Abcam, Cambridge, UK
Antibody cMET	ab39075	Abcam, Cambridge, UK
Antibody ERK1/2 (p42/44 MAPK)	9102	Cell Signaling, Danvers, MA, USA
Antibody GFP	63246	Clontech, Saint-Germain-en-Laye, France
Antibody MACC1 (for IF)	5197	ProSci, Poway, CA, USA
Antibody MACC1 (for WB, IP)	Sc-163595	Santa Cruz Biotechnology, Santa Cruz, CA, USA
Antibody MACC1, blocking peptide	Sc-163595	Santa Cruz Biotechnology, Santa Cruz, CA, USA
Antibody p53	OP29	Calbiochem, Merck, Darmstadt
Antibody pERK (P-p42/44 MAPK)	91015	Cell Signaling, Danvers, MA, USA
Antibody SASH1	Anti-Peptide polylclonal antiserum (rabbit) „pAb1540“[95]	Dr. Markus Moser, Max Planck-Institut, Martinsried[75]
Antibody secondary anti-mouse HRPO (for WB)	115-035-003	Dianova, Hamburg / Jackson Immuno Research, West Grove, PA, USA
Antibody secondary anti-rabbit Alexa488 (for IF)	111-545-003	Dianova, Hamburg / Jackson Immuno Research, West Grove, PA, USA
Antibody secondary anti-rabbit HRPO (for WB)	111-035-003	Dianova, Hamburg / Jackson Immuno Research, West Grove, PA, USA
Antibody Tubulin	CP06	Calbiochem, Merck, Darmstadt
Antibody V5	46-1157	Invitrogen, Darmstadt
Antibody β1-Integrin	MAB2253Z	Chemicon international, Merck, Darmstadt
Antibody β-Catenin	610154	BD Biosciences, San Jose, CA, USA
IgG from goat serum	I5256	Sigma-Aldrich, Steinheim
IgG from rabbit serum	I5006	Sigma-Aldrich, Steinheim
Phalloidin–Tetramethylrhodamine B isothiocyanate (TRITC)	P1951	Sigma-Aldrich, Steinheim

3.8 Primer, Sequences	reference	Company, city
Expression plasmid SASH1-V5 (pBud)	NA	Constructed in own laboratory by Dr. Martini[75]
Expression plasmid SASH1-ΔCter (pBud)	NA	Constructed in own laboratory by Dr. Martini[75]
hBRAF HRMA fwd (HPLC)	ggtgattttggtctagctacag	Metabion international, Martinsried
hBRAF HRMA rev (HPLC)	agtaactcagcagcatctcagg	Metabion international, Martinsried
hHPRT 7300 fwd	gctttccttggtcaggcagtataat	Metabion international, Martinsried
hHPRT 7300 rev	aagggcatatcctacaacaaacttg	Metabion international, Martinsried
hHPRT UPL fwd	gaccagtcaacaggggacat	Metabion international, Martinsried
hHPRT UPL rev	gtgtcaattatatcttccacaatcaag	Metabion international, Martinsried
hKRAS HRMA fwd (HPLC)	tcattatttttattataaggcctgctgaa	Metabion international, Martinsried
hKRAS HRMA rev (HPLC)	caaagactggtcctgcaccagta	Metabion international, Martinsried
hMACC1 UPL fwd	ggcatatgaaattcctcatcg	Metabion international, Martinsried
hMACC1 UPL rev	ggcaggtttccacatcatct	Metabion international, Martinsried
hOsteopontin 7300 fwd	ttgcagccttctcagccaa	Metabion international, Martinsried
hOsteopontin 7300 rev	ggaggcaaaagcaaatcactg	Metabion international, Martinsried
hSASH1 UPL fwd	cagatccgggtgaagcag	Metabion international, Martinsried
hSASH1 UPL rev	gagtccaccacttggaatcg	Metabion international, Martinsried
Negative control siRNA	uucuccgaacgugucacguuu	Qiagen, Hilden
Plasmid pBudCE4.1 -EGFP	V532-20	Invitrogen, Darmstadt
shMACC1 antisense	tcgataaaaagattggacttgt acactgctctcttgaagcagt gtacaagtccaatcggga	Metabion international, Martinsried
shMACC1 sense	gatctcccgattggacttgta cactgcttcaagagagcagtg tacaagtccaatctttta	Metabion international, Martinsried
shRNA plasmid pSUPER.neo+gfp	VEC-PBS-0006	OligoEngine, Seattle, WA, USA
shRNA plasmid SASH1-GFP (pSUPER)	NA	Constructed in own laboratory by Dr. Martini[75]
siRNA APC	ccggugauugacaguguuuca	Qiagen, Hilden
siRNA MACC1	aagauuggacuuguacacugc	Qiagen, Hilden
siRNA SASH1	cagaaauugacaacuaagaaa	Qiagen, Hilden

4 Methods

4.1 Protocols

Hematoxylin and Eosin staining

1. Prepare tissue section on slide
2. 1min, Formalin (4%)
3. 1min, rinse with water
4. 5min, Hematoxylin
5. 5min, rinse with water
6. 1min, Eosin
7. Dip into water, five times
8. Dip into Ethanol (70%), five times
9. Dip into Ethanol (96%), five times
10. 2min, Ethanol (100%)
11. 3min, Xylol (repeat three times)
12. Place covering slide with one drop of Eukit on tissue section

Isolation of DNA from tissue using the Qiagen DNeasy kit

1. Add 350µl of RLT Lysis Buffer to 25mg tissue (approximates 3 slices of a human tumor block á 100µm, stored in a 2ml safelock Eppendorf tube in liquid nitrogen) or cells (Preparation of RLT Lysis Buffer: 1ml RLT + 10µl 2-Mercaptoethanol)
2. TissueLyser II with metal bead, 1:30min, 30 1/min, -20°C
3. 5min, 12 000rpm, room temperature
4. Transfer the supernatant in a white DNA spin column, 15sec, 10 000rpm, room temperature
5. Add 500µl Buffer AW1, 15sec, 10 000rpm, room temperature
6. Add 500µl Buffer AW2, 2min, 10 000rpm, room temperature

7. Ensure that the outside of the spin column is dry, place the spin column in a new 1.5ml Eppendorf tube
8. Add 100µl Buffer EB, 1min, allow to stand, room temperature
9. 1min, 10 000rpm, room temperature
10. Repeat steps 8 and 9 once
11. Store DNA on ice until further processing or storage at 4°C

Isolation of RNA using the Qiagen RNeasy kit

From cultured cells:

1. Resuspend the pellet of the harvested cells in 350µl RTL Lysis Buffer, transfer into purple Qiashredder-column (Preparation of RLT Lysis Buffer: 1ml RLT + 10µl 2-Mercaptoethanol)
2. 2min, 12 000rpm, room temperature
3. Add whole flow-through to 350µl ethanol (prepared in a new collection tube), mix by pipetting up and down, transfer all into a pink RNA spin column
4. Continue with step 9

From tissue:

1. Add 1ml of TRI Reagent to 25mg tissue (approximates 3 slices of a human tumor block á 100µm, stored in a 2ml safelock Eppendorf tube in liquid nitrogen)
2. TissueLyser II with metal bead, 1:30min, 30 1/min, -20°C
3. 5min, allow to stand, room temperature (dissociation)
4. Add 200µl Phenol:Chloroform:Isoamyl Alcohol 25:24:1 (mix well before adding)
5. 5min, allow to stand, room temperature
6. 15min, 12 000rpm, 4°C
7. Transfer 400µl of the clear supernatant phase (containing the RNA) into a new collection tube (prepared with 400µl 70% ethanol), mix by pipetting up and down
8. Transfer all 800µl into a pink RNA spin column
9. 15sec, 12 000rpm, room temperature

10. Add 400µl Buffer RW1, 15sec, 12 000rpm, room temperature
11. Add 10µl DNase (prepared in 70µl Buffer RDD), 15min, allow to stand, room temperature
12. Add 400µl Buffer RW1, 15sec, 12 000rpm, room temperature
13. Add 500µl Buffer RPE, 15sec, 12 000rpm, room temperature
14. Repeat step 13 once
15. Ensure that the outside of the spin column is dry, place the spin column in a new 1.5ml Eppendorf tube
16. Add 30µl RNase free water, 1min, allow to stand, room temperature
17. 2min, 12 000rpm, room temperature
18. Repeat steps 16 and 17 once
19. Store RNA on ice until further processing or freezing at -80°C

RNA integrity control by denaturating gel

---

1. Boil 85ml of DEPC water (see below) together with 1.5g purified agarose
2. Add 10ml of MOPS-Buffer (10x, see below) and 5ml of Formaldehyde (38%)
3. Mount gel chamber, clean inside and all instruments with H_2O_2, insert gel, let cool down, fill up with MOPS (1x)
4. Mix 10µl of the RNA sample and 10µl of RNA-loading buffer (see below), 1min, denaturation, 75°C
5. Add 1µl Ethidiumbromide (diluted 1:10)
6. Run gel at 55V for 2h

DEPC-treatment of water:

1. 0.1% Diethylpyrocarbonate in H_2O (i.e., 2ml in 2l)
2. Mix with magnetic stir bar overnight, room temperature
3. Autoclaving (inactivation of DEPC)

MOPS-Buffer (10x):

1. Dissolve 46.24g MOPS in 800ml DEPC water
2. Adjust pH to 7 by adding NaOH
3. Add 16.6ml of NaAc pH8.0, 3M

4. Add 20ml of EDTA pH8.0, 0.5M
5. Add DEPC water to a total volume of 1l

RNA-loading buffer (2x):
Mix 160µl MOPS (10x), 80µl Bromphenol blue (saturated dilution), 720µl Formamide, 720µl Formaldehyde (37%), 160µl Glycerol, 120µl H_2O

Transcription of RNA into cDNA

1. Add 1µg of RNA to H_2O to a total volume of 25µl
2. Add 1µl random hexamer primer (1:150) and 1 µl dt Oligo (1:20)
3. 10min, incubation, 70°C
4. Cool to 4°C
5. Centrifuge down
6. Add 8µl M-MulV RT (5x RT-Buffer), 2µl dNTPs (10mM, see below), 1µl RNase inhibitor and 2µl Revert Aid RT H-minus M-MulV reverse transcriptase
7. 10min, incubation, room temperature
8. 60min, transcription, 42°C
9. 5min, removal of RNA, 95°C

dNTPs (10mM):
Mix 20µl of dGTP, dCTP, dATP and dTTP each (100mM) with 720µl H_2O (total volume of 800µl).

Determination RNA expression levels by rtPCR

RNA of all stage II patients included in this study was sent to Pia Herrmann for quantification of MACC1 expression levels as described previously[117] (Laboratory of Prof. Dr. rer. nat. Ulrike Stein, Experimental and Clinical Research Center, a joint cooperation of the Charité Medical Faculty and the Max-Delbrück-Center for Molecular Medicine). All other expression analyses were performed in the Munich laboratory using the UPL method and calibration to HPRT expression levels after consecutive dilution series. Only Osteopontin expression was measured using the

7300 Real-Time PCR System according to previously established protocols.[96] All measurements were performed in duplicates, together with a negative (H_2O) and positive control (known cell line cDNA, also for calibration of multiple plates) on every 96-well plate.

rtPCR Quantification using the UPL method and LightCycler 480 II System

1. Prepare the mastermix: 10µl Gene Expression Mastermix Abi, 0.2µl primer left (20µM), 0.2µl primer right (20µM), 4.4µl H_2O, 0.2µl specific UPL-probe (for SASH1 #38, for MACC1 #47, for HPRT #22)
2. Add 5µl of cDNA (10ng/µl)
3. Place in 96-well plate, centrifuge down
4. PCR program according to the manufacturer's protocol (Mono color hydrolysis probe UPL, Relative Quantification)

rtPCR Quantification using the 7300 Real-Time PCR System

1. Preparation of mastermix: 15µl SYBR Green PCR Master Mix, 1µl primer forward (15µM), 1µl primer reverse (15µM), 3µl H_2O
2. Add 10µl cDNA (10ng/µl)
3. Place in 96-well plate, centrifuge down
4. PCR program according to the manufacturer's protocol (58°C)[96]

Detection of KRAS and BRAF mutations using HRM Analysis[134]

---

1. Prepare the mastermix:
   For KRAS, mix 10µl Master Mix (2x concentrated, including ResoLight high-resolution melting dye), 0.8µl primer forward (25mM), 0.8µl primer reverse (25mM), 1.6µl $MgCl_2$ Stock Solution (25 mM), 4.8µl H_2O
   For BRAF, mix 10µl Master Mix (2x concentrated, including ResoLight high-resolution melting dye), 0.2µl primer forward (25mM), 0.2µl primer reverse (25mM), 2.4µl $MgCl_2$ Stock Solution (25 mM), 5.2µl H_2O
2. Add 2µl of genomic DNA (10ng/µl)
3. Centrifuge down

4. PCR program (Endpoint Gene scanning): pre-incubation (95°C, 10 min), amplification (42 cycles, 95°C, 15s / 61°C, 15s / 72°C, 15s), melting point analysis (95°C, 5s / 72°C, 90s, followed by a melting profile ranging from 72°C to 95°C in 19.2min)

For a subset of patient DNA samples, KRAS and BRAF mutational status was determined and validated by pyrosequencing additional to High Resolution Melting Analysis. Pyrosequencing was performed at the department of Pathology of the LMU (Prof. Dr. rer. nat. Andreas Jung) using the PyroMark Test Kit, the PyroMark Q24 Vacuum Workstation, and PyroMark Q24 Software 2.0 for analysis. All steps were performed according to the standard operating protocol of the pathological laboratory, as described in the Master Thesis of Alexander Balmert.[7]

Detection of Microsatellite instability status using Multiplex PCR

Genomic DNA of tumor and corresponding normal colon mucosa were analyzed for microsatellite instability at the department of Pathology of the Technische Universität München by Prof. Dr. rer. nat. Gisela Keller using the Type-it Microsatellite PCR Kit and following procedures for routine diagnostics.[79] Two mononucleotide and three dinucleotide Bethesda markers (BAT25, BAT26, D2S123, D5S346, and D17S250) were investigated. A tumor with five normal markers was defined as microsatellite stable (MSS). Irregularity in one marker was defined as low grade microsatellite instability (MSI-L), irregularity in two or more markers was defined as high grade microsatellite instability (MSI-H).

Detection and sorting of transfected cells by FACS

Cell sorting by FACS according to GFP expression was performed by Lynette Henkel (Group of Dr. rer. nat. Matthias Schiemann at the Institute for Medical Microbiology, Immunology and Hygene of the Technische Universität München). After harvesting (see below), cells were washed and stored in PBS until sorting. Sorting was performed on a flow cytometer type Aria or MoFlo II and the FACSDiva Version 6.1.2

software was used for analysis of the results. Directly after the FACS process, the cells were transferred into FCS until subsequent plating for further expansion.

Monitoring of GFP positive cells by flow cytometry

Monitoring and quantification of GFP positive transfected cells by flow cytometry after cell sorting (see above) was performed in the own laboratory. Cells were prepared in the same manner as described above. According to the manufacturer's protocol, 20 000 cells of each preparation were analyzed, including non-transfection controls. Settings were the following: FSC-H: Voltage E00, AmpGain 1.00, Mode Lin; SSC-H: Voltage 459, AmpGain 1.88, Mode Lin; Threshold: FSC 52. Analysis of the results was performed by the FlowJo software.

Harvesting, counting, splitting of cells

1. Remove culture media from adherent cells
2. Add PBS and remove again to wash, room temperature
3. Add Trypsin, incubation until cells start to detach (approximately 2-10min) at 37°C, saturated humidity
4. Add media and collect cells, transfer all into 15ml Falcon
5. 5min, 1 500rpm, room temperature
6. Discard supernatant
7. Resuspend the cell pellet in media
8. Count cells in microscopic Neubauer counting chamber
9. Dilute the intended number of cells and spread in new culture plate with specific media (see below)
10. Incubate at 37°C, saturated humidity

Culture media for cell lines:

(FCS 30min, 56°C heat inactivation before use)

- SW480, DLD1, HT29, Hek293:
  DMEM (1X), 7% FCS, 1% Pen/Step, 1% Glutamine
- SW620:
  DMEM / Ham's F-12 (1:1), 10% FCS, 1%Pen/Strep
- HCT116:
  McCoy's 5A (1X)+GlutaMAX-I, 7% FCS, 1% Pen/Strep, 1% Glutamine

Freezing cells

---

1. Harvest cells (see above)
2. Instead of media, resuspend the cell pellet in 90% FCS / 10% DMSO
3. Transfer to cryo tube
4. Slowly freeze tube in foamed plastic material at -80°C overnight
5. Transfer into liquid nitrogen after 6-24h
6. Thaw one aliquot of frozen cells as alive control (see below)

Thawing cells

---

1. Thaw cryo tube containing the cells in the palm of the hand
2. Add content to a prepared cell culture plate with media
3. Incubate overnight at 37°C, saturated humidity
4. Replace culture media after 6-24h

Transfection of cells with plasmid DNA / siRNA

---

1. Seed $4x10^5$ cells per well of a six well plate
2. Transfection according to protocol (see below)
3. Incubation over two nights, 37°C, saturated humidity
4. Harvest cells for analysis

Protocol for transfection reagents:

(Fugene for HCT116 / Attractene for SW480 and HT29 / Turbofect for SW620 and DLD1)

1. Mix 2 / 2.5 / 4µg of DNA or siRNA with 98 / 100 / 200µl DMEM
2. Add 5 / 6.76 / 8µl of transfection reagent
3. Mix by vortexing
4. 15min, incubation, room temperature
5. Add to cells
6. Change media after 24 / 6 / 5h

(Calcium chloride for Hek293)

1. Mix 5µg of DNA or siRNA with 135µl H_2O
2. Add 15µl of $CaCl_2$ (2.5M)
3. Mix by vortexing; while vortexing, dropwise add 150µl BES (pH 6.95, see below)
4. 10min, incubation, room temperature
5. Add to cells
6. Change media after 24h

BES:

For 100ml, mix 1.066g BES, 1.636g NaCl, and 21.24mg Na_2HPO_4. Add H_2O to a total volume of 100ml while adjusting the pH to 6.95.

Plasmid construction for stable MACC1 shRNA expressing cells

Preparation of oligos

1. Mix 2.5µg of sense and 2.5µg of antisense DNA (for shRNA) and fill up to a total volume of 100µl with Annealing buffer (= 10mM Tris, 1mM EDTA pH 8)
2. 4min, 94°C (denaturation)
3. 10min, 70°C (annealing)
4. Let cool down and store at 4°

Digestion and purification of the pSUPER plasmid

5. Mix 5µg plasmid pSUPER, 35µl H_2O, 2.5µl XhOI, 2.5µl BglII, 5µl Fast digest buffer (white) and let incubate at room temperature for one hour
6. Mix with Orange G, separate the digested plasmid by running a 1% Agarose gel (1 band) together with the undigested plasmid (2 or 3 bands: supercoiled)
7. Cut out the band containing the linearized plasmid (scalpel) and transfer into a 1.5ml Eppendorf tube
8. Purify the containing DNA according to the Qiagen Gel extraction kit protocol

Ligation of prepared oligos and plasmid

9. Mix 1µl of the prepared oligos, 1µl of the purified plasmid, 13µl H_2O, 2µl Ligase buffer and 2µl T4 Ligase
10. 30min, incubation, room temperature

Transformation of the ligated plasmid into chemocompetent E. coli bacteria (DH5α)

11. Thaw 100µl of E. coli preparation on ice
12. Add 10µl of the ligated plasmid
13. 30min, on ice
14. 90s, 42°C
15. 2min, on ice
16. Add 600µl of SOC medium (see below)
17. 45min, 37°C, shaking in incubator
18. Spread the whole preparation on a LB-Ampi plate
19. Incubation overnight, 37°C, saturated humidity

Mini-preparation and control of E. coli clones

20. Mix 3ml of LB medium (see below) with 3µl Ampicillin in a snap-cap falcon (several preparations)
21. Pick single clones of the bacteria plate by touching them with a pipet tip and drop into the prepared falcons
22. Incubation overnight, 37°C, shaking, saturated humidity
23. Transfer 1.5ml into a new Eppendorf tube
24. 3min, 13 000rpm, discard supernatant
25. Mini-preparation according to the QIAprep Spin Miniprep Kit protocol

26. Control the purified DNA by digestion (5µl DNA, 2µl Fast digest buffer (green), 13µl H_2O, 0.2µl of restriction enzymes XhOI and BglII in two different preparations; 30min,incubation, 37°C) and separation on a 1% Agarose Gel

Maxi-Preparation of a positive clone

27. Maxi-Preparation of a positive clone according to the QIAGEN Plasmid Plus Maxi Kit protocol
28. Validation by sequencing of the prepared DNA fragment via Eurofins (www.eurofinsdna.com)

Transfection and cultivation of stable clones

29. Transfection of cells according to the specific protocol (see above)
30. Expansion of positive clones by cultivation under G418 antibiotic selection pressure after the first day of transfection, until formation of colonies
31. Pick GFP positive colonies with a Trypsin soaked piece of Whatman paper, expansion under G418 antibiotic selection pressure
32. If necessary, repeated steps of purification for positive clones by GFP dependent cell sorting during expansion

SOC medium:

2% Trypton, 0.5% yeast extract, 10mM NaCl, 2.5mM KCl, 10mM $MgCl_2$, 10mM $MgSO_4$, 20mM Glucose

LB medium (pH 7.0):

1% Trypton, 0.5% yeast extract, 1% NaCl

Separation of cell compartments

---

1. Mix pellet of harvested cells with 1ml PBS (4°C)
2. 5min, 1 500 rpm, 4°C
3. Discard supernatant, resuspend pellet in 100µl of CLB Buffer per $1x10^6$ cells (see below, with protease inhibitors PIC and Pefa, see “Detection of protein by Western Blotting”)

4. 10min, on ice, incubation
5. 50 times douncing, on ice, transfer in new Eppendorf tube
6. Transfer 50µl in new Eppendorf tube, add 25µl SDS (3x, see “Detection of protein by Western Blotting”), heat for 1min at 95°C, freeze at -20°C (input)
7. Continue with the remaining preparation: 5min, 3 000rpm, 4°C
8. Transfer the supernatant (cytoplasm and membrane compartments) from the pellet (nuclear fraction), store the pellet on ice.
9. Continue with the supernatant: 15min, 39 000g, 4°C
10. Transfer 100µl of the new supernatant in a new Eppendorf tube, add 50µl SDS (3x), heat for 1min at 95°C, freeze at -20°C (cytoplasm)
11. Continue with the pellet from step 9: discard any remaining supernatant, resuspend the pellet in 50µl SDS (1x, corresponds to SDS 3x diluted with H_2O), heat for 1min at 95°C, freeze at -20°C (membranes)
12. Continue with the pellet from step 8: resuspend in 800µl TSE Buffer (see below, with protease inhibitors PIC and Pefa, see “Detection of protein by Western Blotting”)
13. 30 times douncing, on ice, transfer in a new Eppendorf tube
14. 5min, 3 000rpm, 4°C
15. Discard supernatant, again resuspend the pellet in 800µl TSE Buffer
16. 5min, 3 000rpm, 4°C
17. Discard supernatant, resuspend the pellet in 100µl RIPA Buffer (with protease inhibitors PIC and Pefa, and 20% SDS, see “Detection of protein by Western Blotting”), add 50µl SDS (3x), heat for 1min at 95°C, freeze at -20°C (nucleus)

CLB Buffer:

For 50ml, mix 5ml Hepes (pH 7.4), 100µl NaCl (5M), 250µl $NaHCO_3$ (1M), 20µl $CaCl_2$ (2.5M), 500µl EDTA (pH 8.0, 0.5M) and fill up to a total volume of 50ml with H_2O.

TSE Buffer:

For 50ml, mix 500µl Tris (pH 7.5, 1M), 15ml Saccharose (1M), 100µl EDTA (0.5M), 500µl NP-40 (10%), and fill up to a total volume of 50ml with H_2O.

1. Preparation: Let cells grow on covering slide (preincubated with 0.1% Gelatine for one hour); respectively, circumscribe tissue section on slide by fat pen

PFA-fixation

2. Wash with PBS
3. 20min, PFA (3%, see below) fixation, room temperature
4. Wash with PBS (three times)
5. 20min, PBS / NH_4Cl (40mM), room temperature
6. 3min, PBS / Triton X 100 (0.1%) permeabilization, room temperature
7. Wash with PBS (three times)
8. 20min, PBS / BSA (2%) blocking, room temperature

Antibody labeling

9. 1h, incubation with primary antibodies (in PBS / BSA 2%, for dilution see Table 1), room temperature
10. Wash with PBS (three times)
11. 1h, incubation with secondary antibodies (in PBS / BSA 2%, for dilution see Table 1), room temperature
12. Wash with PBS (three times)
13. Cover by a microscopic slide / covering slide and Glycerin (90%) / PBS (10%), fix cover with nail polish

PFA 3%:

Mix 3g Paraformaldehyde with 90ml PBS (pH7.4), warm to dissolve and let cool to room temperature again. Add 10µl $CaCl_2$ (1M) and 10µl $MgCl_2$ (1M). Adjust pH to 7.4 and add PBS to a total Volume of 100ml. Sterile filtration (0.4µm), store aliquots at -20°C.

Table 1: Antibody dilutions for immunofluorescence.

Primary Antibody / Staining	**Secondary Antibody**
SASH1 (“1540”, 1:200)	Anti-rabbit Alexa488 (1:300)
MACC1 (ProSci, 1:400)	
DAPI (1:1000)	none
TRITC (1:500)	none

Detection of protein by Western Blotting

Preparation of material:

1. Mix pellet of harvested cells with 1ml PBS (4°C)
2. 5min, 1 500 rpm, 4°C
3. Discard supernatant, resuspend pellet in 300µl of RIPA Buffer (with protease inhibitors, see below)
4. 15min, rotation, 4°C
5. 15min, 14 000rpm, 4°C
6. Transfer supernatant in new 1.5ml Eppendorf tube, add 150µl SDS Loading Buffer (3x, see below)
7. 1min, boiling, 95°C
8. Store at -20°C

SDS PAGE:

9. Boil sample before application (1min, 95°C), mount gel chamber, fill with Resolving and Stacking gel and Running buffer (see below)
10. 20µl of sample and 5µl of Page ruler in pocket of stacking gel, 80V until sample has reached resolving gel
11. 120V until sample has dispersed

Transfer to membrane:

12. Place the gel in a Whatman chamber and moisten with transblot buffer (see below): three layers of Whatman paper, membrane, SDS PAG, another three layers of Whatman paper
13. 45min, 20V
14. Ponceau red staining to confirm protein transfer: place membrane in Ponceau red (1min, see below), strip in water until bands become visible

Incubation and protein detection by specific antibodies:

15. 5min, shaker with 0.1% PBST / milk (5%), room temperature (repeat three times overall)
16. Primary antibody (for dilution see Table 2): incubation overnight in 0.1% PBST / milk (5%), shaker, 4°C
17. 5min, shaker with 0.1% PBST, room temperature (repeat three times overall)
18. Secondary antibody (for dilution see Table 2): incubation 1h in 0.1% PBST / milk (5%), shaker, room temperature
19. 5min, shaker with 0.1% PBST, room temperature (repeat three times overall)
20. Detection: incubate membrane with Detection Reagent 1 and 2 (prepared 1:1), 1min, room temperature
21. Dry membrane on Whatman paper, place in film chamber for 10sec up to 5min, development of film in developing machine, protein quantification by "Analyze Gels" function of ImageJ
22. Counterstaining with another antibody if needed: For stripping, incubate with Re-Blot Plus Mild Solution (10x, diluted with water 1:10), 15min, shaker, room temperature
23. Continue with step 15

RIPA-Buffer:

For 100ml RIPA-Buffer, mix 5ml TrisHCl (1M, pH 7.4), 10ml NP-40 (10%), 2.4ml Na-deoxycholate (10%), 3ml NaCl (5M), 0.2ml EDTA and fill up to a total volume of 100ml with H_2O. Adjust pH to 7.4 and store at 4°C. Directly before use, add protease inhibitors to 2ml RIPA: 20µl Pefabloc (100mg in 4ml H_2O), 10µl SDS (20%), 200µl PIC (25 tablets / 250ml in 12.5ml H_2O), 20µl Benzamidine (78mg in 5ml H_2O), PMSF 20µl (fill up 348.4mg of PMSF (100mM) to a total volume of 20ml Isopropanol), 10µl Na_3VO_4 (200mM, adjust pH 10.0, boil until colorless, cool down to room temperature, again adjust pH 10.0, again boil until colorless, cool down to room temperature), 20µl NaF (16.8mg in 4ml H_2O), 20µl β-Glyc.phos (86.4mg in 4ml H_2O), 2µl Pepstatin (5mg in 5ml Ethanol, heated to dissolve).

SDS Loading Buffer (3x):
Mix 2.4ml Tris (1M, pH 6.8), 3ml SDS (20%), 3ml Glycerol (100%), 1.6ml 2-Mercaptoethanol and a small amount of Bromphenol blue (tip of a spatula, until desired color is reached).

Stacking (5%) / Resolving (10%) gel:
3.4/1.9ml H_2O, 0.83/1.7ml Acrylamide mix (30%), 0.63ml Tris (1.0M, pH 6.8)/1.3ml Tris (1.5M, pH 8.8), 0.05/0.05ml SDS (10%), 0.05/0.05ml Ammonium persulfate (10%), 0.005/0.002ml TEMED

Running Buffer:
For 1l Running Buffer (5x), mix 30g Tris, 144g Glycin and 5g SDS and fill up to a total volume of 1l with H_2O. For 1l Running Buffer (1x), use 200ml Running Buffer (5x) and fill up to a total volume of 1l with H_2O.

Transfer Buffer (Transblot):
For 1l Transblot (10x), mix 58.15g Tris and 29.28g Glycin and fill up to a total volume of 1l with H_2O. For 500ml Transblot (1x), mix 100ml Methanol (100%), 50ml Transblot (10x) and fill up to a total volume of 500ml with H_2O.

Ponceau red solution:
For 100ml, mix 0.2g Ponceau red, 5ml Acetic acid and 95ml H_2O.

Table 2: Antibody dilutions for Western Blot.

Primary Antibody	**Secondary Antibody**
Actin (1:2 000)	Anti-mouse (1:4 000)
CDC5L (1:100)	Anti-mouse (1:4 000)
cMET (1:250)	Anti-rabbit (1:4 000)
ERK1/2 (p42/44 MAPK) (1:1 000)	Anti-rabbit (1:4 000)
GFP (1:2000)	Anti-rabbit (1:4 000)
MACC1 (Santa Cruz, 1:1 000)	Anti-goat (1:4 000)
p53 (1:20)	Anti-mouse (1:4 000)
pERK1/2 (P-p42/44 MAPK) (1:1 000)	Anti-rabbit (1:4 000)
SASH1 (“1540”, 1:200)	Anti-rabbit (1:4 000)
Tubulin (1:2 000)	Anti-mouse (1:4 000)
V5 (1:2 000)	Anti-mouse (1:4 000)
β1-Intergrin (1:2 500)	Anti-mouse (1:4 000)
β-Catenin (1:4 000)	Anti-mouse (1:4 000)

Detection of protein-protein interactions by Immunoprecipitation

1. Harvest material as described for Western Blot analysis (“Preparation of material”, steps 1 to 5)
2. Transfer 50µl of the supernatant to a new Eppendorf tube, add 25µl of SDS (3x), boil for 1min, 95°C, store at -20°C (positive control)
3. Add 1.5µl of antibody to 400µl of the remaining supernatant (two preparations: specific antibody and negative/isotype control)
4. 2h, incubation (rotation), 4°C
5. Prepare beads (Sepharose G for SASH1 and MACC1): 120µl per IP, wash with PBS (once) and RIPA-Buffer (twice)
6. Add beads to the lysate-antibody-solution, 1h incubation (rotation), 4°C
7. Wash with 1ml RIPA three times (centrifuge down after each washing step)
8. Add 60µl SDS (1x: SDS 3x diluted in H_2O)
9. 1min, boiling, 95°C
10. Store at -20°C

Determination of cell proliferation by XTT assay

1. Seed 0.5 x10^4 cells in 200µl media (0.5% FCS) in a 96-well plate
2. Incubation, overnight, saturated humidity, 37°C
3. Prepare 6ml XTT labeling reagent and mix with 100µl electron coupling reagent for one 96-well plate
4. Add 10.2ml media (3% FCS) to the preparation
5. Pipet 150µl in every well of a 96-well plate
6. Measurement of cell proliferation by time dependent change of absorption (wave length 450-500nm, reference 650nm, filter B)

Determination of cell migration by wound healing assay

1. Pretreatment of cells with Mitomycin C (0.625 µg/ml) to block cell invasion: 2.5h incubation, saturated humidity, 37°C
2. Wash with PBS (three times), harvest cells

3. Seed 1x10^5 cells in both fields of migration chamber, fill up both fields to 70µl with media, add 1ml media outside of the fields
4. Overnight incubation, saturated humidity, 37°C
5. Remove migration chamber by forceps
6. Replace media after washing with 2ml DMEM once
7. Photo documentation of time dependent cell migration into migratory space

4.2 Patient tissue and data

Surgical specimen collection

Human tissue was collected from operations between 1987 and 2012 and stored at the Surgical Department of the Klinikum rechts der Isar. Approved by the ethics committee of the Klinikum rechts der Isar (no. 1926/7), the samples were obtained after prior informed written patient consent. Tumor samples were obtained usually within one hour after surgical resection by a trained pathologist or surgeon and immediately transferred into liquid nitrogen. Specimens were then stored at -80°C until further processing. Histology-guided sample selection[134] was performed to ensure a sufficient amount of tumor cells (more than 30%) or normal tissue.

Patient data and follow-up

Clinical and histopathological data of all patients were prospectively collected and documented in an Excel list. After transferring in a Macro-based database, clinical records were updated continuously.[99] Follow-up data was obtained by reviewing medical reports, the documentation system of the Klinikum rechts der Isar and demographical data of the Tumorzentrum München. Patients with insufficient documented follow-up data were contacted by telephone or via their attending doctors. Distant metastasis free survival was defined as the primary end point for survival analysis.

4.3 Statistical analysis

All repeatable experiments were carried out in at least three independent procedures. Statistical evaluation was performed using SPSS. For descriptive analysis, the number or relative frequency in percent is indicated. Quantitative data are reported as mean±standard deviation, respectively median and range. The distribution of nominal or ordinal scaled variables was compared using Pearson's chi-squared test. Cardinal variables were tested for normal distribution by the Kolmogorov-Smirnov test. For further explorative comparison of independent groups, the t test (for normal distribution) or Mann-Whitney U (for non-normal distribution) was used. All statistical tests were performed two-sided, and *p*-values less than 0.05 were considered to be statistically significant. No correction of *p*-values was applied to adjust for multiple test issue. However, results of all statistical tests being conducted were thoroughly reported so that an informal adjustment of *p*-values can be performed while reviewing the data.[104]

In order to derive optimal cut-off values of gene expression levels, maximally selected log-rank statistics performed by R Software were used. To consider multiple test issue within these analyses, the R-function *maxstat.test* was employed.[50]

Time-dependent patient survival probabilities were estimated with the Kaplan-Meier method, and the log-rank test was used to compare independent subgroups. Recurrence-free patient survival (i.e., distant metastasis-free survival) was considered as primary end point. To investigate the effect on survival of multivariable relationships among covariates, Cox proportional hazard models were used. Recurrence-free survival times as well as estimated hazard ratios (HRs) were calculated and reported in 95% confidence intervals (95% CIs).

Multivariable analysis of binary outcome data was assessed by logistic regression. A post-hoc power analysis using N-Query Software revealed that with the total number

of 22 distant-recurrent cases in the stage II cohort, hazard ratios of ≥3.2 were detectable with a type-2 error ≤20% (power 80%) at a two-sided level of significance of 5%, when using a log-rank test. For purpose of illustration and clinical applicability, a nomogram was created based on the final regression model (using the 'nomogram' function from Frank E Harrell Jr (2008). Design: Design Package. R package version 2.1-2. http://biostat.mc.vanderbilt.edu/s/Design, http://biostat.mc.vanderbilt.edu/rms). In this figure, model-based score points are displayed for each predictor variable category, which have to be summarized for any individual patient. For the resulting total number of points, the corresponding predicted survival probabilities can be read from the nomogram.

Area-under-curve [98] values were calculated by time-dependent receiver operating-characteristic (ROC) analyses for censored survival data. To calibrate calculated AUC values and therefore to correct for over optimism in the estimated model performance, the R function *validate.cph* employing enhanced bootstrap was used.[48] The Bayesian Information Criterion[90] was used to assess the overall prognostic performance of the different classification systems via bootstrap-resampling analysis.

Clustering of patients into different groups was performed by the SPSS Hierarchical Cluster and Two-step Cluster analysis function.

Decrease of mRNA after treatment with Actinomycin D was quantified by rtPCR and the relative reduction of mRNA transcripts was indicated, based on previous illustrations.[2] Assuming that C_t^x means the C_t value at a specific point of time, C_t^0 means the C_t value without treatment, and a rise of the C_t value of one cycle means a reduction of the quantity of RNA of 50%, it was calculated by the formula

$$\text{mRNA reduction in per cent} = \frac{100\%}{2^{C_t^x - C_t^0}}$$

.

5 Results

5.1 Part I: Molecular genetic characterization of colon cancer samples

5.1.1 Feasibility of biomarkers for risk prediction in disease stage II

Patient cohort

This work is based on the hypothesis that the integrative analysis of a biomarker panel may allow identification of colon cancer patients with a high risk of disease recurrence. This high-risk subgroup remains hitherto ill-defined in molecular genetic and clinical terms. Therefore, tumor tissue from 232 patients with histopathologically confirmed stage II colon cancer was selected for this project for subsequent analysis. All patients underwent complete surgical resection (R0), and the median of histologically reviewed lymph nodes per patient was 21 (range 7-72), implying an adequate nodal negative staging. The median follow-up was 97 months (range 39-210). Additionally, samples of histologically confirmed normal colon mucosa from resected specimen (n=11) were analysed to provide reference calibrators. None of the patients received neoadjuvant treatment. Ten patients with T4 tumors underwent adjuvant chemotherapy because of tumor perforation or invasion into other organs. Patient characteristics are shown in Table 3. Five patients developed local recurrence and were excluded from the study prior to analysis since this recurrence may have been a result of residual disease rather than metastatic tumor.[61] "Metachronous metastasis" was defined as distant organ metastases during follow-up (>30 days post-surgery). Median time to diagnosis of metastasis was 29 months. All patients with recurrence had metachronous metastasis, in liver (n=8), lung (n=5), or in both liver and lung (n=9). Two patients had peritoneal carcinomatosis. Brain

metastasis or involvement of the bladder and ovary were observed in one patient, respectively. No metachronous tumors were found in the colon or rectum.

Table 3: Clinical characteristics of all investigated patients with stage II colon cancer.

Category	Specification	Patients	
		232	(100%)
Sex	Male	132	(57%)
	Female	100	(43%)
Age (years, median)		66	(range 15-91)
Location	Right colon	124	(53%)
	Left colon	108	(47%)
T	T3	197	(85%)
	T4a	16	(7%)
	T4b	19	(8%)
Lymphatic invasion (L)	L0	208	(90%)
	L+	24	(10%)
Angioinvasion (V)	V0	226	(97%)
	V+	6	(3%)
Grading (G)	G1-2	159	(69%)
	G3-4	73	(31%)
Recurrence	No recurrence	210	(91%)
	Distant metastasis	22	(9%)

Analysis of nucleic-acid based molecular markers

Genomic DNA was extracted from all 232 tumors. Oncogenic mutations in exon 2 of KRAS and in exon 15 of BRAF were detected by High resolution melting (HRM) analysis.[7] KRAS and BRAF mutations were identified in 70 samples (30%), respectively in 35 samples (15%). KRAS and BRAF mutations were mutually exclusive. Normal mucosal control tissue of 11 patients harbored no KRAS or BRAF mutations (Figure 10). HRM analysis is a feasible method to detect mutations in double-stranded DNA and was therefore established in the laboratory prior to characterization of the patient cohort. After PCR-amplification of the potentially mutated DNA fragments, a real-time monitored melting curve was performed with an intercalating saturating DNA dye.[127] Shifts of the normalized melting curve allowed detection of mutations in the genomic DNA. By cell line experiment with known mutational status, the distinction of amplicons differing in a single base was

confirmed, and by serial dilution experiments, a still reliable detection of 5% mutated DNA was confirmed (Figure 9). Further validation of the HRM method by pyrosequencing in a subgroup of 118 randomly selected samples revealed highly congruent results, with 92%, 95%, and 93% consistency for KRAS, BRAF, and overall, respectively (Table 4 and Table 5).[7]

Figure 9: Dilution series of mutated and wild type DNA for determination of sensitivity of HRM. Differences of the melting curve behavior allowed reliable detection of (a) KRAS and (b) BRAF mutations down to a content of 5% mutated DNA.

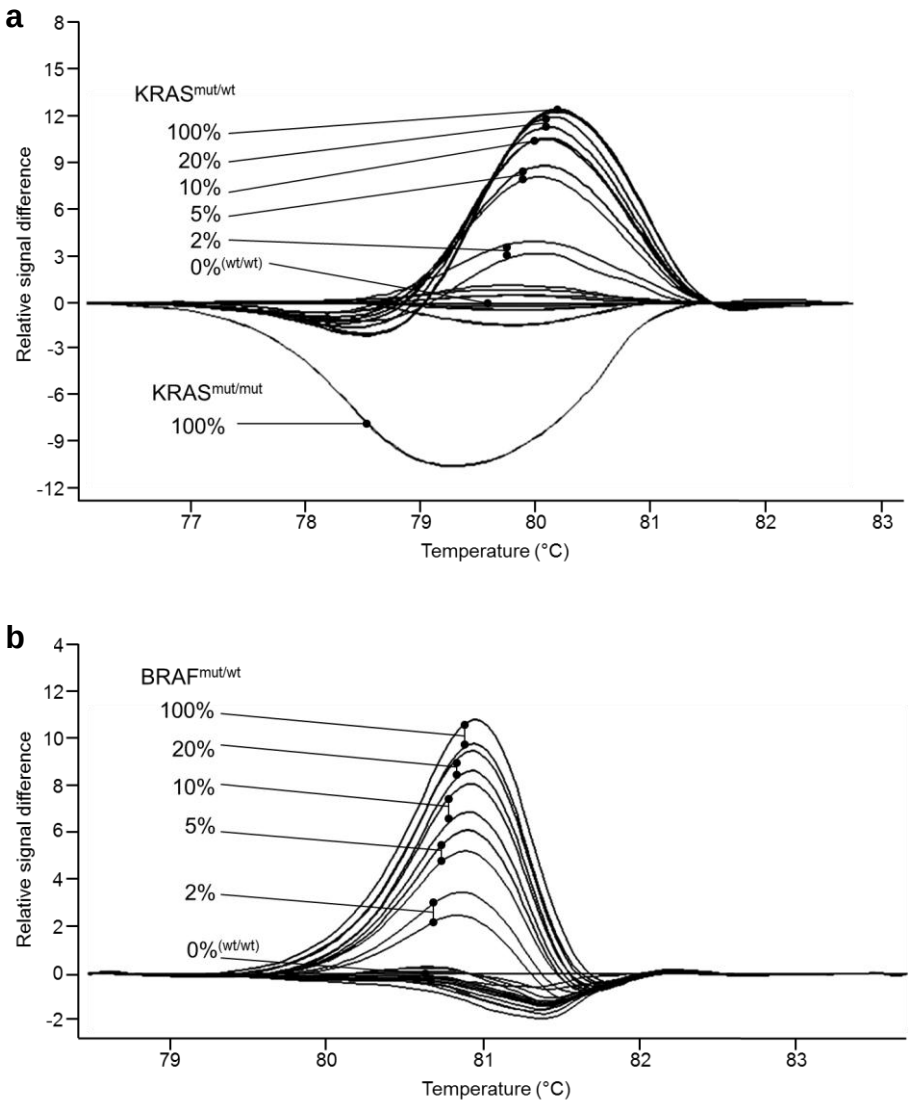

Table 4: Comparison of High resolution melting and pyrosequencing results regarding KRAS mutational status. The numbers indicate the patients in each group.

		Result HRM		
		wt	**mut**	
Result pyrosequ.	wt	78	0	78
	mut	10	30	40
		88	30	118

Table 5: Comparison of High resolution melting and pyrosequencing results regarding BRAF mutational status. The numbers indicate the patients in each group.

		Result HRM		
		wt	**mut**	
Result pyrosequ.	wt	95	0	95
	mut	6	17	23
		101	17	118

Analysis of microsatellite instability was performed by Prof. Dr. rer. nat. Gisela Keller, department of Pathology, Technische Universität München, according to a standard panel of five Bethesda microsatellite markers also used for routine clinical diagnosis.[79] High-grade microsatellite instability occurred in 26% (MSI-H, 61 patients). All other tumors and normal mucosal control tissues of 11 patients were microsatellite stable (MSS). No-low grade microsatellite instability (MSI-L) was detected (Figure 10).

Figure 10: Proportion of patients with (a) mutations in KRAS, (b) mutations in BRAF, and (c) microsatellite instable (MSI-H) tumors. 11 normal colon mucosa samples were analyzed as reference.

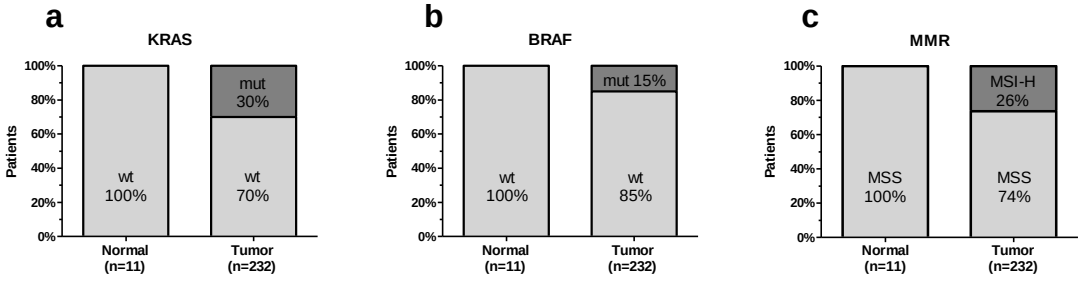

Next, RNA was extracted from all samples for expression analysis. RNA integrity was monitored in a semi quantitative fashion by denaturing gel electrophoresis and

monitoring rRNA 18S- and 28S-subunit bands for each sample (Figure 11). Overall, 53 samples were excluded and RNA of the remaining 179 patients was transcribed into cDNA. Clinical characteristics of this subgroup did not differ significantly from the whole patient group (Table 6).

Figure 11: Representative results of RNA gel electrophoresis.#1 indicates a degraded RNA sample, while #2 and #3 are of high integrity with clear 18S and 28S bands.

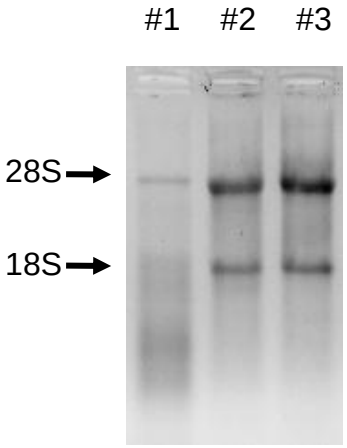

Table 6: Characteristics of the subgroup of 179 patients with RNA of high integrity.

Category	Specification	Patients	
		179	(100%)
Sex	Male	103	(58%)
	Female	76	(42%)
Age (years, median)		66	(range, 15-91)
Location	Right colon	102	(57%)
	Left colon	77	(43%)
T	T3	153	(85%)
	T4a	13	(7%)
	T4b	13	(7%)
Lymphatic invasion (L)	L0	161	(90%)
	L+	18	(10%)
Angioinvasion (V)	V0	173	(97%)
	V+	6	(3%)
Grading (G)	G1-2	123	(69%)
	G3-4	56	(31%)
Recurrence	No recurrence	161	(90%)
	Distant metastasis	18	(10%)

Compared to control mucosa from 11 patients, gene expression of the candidate tumor suppressor SASH1 was significantly downregulated in tumor tissue (relative mean expression decreased 1.95 fold, $p<0.001$), whereas transcripts of the Wnt pathway surrogate marker Osteopontin and the metastasis-associated gene MACC1 were upregulated (relative mean expression Osteopontin: increased 3.74 fold, $p<0.001$, relative mean expression MACC1: increased 4.68 fold, $p<0.001$, Figure 12).

Figure 12: Gene expression levels of (a) Osteopontin and (c) MACC1 were significantly increased in tumor tissue compared to normal mucosa, whereas (b) expression levels of the candidate tumor suppressor gene SASH1 were decreased. 11 normal colon mucosa samples were analyzed as reference. The boxes indicate the 25th, 50th, and 75th percentiles. The whiskers include values within 1.5 interquartile ranges (Tukey). The t test for independent samples has been performed.

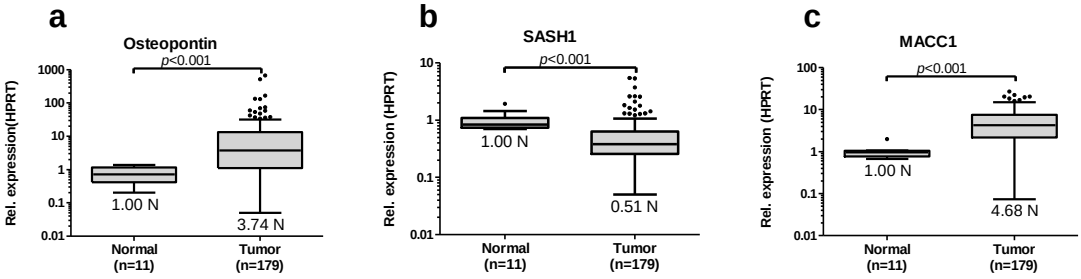

Moreover, Osteopontin was validated *in vitro* for its association with activation of the canonical Wnt pathway, either by siRNA-mediated knockdown of the tumor suppressor APC (Figure 6), or by pharmacological inhibition of the protein kinase GSK, a central component of the "destruction complex" with Lithium chloride. In both cases, significant upregulation of Osteopontin expression was found, in line with earlier observations (APC data from Dr. Melanie Martini and Alexandra Gnann, Figure 13).[96]

Figure 13: Expression levels of Osteopontin. This experiment was carried out in a non-tumor derived cell line (Hek293) with no previous activating mutations in the Wnt pathway, and the results confirm the usefulness of Osteopontin expression to serve as a surrogate marker for activation of the canonical Wnt pathway. (a) Increased Osteopontin mRNA expression levels 24 hours and 48 hours after APC knockdown by siRNA. Transfection with scrambled control siRNA did not lead to significant changes in Osteopontin expression (not shown). (b) Increased Osteopontin expression was detected after Lithium chloride treatment for 24 hours (20mM). Lithium chloride inhibits the Glycogen synthase kinase 3β, leading to increased β-Catenin levels and thus enhanced transcription of Wnt target genes. Results of at least three independent experiments are shown. The boxes indicate the 25th, 50th, and 75th percentiles. The whiskers include values within 1.5 interquartile ranges (Tukey). The t test for independent samples has been performed.

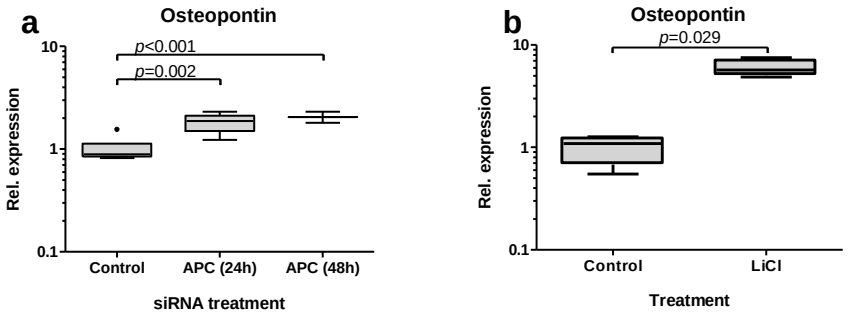

Correlation of individual biomarkers

Microsatellite instable tumors occurred preferentially in patients with BRAF mutation (24 of the 35 BRAF mutated patients, $p<0.001$), and were located in the right colon in 85% of the cases (52 of 61, $p<0.001$). Accordingly, right-sided tumors were more likely for BRAF mutation ($p<0.001$). Microsatellite instability ($p=0.009$) and BRAF mutation ($p<0.001$) occurred more frequently in female patients. These findings are in accordance with large datasets reported earlier, and confirm that the collective analyzed here is in good accordance with the general patient population.[66] MACC1 has previously been described as a metastasis-associated gene.[33, 112, 117] However, limited data are available regarding its interactions with other genetic markers. Patients with microsatellite instable tumors ($p<0.001$) or BRAF mutation ($p=0.039$) had significantly reduced MACC1 expression levels. Interestingly, there was an inverse correlation of the expression levels of SASH1 and MACC1 ($p=0.006$). Furthermore, high Osteopontin expression levels were associated with microsatellite

instability (p=0.005) and increased SASH1 expression (p=0.023). A comprehensive list of all apparent associations including clinical data is shown in Table 7.

Table 7: Correlation of molecular and clinical parameters. The upper number in each box indicates the correlation coefficient (Spearman's rho). Negative values reflect inverse correlations. The lower number depicts the corresponding p-value. Significant correlations are highlighted by gray shading.

	KRAS (mutated)	BRAF (mutated)	MMR (MSI-H)	Osteopontin (continuosly)	SASH1 (continuosly)	MACC1 (continuosly)	Sex (female)	Age (continuosly)	Location (left)	T status (high)	L status (positive)	V status (positive)	Grading (G3-4)	Distant metastasis
KRAS (mutated)		**-0.277** **<0.001**	-0.73 0.271	-0.080 0.289	-0.135 0.071	0.071 0.343	-0.098 0.136	-0.097 0.140	-0.124 0.059	-0.056 0.392	-0.100 0.129	-0.048 0.467	0.040 0.545	**0.140** **0.033**
BRAF (mutated)	**-0.277** **<0.001**		**0.405** **<0.001**	0.103 0.170	-0.064 0.389	**-0.154** **0.039**	**0.217** **0.001**	**0.184** **0.005**	**-0.297** **<0.001**	-0.044 0.507	-0.064 0.331	0.007 0.913	0.026 0.698	-0.054 0.411
MMR (MSI-H)	-0.73 0.271	**0.405** **<0.001**		**0.207** **0.005**	-0.060 0.427	**-0.310** **<0.001**	**0.172** **0.009**	-0.009 0.886	**-0.381** **<0.001**	0.082 0.211	-0.042 0.523	0.026 0.693	**0.186** **0.005**	**-0.160** **0.015**
Osteopontin (continuosly)	-0.080 0.289	0.103 0.170	**0.207** **0.005**		**0.170** **0.023**	0.081 0.281	**0.148** **0.049**	0.044 0.557	-0.107 0.152	0.027 0.719	-0.014 0.852	0.078 0.299	0.040 0.596	-0.069 0.356
SASH1 (continuosly)	-0.135 0.071	-0.064 0.389	-0.060 0.427	**0.170** **0.023**		**-0.203** **0.006**	-0.061 0.416	-0.042 0.578	0.106 0.158	0.114 0.130	-0.044 0.555	0.093 0.218	0.068 0.364	-0.003 0.970
MACC1 (continuosly)	0.071 0.343	**-0.154** **0.039**	**-0.310** **<0.001**	0.081 0.281	**-0.203** **0.006**		0.065 0.385	-0.001 0.993	0.099 0.188	0.004 0.960	0.027 0.720	0.057 0.448	-0.029 0.699	**0.179** **0.016**
Sex (female)	-0.098 0.136	**0.217** **0.001**	**0.172** **0.009**	**0.148** **0.049**	-0.061 0.416	0.065 0.385		**0.078** **0.238**	**-0.202** **0.002**	-0.025 0.706	-0.038 0.560	-0.032 0.626	0.085 0.197	**-0.133** **0.043**
Age (continuosly)	-0.097 0.140	**0.184** **0.005**	-0.009 0.886	0.044 0.557	-0.042 0.578	-0.001 0.993	0.078 0.238		**-0.134** **0.041**	-0.002 0.977	0.013 0.846	0.077 0.243	**0.139** **0.034**	-0.095 0.151
Location (left)	-0.124 0.059	**-0.297** **<0.001**	**-0.381** **<0.001**	-0.107 0.152	0.106 0.158	0.099 0.188	**-0.202** **0.002**	**-0.134** **0.041**		**0.138** **0.036**	0.023 0.722	-0.043 0.513	**-0.130** **0.048**	-0.037 0.579
T status (high)	-0.056 0.392	-0.044 0.507	0.082 0.211	0.027 0.719	0.114 0.130	0.004 0.960	-0.025 0.706	-0.002 0.977	**0.138** **0.036**		**0.134** **0.041**	0.082 0.214	0.004 0.956	0.064 0.328
L status (positive)	-0.100 0.129	-0.064 0.331	-0.042 0.523	-0.014 0.852	-0.044 0.555	0.027 0.720	-0.038 0.560	0.013 0.846	0.023 0.722	**0.134** **0.041**		**0.212** **0.001**	0.044 0.503	**0.132** **0.045**
V status (positive)	-0.048 0.467	0.007 0.913	0.026 0.693	0.078 0.299	0.093 0.218	0.057 0.448	-0.032 0.626	0.077 0.243	-0.043 0.513	0.082 0.214	**0.212** **0.001**		0.065 0.324	0.040 0.545
Grading (G3-4)	0.040 0.545	0.026 0.698	**0.186** **0.005**	0.040 0.596	0.068 0.364	-0.029 0.699	0.085 0.197	**0.139** **0.034**	**-0.130** **0.048**	0.004 0.956	0.044 0.503	0.065 0.324		0.002 0.970
Distant metastasis	**0.140** **0.033**	-0.054 0.411	**-0.160** **0.015**	-0.069 0.356	-0.003 0.970	**0.179** **0.016**	**-0.133** **0.043**	-0.095 0.151	-0.037 0.579	0.064 0.328	**0.132** **0.045**	0.040 0.545	0.002 0.970	

Biomarker correlation with patient prognosis and survival

In order to test the working hypothesis underlying this study, the candidate biomarkers were analyzed for their usefulness as prognostic parameters. Five-year recurrence free survival for the entire patient group was 91±2% (mean±standard deviation). Distant metastases were more likely in male patients (p=0.040, log rank) and, as expected, in patients with lymphatic vessel invasion (L+, p=0.042, log rank). KRAS mutation was associated with distant metastases in general (p=0.033, chi square, Table 7). However, the time-dependent metastasis risk for KRAS-mutant

patients was not significantly elevated upon Kaplan-Meier analysis (p=0.062, log rank, Figure 15). BRAF status did not correlate with the risk of metastasis (p=0.447, log rank). In accordance with published findings, patients with microsatellite instable tumors had increased metastasis free survival rates (p=0.017, log rank). In contrast to discrete or categorical parameters (e.g., mutated or wild-type), the measured expression values for Osteopontin, MACC1 and SASH1 are of a continuous type. For practical reasons, threshold (or cut-off) values were determined by maximally selected log rank statistics (Figure 14). This analysis revealed no prognostic effect for the Wnt-surrogate marker Osteopontin expression, whereas downregulation of the tumor suppressor SASH1 was associated with poor prognosis. Interestingly, increased SASH1 expression may have a protective effect, since patients with intratumoral SASH1 expression elevated more than 0.96 fold compared to normal mucosa did not develop distant metastases (n=29, p=0.049, log rank). Figure 15 depicts the Kaplan-Meier curves for recurrence free survival, indicating the risk of distant metastasis.

Figure 14: Cut-off determination for (a) Osteopontin, (b) SASH1 and (c) MACC1 using maximally selected log-rank statistics. Time dependency of the events was considered for this calculation.

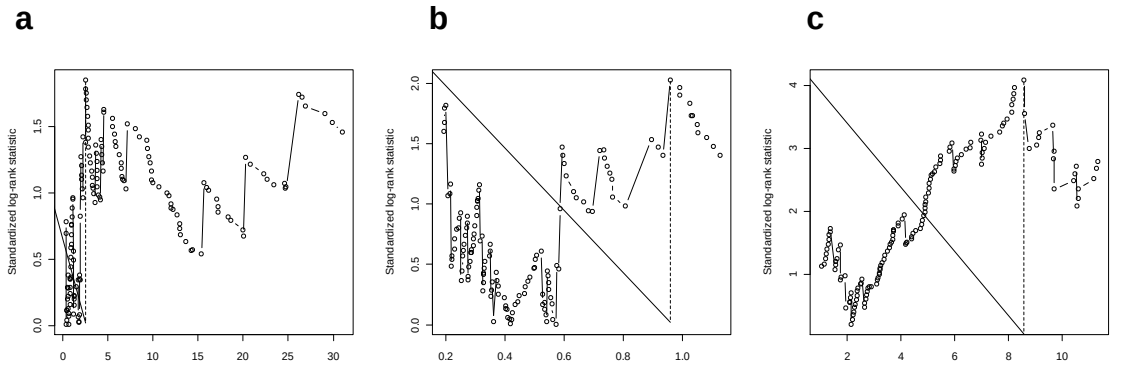

Figure 15: Distant metastasis free survival as a function of the mutational status of (a) KRAS, (b) BRAF, (c) mismatch repair (MMR) status, and of expression levels higher or lower than the calculated cut-off values for (d) Osteopontin, (e) SASH1 and (f) MACC1. Kaplan-Meier *p*-values refer to log rank (Mantel Cox) statistics.

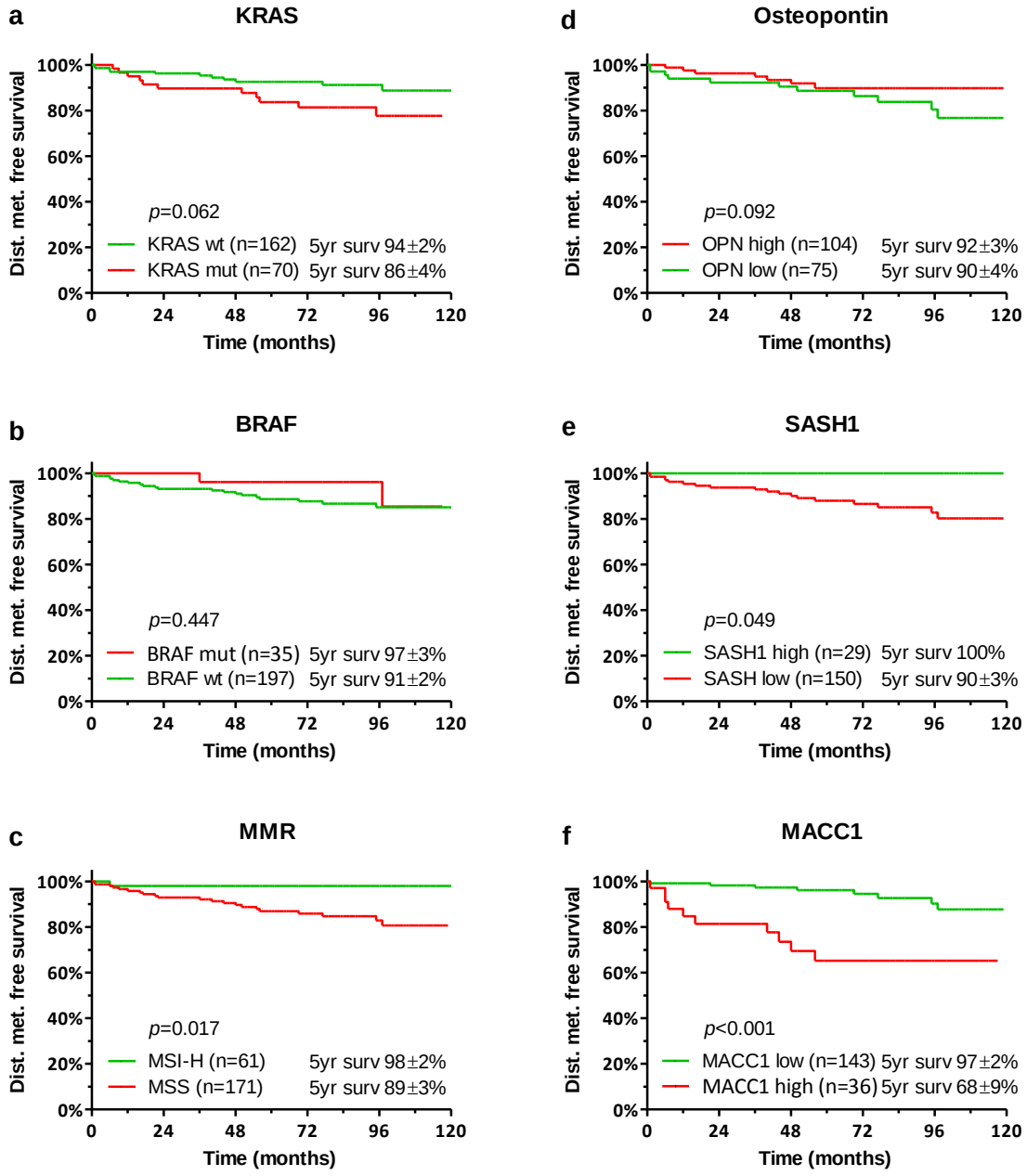

MACC1 overexpression was the only biomarker in the panel tested here which was highly significantly associated with occurrence of distant metastases ($p<0.001$, log rank). The hazard ratio for patients with over-threshold expression of MACC1 was 6.2 (95% CI 2.4–16; $p<0.001$) for development of metachronous metastasis. Based

on this cut-off value of MACC1 expression, sensitivity was 55.6% and specificity was 83.9% (Table 8).

Table 8: Prognostic characteristics for the MACC1 cut-off value. The numbers of patients in the particular groups are indicated. Sensitivity indicates the likelihood to identify a high risk patient, Specificity indicates the likelihood to identify a low risk patient, Negative predictive value (NPV) indicates the likelihood that a patient identified as low-risk does not develop metastasis, Positive predictive value (PPV) indicates the likelihood that a patient identified as high-risk does develop metastasis, and Accuracy indicates the percentage of patients stratified correctly into high or low risk.

	No metastasis	Metastasis		
MACC1 low	135	8	143	NPV 94.4% $\left(\frac{135}{143}\right)$
MACC1 high	26	10	36	PPV 27.8% $\left(\frac{10}{36}\right)$
	161	18	179	
	Specificity 83.9% $\left(\frac{135}{161}\right)$	Sensitivity 55.6% $\left(\frac{10}{18}\right)$		Accuracy 81.0% $\left(\frac{135+10}{179}\right)$

Multivariable analysis and risk assessment

Upon multivariable analysis of the six molecular markers, MACC1 expression remained the only independent parameter predicting distant metastasis (Table 9). Importantly, essentially the same results were obtained when the 10 patients receiving chemotherapy were excluded from analysis. Furthermore, removing or including established clinical factors resulted in no substantial improvement of the multivariable Cox regression model (not shown). The results of risk prediction by the molecular markers obtained in the multivariable model can be visualized in a nomogram, which allows estimating the weight of each parameter (Figure 16). Due to the lacking prognostic power of Osteopontin, it was omitted to avoid distortion of the results.

Table 9: Multivariable analysis including clinical factors and molecular markers. MACC1 remained the only independent parameter predicting the risk of developing metachronous metastasis (a) for all patients, (b) without relevant changes after exclusion of n=10 patients who were treated with chemotherapy due to T4 tumors or tumor perforation. Asterisks (*) highlight parameters that were analyzed continuously. The hazard ratio (HR) of 1.01 for MACC1 relies on the continuous measurement scale of MACC1 and describes the risk increment per one-unit change of MACC1. A difference in MACC1 expression of, e.g., 5 units is therefore associated with an estimated risk increase of 1.05 (5%).

	a		95% CI		**b**		95% CI	
	p	HR	Lower	Upper	*p*	HR	Lower	Upper
Sex (female)	0.185	0.48	0.16	1.43	0.343	0.58	0.19	1.78
Age*	0.059	0.96	0.91	1	0.055	0.96	0.91	1.00
Location (left)	0.052	3.65	0.99	13.4	0.07	0.28	0.7	1.11
T3		1				1		
vs. T4a	0.056	0.19	0.03	1.04	0.224	3.52	0.46	26.8
vs. T4b	0.819	0.79	0.11	5.96	0.431	2.44	0.27	22.4
Lymph. (L+)	0.199	0.41	0.11	1.6	0.123	2.98	0.75	11.9
Angio. (V+)	0.498	2.83	0.14	57.4	0.686	0.54	0.03	11.0
Grading (G3-4)	0.520	0.69	0.22	2.17	0.941	1.05	0.28	3.94
KRAS (mut)	0.636	1.34	0.40	4.44	0.461	1.62	0.45	5.85
BRAF (mut)	0.750	1.32	0.24	7.26	0.592	1.62	0.28	9.52
MMR (MSI-H)	0.061	0.11	0.01	1.10	0.110	0.15	0.02	1.53
Osteopontin*	0.334	1	0.99	1	0.334	0.98	0.93	1.03
SASH1*	0.459	0.9	0.69	1.18	0.651	0.75	0.22	2.56
MACC1*	0.006	1.01	1	1.02	0.012	1.15	1.03	1.28

Figure 16: Nomogram for integrative metastasis free survival risk assessment, including the molecular parameters that were relevant for prediction of prognosis. To obtain an individual patient's score, a straight line is drawn from each marker scale to the axis, yielding a point score. SASH1 and MACC1 refer to expression values relative to normal mucosa. The points gained from analysis of each prognostic variable are summed up, and this number is then indicated on the total points axis. Next, a straight line is drawn down from the total points to the estimated survival probability to ascertain the patient's specific risk.

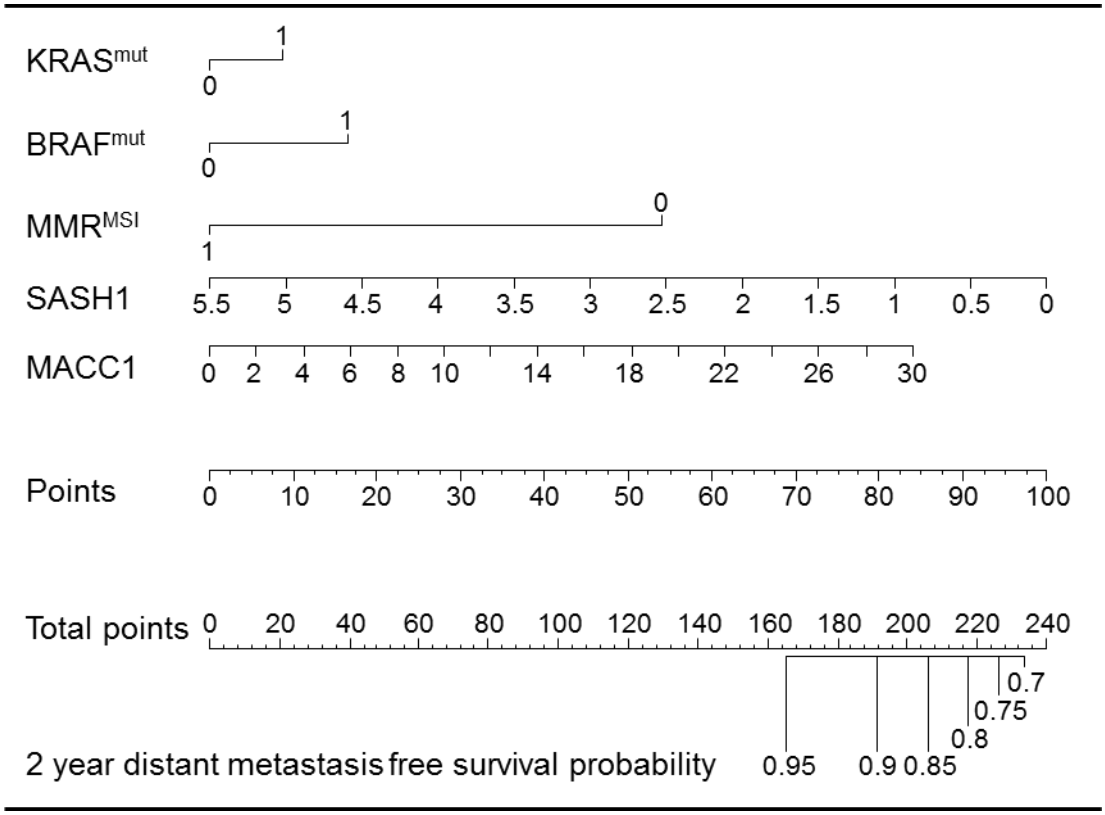

When analyzing the time-dependent area under the curve[98], an integrative model containing the molecular markers revealed a continuously higher prognostic impact than a model based on clinical factors, even though this difference did not attain significance (Figure 17). Further, the AUC obtained by analysis of MACC1 alone was slightly, but not significantly lower than by the integrative molecular marker model containing additionally KRAS, BRAF, MMR, Osteopontin, and SASH1 (data not shown). Cross-validation via enhanced bootstrap method was performed to provide unbiased estimates of prediction error. Therefore, the AUC values are corrected for over-optimism and represent confident estimates for the true underlying discriminative ability of the respective prediction model.

Figure 17: Comparison of the prognostic impact of the analyzed molecular markers (KRAS, BRAF, MMR, Osteopontin, SASH1, MACC1) and clinical factors (patient sex, age, tumor location, T stage, lymphatic invasion, angioinvasion, grading). Time-dependent calibrated areas under the receiver operating curves[98] illustrate a slight advantage of the molecular markers over the clinical factors.

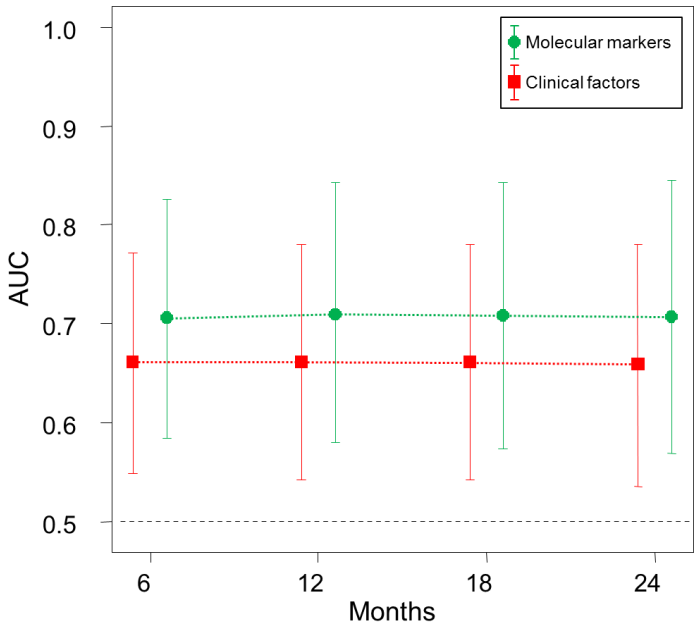

Finally, the prognostic performance of MACC1 alone was compared with the performance of the multivariable molecular marker model using the Bayesian Information Criterion.[90] BIC is a measure of the goodness of fit of an estimated statistical model. In contrast to AUC, it accurately considers the number of parameters included in the model.[82] In return, no absolute values are obtained but solely a relative comparison of different models against each other is possible. With delta BIC = 15.1 (95% CI 1.92-22.9; p<0.001), there was a significant advantage for the multivariable model over risk prediction by MACC1 alone.

Molecular subgroups with distinct risk profiles

Allocation of patients into molecular genetic cohorts should coincide with different risk groups. In order to test this hypothesis, a hierarchical cluster was created, which defined different groups of patients depending on their molecular tumor characteristics and development of metastasis. However, the visualization of group

relations by a dendrogram did not show a clear relation between the analyzed molecular markers and the recurrence risk (Figure 18).

Figure 18: Hierarchical cluster analysis. Horizontal distances in the dendrogram tree depict the level of analogy between individual clusters. Patients with recurrent disease are scattered throughout the whole cohort. Red: high Osteopontin and MACC1 expression/low SASH1 expression/MSS/mut/recurrence; green: low Osteopontin and MACC1 expression/high SASH1 expression/MSI-H/wt/no recurrence.

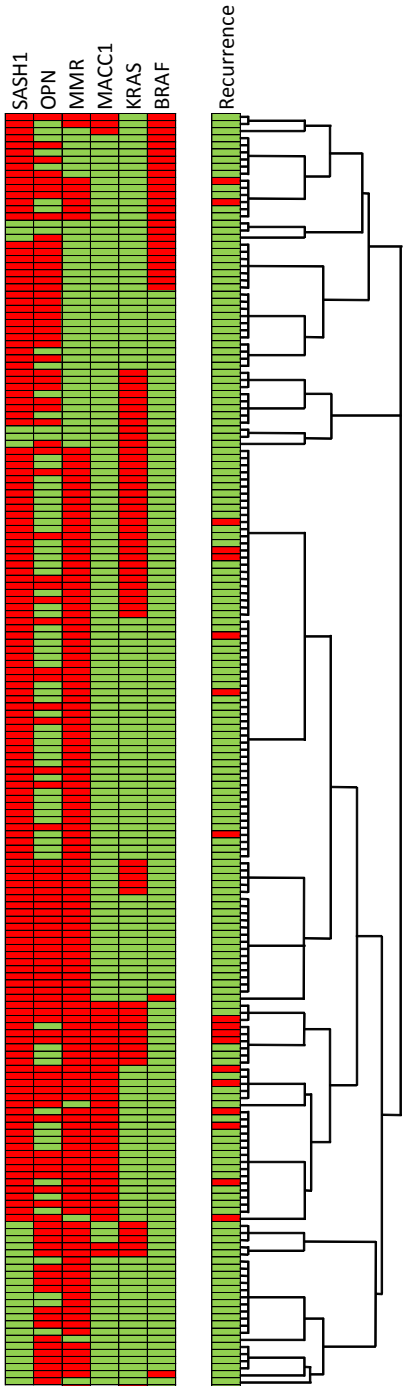

In a next approach, a two-step cluster analysis was performed. It determines the number of existing clusters automatically and allows the integration of both, continuous and categorical variables (Table 10). According to their genetic profile, and in concordance with previously described colorectal cancer pathways[66], four patient cohorts with different risk of recurrence were identified. However, differences in prognosis between the groups did not attain significance due to relatively small sample size (p=0.344, log rank test). Microsatellite instable tumors were preferably located in the right colon, often associated with a BRAF mutation, and had a favorable prognosis. The recurrence rate for this group was 6% (4% for BRAF wild type, cluster #1, and 7% for BRAF mutated, cluster #2).[17, 66] Patients with low MACC1 expression levels were grouped in clusters #1 and #2. Cluster #3 comprised microsatellite stable patients with no mutation of KRAS or BRAF. No obvious alterations other than elevated expression of the tumor suppressor gene SASH1 were detected in this cluster. The patients had an intermediate recurrence risk of 10%. Patients with KRAS mutation (cluster #4) had the highest recurrence risk (16%). Clusters #3 and #4 contained the patients with high MACC1 expression levels. Taken together, two-step cluster analysis classifies patients according to their genetic alterations and their resulting risk profiles.

Table 10: Two-step cluster analysis. Depending on their molecular signature, four groups of patients were identified. The descending order of the markers reflects the assumed significance of the predictor. Upward arrows indicate high (↑), respectively very high (↑↑) expression; downward arrows indicate low (↓), respectively very low (↓↓) expression. *15 of 26; **17 of 27.

Cluster Size	#1 n=26	#2 n=27	#3 n=83	#4 n=43
BRAF	wt (100%)	mut (100%)	wt (100%)	wt (100%)
KRAS	wt (58%)*	wt (100%)	wt (100%)	mut (100%)
MMR	MSI-H (100%)	MSI-H (63%)**	MSS (100%)	MSS (100%)
MACC1 expr.	↑	↑	↑↑	↑↑
SASH1 expr.	↓↓	↓↓	↓	↓↓
OPN expr.	↑↑	↑↑	↑	↑
Risk of distant metastasis	4% (1/26)	7% (2/27)	10% (8/83)	16% (7/43)
	6% (3/53)		12% (15/126)	
	10% (18/179)			

5.1.2 Molecular changes during the development of metastasis

In the previous part of this work, the aim was to gain prognostic information by molecular analysis of primary tumors. However, due to intratumoral heterogeneity and possible clonal selection during the presumably long metastatic process, disseminated cancer cells may actually differ substantially from the primary tumor. Therefore, it would be crucial to directly compare the panel of candidate biomarkers analyzed here in primary tumors and their matched metastasis. For nine patients (colon cancer, n=6 and rectal cancer, n=3), corresponding tissue of normal mucosa, primary tumor and liver metastases was analyzed for the markers discussed above (KRAS, BRAF, MMR, Osteopontin, SASH1, MACC1). All nine primary tumors were T3-4 N+ M1 G2-3. One patient with colon cancer underwent resection of liver metastases in a second approach after initial surgery of the primary tumor.

KRAS mutations were detected in five primary tumors (56% of patients), together with their corresponding liver metastases. A BRAF mutation was found in one primary tumor (11% of patients), together with the corresponding liver metastasis. Another female patient without KRAS or BRAF mutation was microsatellite stable for the primary tumor, while her liver metastasis was microsatellite instable. Interestingly, this liver metastasis had the highest MACC1 RNA expression of all. Likely due to sample size, variation of mRNA expression in normal mucosa, tumor, and liver metastasis was not significant (Spearman-Rho). However, if metastases are regarded as the consecutive step after malignant formation of normal colon tissue, the tumor suppressor SASH1 was rather downregulated in the metastatic tissue while Osteopontin was even more strongly upregulated as compared to primary tumors, in all except one patient. Interestingly, the metastasis marker MACC1 showed a bi-phasic pattern, it was elevated in the primary tumor compared to normal mucosa, and decreased again in most of the metastatic tissues (Figure 19).

Figure 19: Corresponding incidence and expression patterns for (a) KRAS and (b) BRAF mutations, (c) microsatellite instability, and (d) Osteopontin, (e) SASH1 and (f) MACC1 in normal colon tissue, colorectal cancer and liver metastases from nine patients. mRNA expression values are calibrated to the mean expression of normal tissue for each marker.

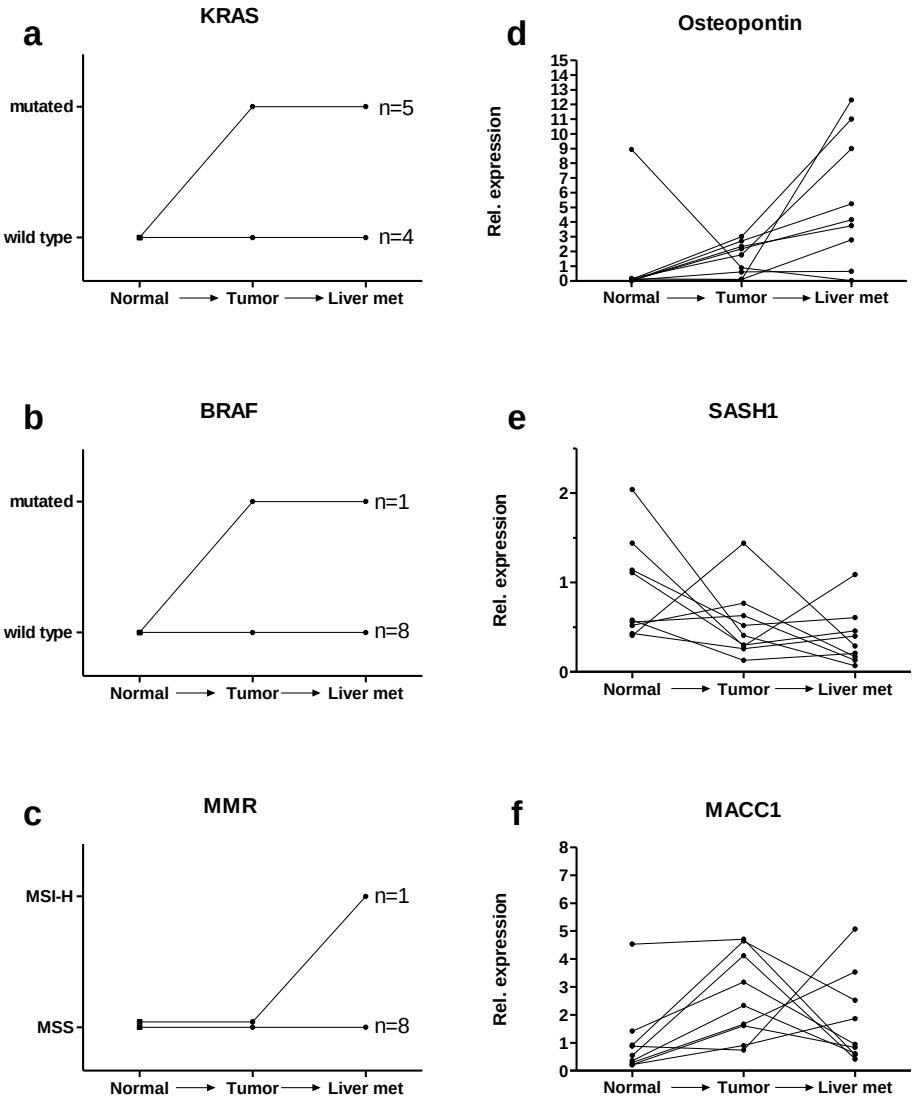

5.2 Part II: In vitro characterization of the candidate metastasis-markers SASH1 and MACC1

5.2.1 Expression of SASH1 and MACC1 differs in cell lines and tissue

Our results obtained on clinical samples of colon cancer indicated a significant association of reduced SASH1 expression with prognosis, and a highly significant correlation of increased MACC1 expression with metastatic disease. Moreover, there was a significant inverse correlation between the expression levels of both genes. Thus, especially MACC1 might qualify as candidate marker for risk prediction in colorectal cancer. However, both genes are not well characterized in molecular genetic and biochemical terms, and their role in cellular physiology, or in tumor biology, is still far from being resolved. SASH1 is ubiquitously expressed in human and murine tissues, with high levels in the brain, lung, placenta, spleen and colon.[75, 135] No SASH1 expression is detectable only in lymphocytes and dendritic cells.[95, 135] MACC1 expression levels vary in human tissues, with the highest levels in tissue arising from the endoderm (intestine and stomach), pituitary gland, kidney and trachea; followed by pancreas, mammary gland, bone marrow, ovary, lung, heart, liver, and B-lymphoblasts.[95, 115] Here, we first analyzed the endogenous expression of SASH1 and MACC1 within established colorectal cancer cell lines, providing the possibility for different intervention assays. There was no MACC1 expression detectable in a non-malignant cell line (Hek293). HCT116 colon cancer cells had low MACC1 mRNA levels, while expression in DLD1 and HT29 was higher. SW480 colon cancer cells express low mRNA levels of both SASH1 and MACC1, whereas transcription of both genes is upregulated in SW620 cells, a cell line raised from a lymph node and abdominal mass recurrence of the same patient.[6, 117] SASH1 levels were highest in HT29 and HCT116 (Figure 20). HT29 has 3 copies of chromosome 6 (trisomy), where SASH1 is localized, a possible explanation for increased levels. HCT116 is the only cancer cell line investigated here which does not have a mutation in the APC gene, and the only with no mutation in the p53 gene.[114] However, it

harbors a deleted β-Catenin allele, which may lead to even higher Wnt activity. The Wnt surrogate marker Osteopontin was correlated with high SASH1 expression levels in the clinical stage II patient cohort previously (Table 7). This could indicate a functional connection of SASH1 and Wnt signaling.

Figure 20: (a) Expression levels of SASH1 and MACC1 in different cell lines under normal growth conditions. Mean and standard error of the mean are indicated. (b) All investigated cell lines together revealed no significant correlation of SASH1 and MACC1 expression levels (interpolated dashed line, linear regression analysis). However, for Hek293, SW480, DLD1, and SW620 cells, SASH1 and MACC1 expression levels were directly proportional (full line, linear regression analysis). For all cell lines, SASH1 and MACC1 expression levels refer to HPRT-calibrated SASH1 expression of SW480. Results of at least three independent experiments per cell line are shown.

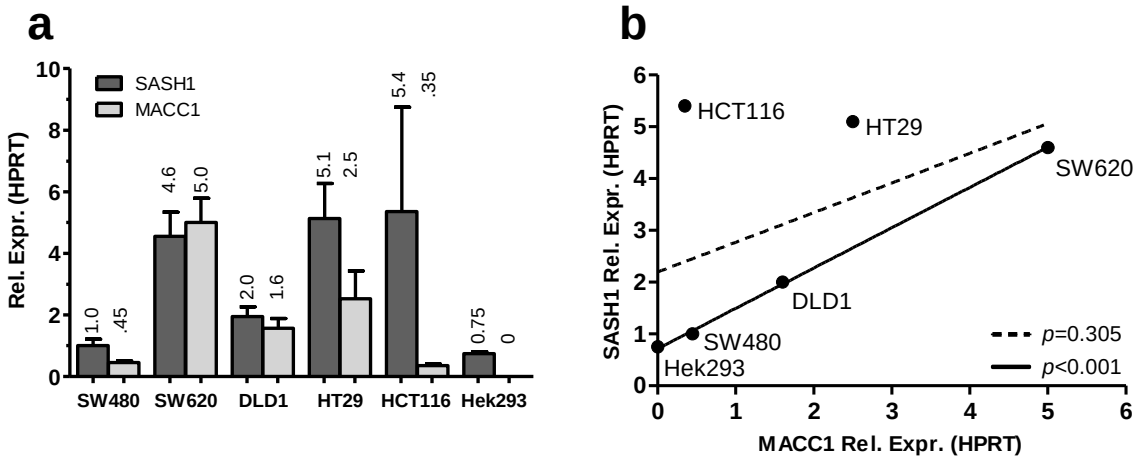

SW620 cells have increased mRNA levels of both transcripts compared to SW480 cells (Figure 20). The association of mRNA levels and protein levels of MACC1 was tested exemplarily on these well characterized cell lines which originate from the very same patient (Figure 21 and Figure 22). Likewise, MACC1 overexpression on protein level was detected in SW620 cells compared to SW480, a finding which was not confirmed for SASH1 (using the polyclonal SASH1 antibody “1540” generated in our laboratory: Figure 36 and data by Alexandra Gnann, personal communication, not shown). SASH1 is mainly found in the nucleus. MACC1 was described to be a transcription factor of cMET and thus is expected to be active inside the nucleus.[117] To investigate the subcellular localization and function of MACC1, separation of cell compartments with consecutive immunoblotting was performed. Here, the nuclear

localization of MACC1 protein was confirmed in both SW480 and SW620 cells, with again reduced total protein levels in SW480 cells (Figure 23). Thus, the regulation of MACC1 appears to take place on the DNA transcription level, but not by restriction of the posttranslational transport from the cytoplasm to the nucleus. The exclusive nuclear appearance of MACC1 in two cell lines strengthens the postulated main function as transcription factor and argues against any further direct involvement in extra nuclear signaling or cell motility processes. Thus, nuclear fractioning provides a feasible tool to narrow down the field of further experiments for characterizing the function of MACC1, as well as postulated connections to SASH1.

Figure 21: (a) Immunofluorescence labeled SW480 and SW620 cells. SW480 cells have a spindle-like shape, while SW620 cells show a round morphology and a higher nucleus to cytoplasm ratio. Both cell types were mixed at a 1:1 ratio, and kept in co-culture prior to the staining experiment. Tissue sections of (b) normal human colon mucosa, (c) colon cancer expressing low MACC1 RNA levels and (d) colon cancer expressing high MACC1 RNA levels indicate limited interpretation capacity. Overall, tissue of three representative patients was stained (two patients of the stage II collective and one patient of the stage IV collective described above). All experiments were repeated in at least two independent preparations. Scale bar: 20µm (400x magnification); blue: DAPI (nuclear staining), green: F-Actin, red: MACC1. For immunofluorescence, a polyclonal rabbit anti-MACC1 antibody by ProSci was used, while for Western blotting a polyclonal goat anti-MACC1 antibody by Santa Cruz was used, as described in the material and methods section.

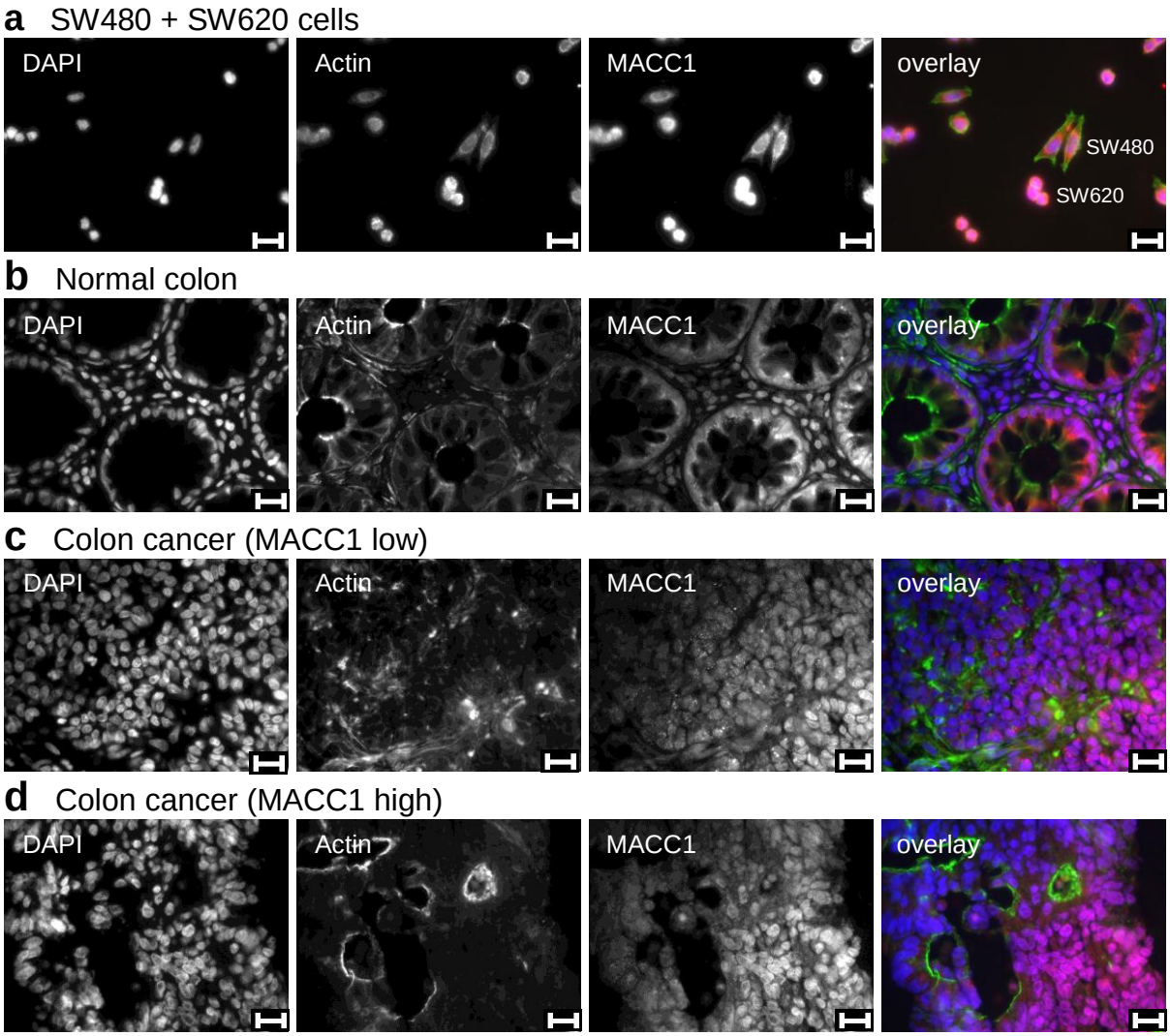

Figure 22: Lower MACC1 protein concentration in SW480 cells compared to SW620 in Western Blots analysis. After incubation of the MACC1 antibody (Santa Cruz) with blocking peptide, no related bands were visible, indicating the specificity of the antibody. Preincubation of one volume fraction blocking peptide with two volume fractions antibody was performed for one hour prior to use, approximating a 40-fold molar abundance of blocking peptide (blocking peptide 50nM; antibody 1.3nM).

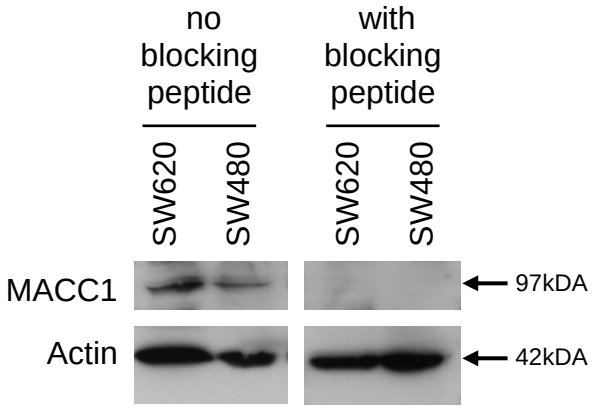

Figure 23: Separation of subcellular compartments and subsequent Western Blot analysis. Positive/loading controls were Cell division cycle 5-like protein (CDC5L) for the nuclear fraction, β-Integrin for the crude membrane fraction, and tubulin for cytoplasm. An additional smaller product was detected by the antibody against MACC1, which presumably represents partial degradation due to the time consuming protocol.

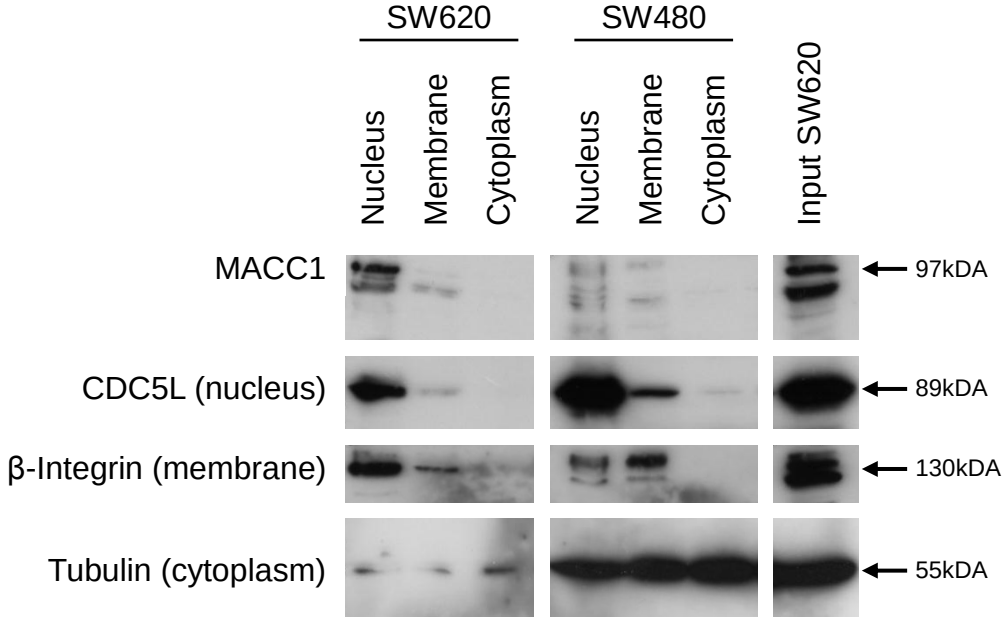

5.2.2 MACC1 expression is regulated by HGF stimulation

MACC1 has been identified as transcription factor directly binding to the cMET promoter. Its binding leads to enhanced transcription of cMET, the membrane located receptor of the hepatocyte growth factor (HGF).[117] By a positive feedback loop, elevated HGF levels were described to lead to upregulation of MACC1 transcripts.[117] To further investigate this regulatory loop, cells were treated with HGF. First, the dose dependent effect of HGF was confirmed. SW620, HT29 and DLD1, but not SW480 cells express the cellular HGF receptor cMET (Figure 24).[136] Stimulation of cells with HGF leads to activation of the HGF/cMET signaling pathway, resulting in phosphorylation of the extracellular signal-regulated kinase (ERK1/2, MAP kinase).[69] This effect was detected in HCT116 cells, and to a lesser extent in the other cell lines.[69] SW620 cells showed relatively strong phospho-ERK1/2 (pERK1/2) levels already under baseline conditions (Figure 24).

Figure 24: Increasing phosphorylation of ERK1/2 due to activation of the cMET pathway by HGF. After serum starvation for nine hours, cells were treated overnight with different HGF concentrations (indicated below) or control incubated with normal growth media containing fetal calf serum (FCS, 7% for SW480, HCT116, and DLD1; 10% for SW620). Total ERK1/2 protein served as loading control.

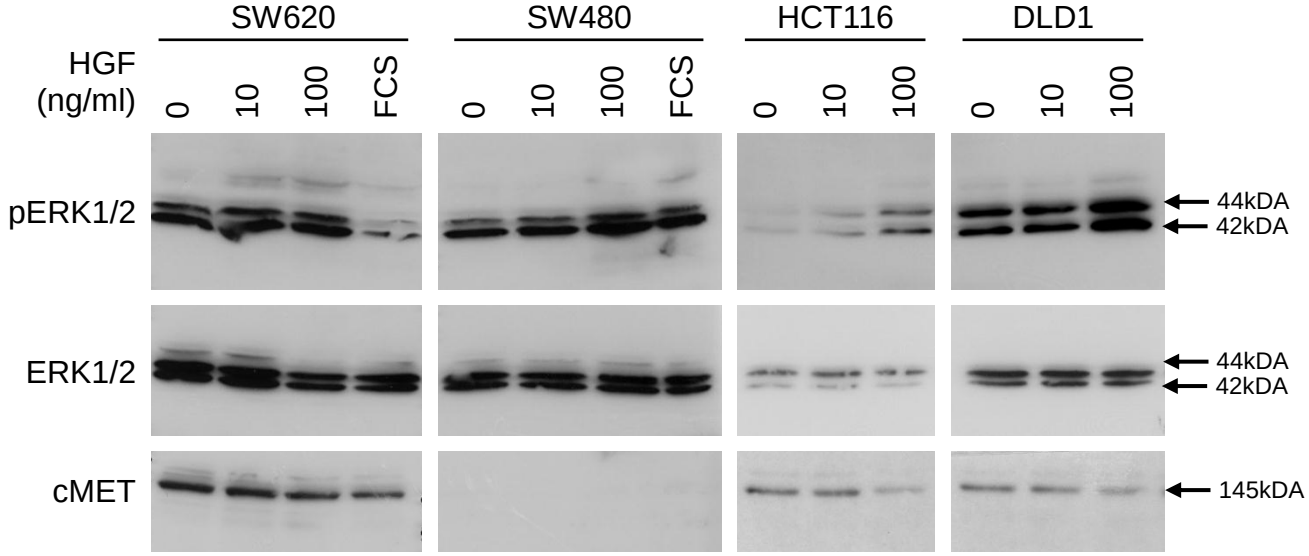

In order to investigate a putative role of MACC1 in the HGF pathway, transcript levels of MACC1 and SASH1 were determined after HGF stimulation. While SASH1 levels remained essentially unchanged, growth-factor treatment led to increased MACC1 expression in SW620, and to a lesser amount in DLD1 cells (Figure 25).

Figure 25: MACC1 and SASH1 expression levels after HGF treatment. Cells were plated out, grown overnight, serum starved for seven hours, and finally treated with HGF (100ng/ml) overnight before harvesting. While HGF-signaling competent cells (Figure 24) increased MACC1 expression after HGF stimulation, no relevant changes were identified for SASH1 levels. Results of at least three independent experiments per cell line are shown. Mean and standard error of the mean are indicated.

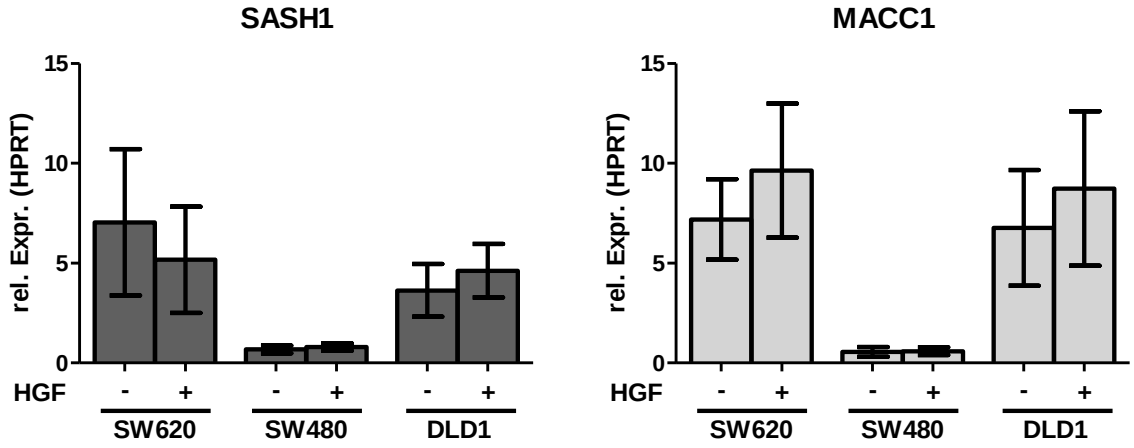

Finally, the effect of HGF stimulation on cell proliferation was analyzed by spectrophotometric quantification. As expected, due to its role regarding cell invasiveness and scattering rather than enhancing cell growth, HGF stimulation did not influence the cell proliferation rate (Figure 26).[118]

Figure 26: Proliferation is not increased upon HGF treatment. As described in the methods section, cells were plated and grown overnight in medium containing 0.5% FCS. On the next day, the medium was replaced by new medium containing 3% FCS with or without HGF (100ng/ml), and the cell growth was quantified over the next 72 hours. The results of three independent experiments are shown.

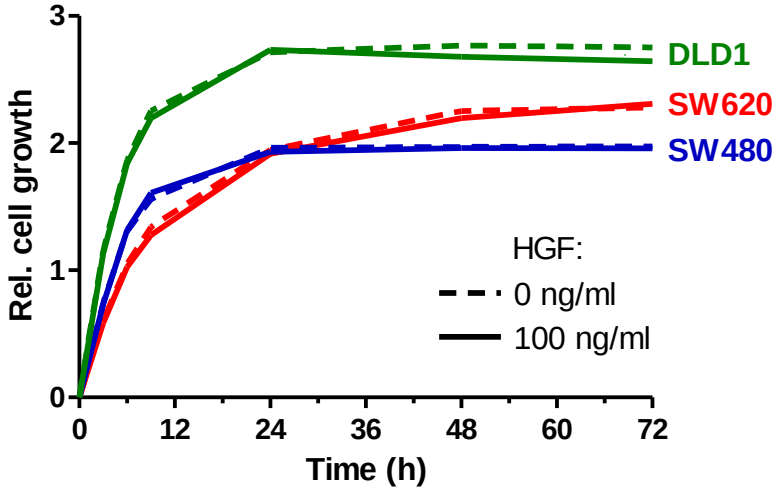

5.2.3 Analysis of putative interactions between MACC1 and SASH1 expression, and their role in cancer cell biology

Transient transfection reveals relations between SASH1 and MACC1

A significant inverse correlation of SASH1 and MACC1 expression levels was detected in human colon cancer tissue (see above). Moreover, earlier results from our group indicated a negative effect of SASH1 on MACC1 transcription, with down-regulated SASH1 leading to increased MACC1 expression.[75] To further investigate this possible connection, knockdown experiments were performed in cell lines. Transient SASH1 knockdown by small interfering RNA (siRNA) was induced in SW620 and DLD1 cells, as well as MACC1 knockdown in SW480, SW620, and DLD1 cells (Figure 27). For the effect of SASH1 knockdown in SW480 cells, previously established cell clones with stable shRNA expression were used (SW480 clones by Alexandra Gnann). As expected, SASH1 knockdown led to a significant reduction of its transcripts in SW480 and DLD1 cells. While SASH1 knockdown

resulted in significant upregulation of MACC1 expression in SW480 cells, confirming earlier findings, there was no effect observable in DLD1 cells. MACC1 knockdown led to reduced MACC1 levels in all cell lines, as expected. However, no significant downregulation could be achieved by the RNA-interference method in SW480 cells, which already display relatively low endogenous MACC1 expression levels (Figure 20). However, there was a trend towards increased SASH1 expression after MACC1 knockdown in SW480 and SW620 cells. Interestingly, DLD1 cells responded by significant downregulation of SASH1 after MACC1 knockdown, displaying a strikingly different behavior than both SW cell lines. Interpretation of the results may be limited because changes on protein level were not investigated.

Figure 27: Knockdown of (a, b, c) SASH1 and (d, e, f) MACC1 in (a, d) SW480, (b, e) SW620 and (c, f) DLD1 cells and resulting mRNA expression levels of SASH1 and MACC1. *p*-values are indicated for significant effects (t test). For all experiments, siRNA was used (except for SASH1 knockdown in SW480, see text above). Cells were transfected directly after plating, as described in detail in the methods section. After incubation over two nights, mRNA levels were quantified by rtPCR. The graphs summarize the results of at least four independent experiments. Mean and standard deviation are indicated.

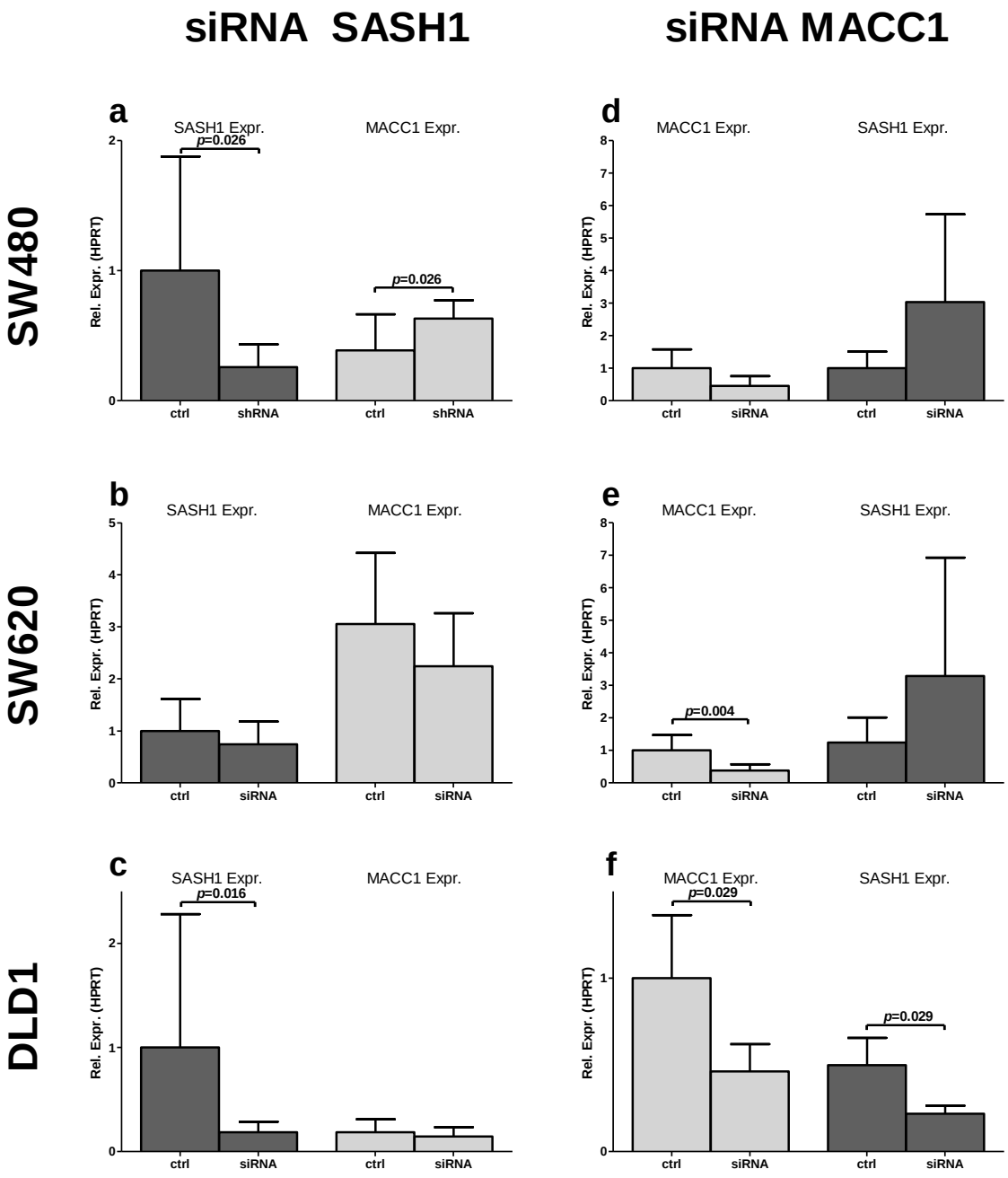

After the initial transfection tests with siRNA had strengthened the evidence for a suspected co-dependency of the two transcripts of SASH1 and MACC1 (see above), cell clones with stable MACC1 knockdown by expression of small hairpin RNA (shRNA) were established, in order to further elucidate cellular characteristics and functional connections. Cells were transfected with the pSUPER plasmid, which contains a G418 resistance cassette, a green fluorescence protein (GFP)-gene which allows identification and sorting by FACS, and had previously been used to establish a SW480 stable SASH1 knockdown cell line (see above, described by Dr. Melanie Martini[75]). Serial dilution revealed cell line specific concentrations of G418 antibiotic which were necessary to warrant positive selection after transfection (Table 11, so-called “killing curve” for G418 selection). The concentration was considered appropriate when approximately 1% of the cells were alive after one week of incubation.

Table 11: Stable SASH1 and MACC1 knockdown cells. The second column indicates the identified concentrations of G418 in cell culture media to provide permanent selective pressure of pSUPER transfected cells. The third column lists the clones that were available for the following experiments.

Cell line	Concentration	Established cell lines (Figure 29)
SW480	1.8 mg/ml	1x empty vector control*, 1x shSASH1*
SW620	3.0 mg/ml	1x empty vector control, 1x shMACC1
HCT116	1.0 mg/ml	3x empty vector control, 3x shSASH1, 2x shMACC1
HT29	1.0 mg/ml	None (see text)

*Previously generated by Alexanda Gnann.

In SW480 (shMACC1) and HT29 cells (any plasmid), no clone selection was achieved despite repeated transfection experiments. One SASH1 knockdown clone was selected initially for the SW620 cell line. However, it had to be discarded due to a lack of effect on expression, despite positive G418 selection and GFP positivity. The other two SW620 clones (empty vector control and shMACC1) were enriched for GFP in repeated FACS passages at the Institute for Medical Microbiology, Immunology and Hygiene of the Technische Universität München, and further monitored by flow cytometry in our laboratory (Figure 28). All HCT116 clones had a

mean GFP positivity rate of 93.5% (range, 35.2 to 97.3%) after a single FACS passage. Changes for MACC1 or SASH1 knockdown cells were quantified relative to the expression in pSUPER empty vector control transfectants (Figure 29).

Figure 28: Exemplary FACS enrichment of GFP positive SW620 cells, transfected with a plasmid containing GFP together with the shRNA sequence for MACC1 knockdown. (a) Transient transfection led to a relatively high initial transfection rate of 43%, which was reversible during consecutive passages under antibiotic selection pressure. In the further course, the rate of stable plasmid expressing positive clones was raised by a single FACS passage from (b) 9% to (c) 31%, with a clearly visible subpopulation (red arrow). Overall, four successive steps of FACS were performed for the transfected SW620 cells. Blue indicates MOCK control transfected cells, red indicates GFP positive transfected cells.

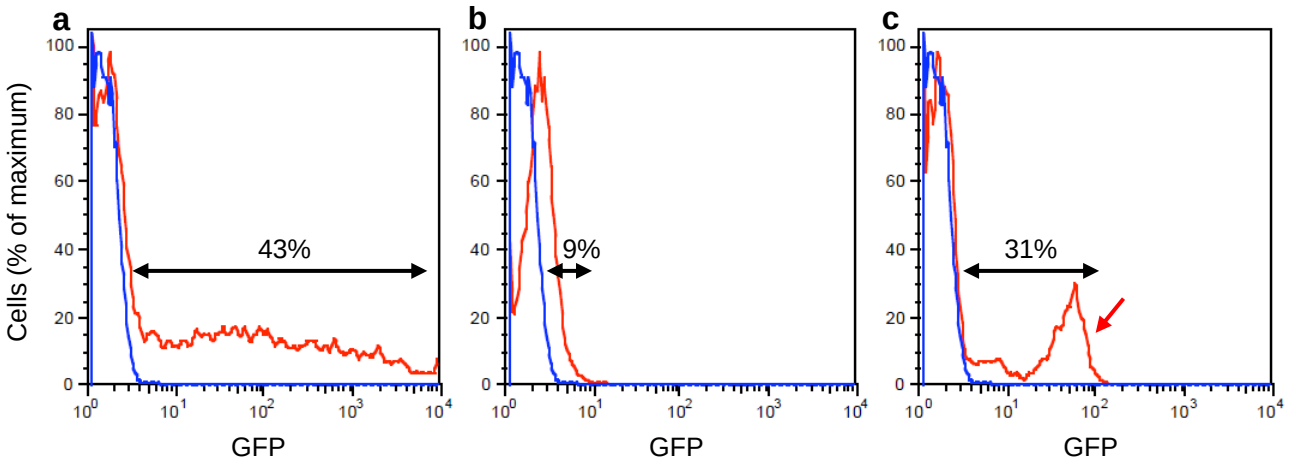

Figure 29: Expression analysis of the 12 generated stably transfected cell lines that were used for further experiments (see also Table 11). Results of at least three independent experiments per cell line are shown. Mean and standard deviation are indicated.

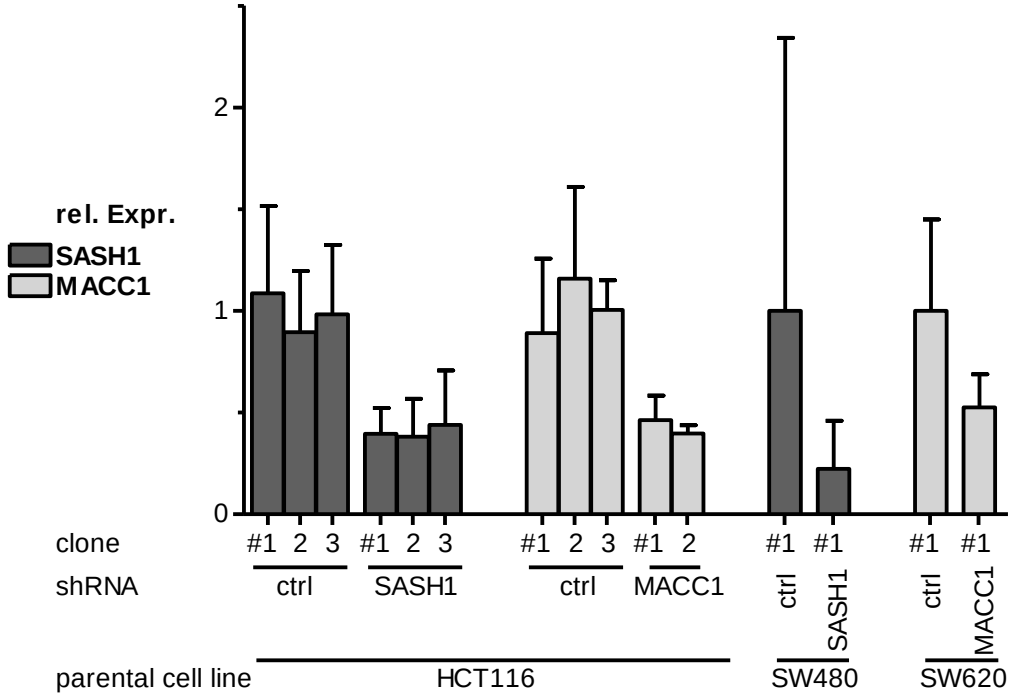

In the newly generated HCT116 cells, a significantly reduced expression was observed for SASH1 and for MACC1 (Figure 30). However, SASH1 knockdown did not lead to relevant alterations of MACC1 expression and vice versa, in contrast to earlier findings after transient siRNA transfection (Figure 27).

Figure 30: Pooled expression levels of the stably transfected cell clones. *p*-values for significant differences are indicated (t test). Results of at least three independent experiments per cell line are shown. Mean and standard deviation are indicated.

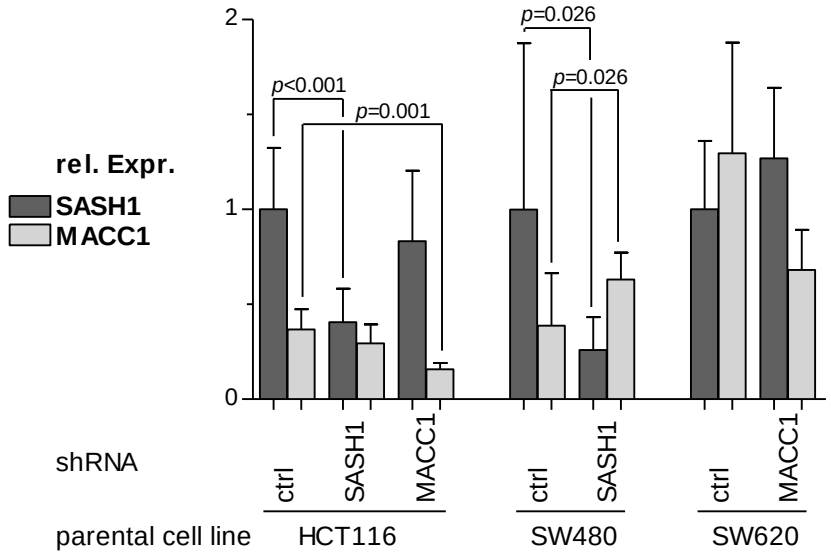

No direct protein-protein interactions between MACC1 and SASH1 by co-immunoprecipitation

---

The observed inverse correlation of SASH1 and MACC1 in both, human cancer samples and cell lines, supports evidence for cross pathway signaling. E.g., SASH1 could bind to the MACC1 promoter, or to MACC1 mRNA. In order to characterize the putative connection between SASH1 and MACC1, it was first analyzed if direct protein-protein interaction occurs. For this purpose, MACC1 protein was pulled down by antibody labeled beads with accompanying detection of SASH1 protein. Vice versa, recombinant SASH1 was precipitated with anti-V5 peptide antibodies, followed by the accompanying detection of MACC1 (co-immunoprecipitation). For the experimental setup, endogenous MACC1 in SW620 cells was detected. However, the polyclonal SASH1 antibody ("1540") generated in our laboratory does not allow immunoprecipitation.[75] Therefore, SW620 cells were transiently transfected by a plasmid encoding full-length SASH1 together with a V5 peptide tag, and subsequent immunoprecipitation was performed by anti-V5 tag antibody "pulldown". As expected, transient SASH1-V5 transfection led to significant upregulation of SASH1, which had been confirmed previously in DLD1 cells (Figure 31 and Figure 32).

MACC1 has been described as mainly nuclear protein with transcription-factor activity. Because V5 tagged SASH1 does not enter the nucleus after transfection in large amounts[75], for some experiments a V5 tagged SASH1 construct lacking the C-terminal amino acid sequence (ΔCter) was used. This deletion construct has been found to strongly accumulate in the nucleus in transfected cells[75], and may therefore be more appropriate to study intra-nuclear interactions with MACC1. No co-precipitation was found in SW620 cells under normal growth conditions, suggesting no direct protein binding between SASH1 and MACC1, at least under the conditions tested here (Figure 33). However, this approach would require potential binding sites for MACC1 residing in the amino-terminal domain of SASH1 and the restricted effectiveness of the SASH1 precipitation should be noticed.

Figure 31: (a) Transfection of DLD1 cells with V5 tagged whole SASH1 led to more than 2000-fold upregulation of SASH1 transcripts. However, MACC1 expression was not affected by SASH1 overexpression. The *p*-value refers to the t test. Results of three independent experiments are shown. Mean and standard deviation are indicated. (b) Immunoblotting of DLD1 cells after transfection with V5 tagged SASH1-ΔCter revealed higher levels of SASH1-V5 protein compared to MOCK transfection (V5 antibody).

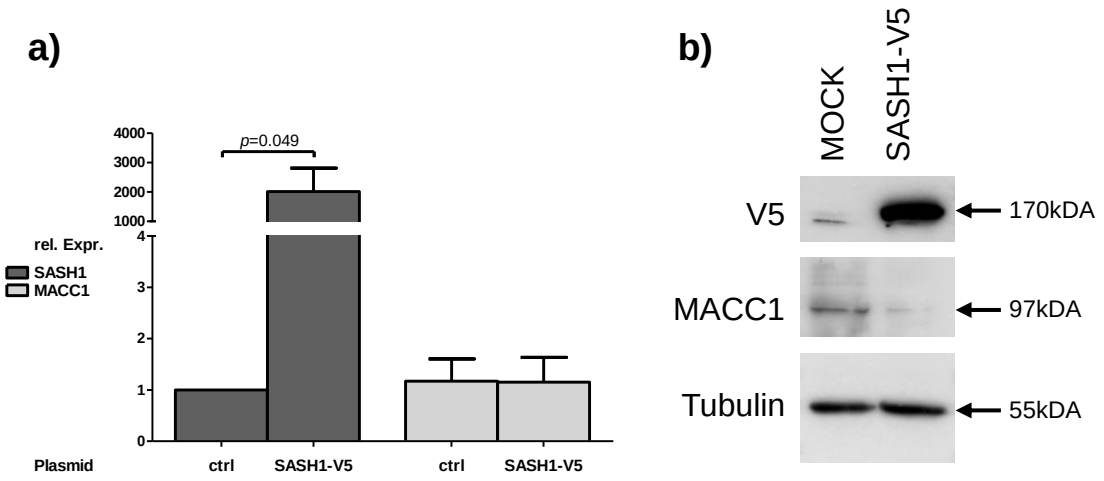

Figure 32: Immunofluorescence labeled DLD1 cells after transfection with V5 tagged whole SASH1 revealed higher levels of SASH1 protein compared to MOCK transfection. Scale bar: 20µm (630x magnification); blue: DAPI (nuclear staining), green: F-Actin, red: anti-SASH1 antiserum #1540.

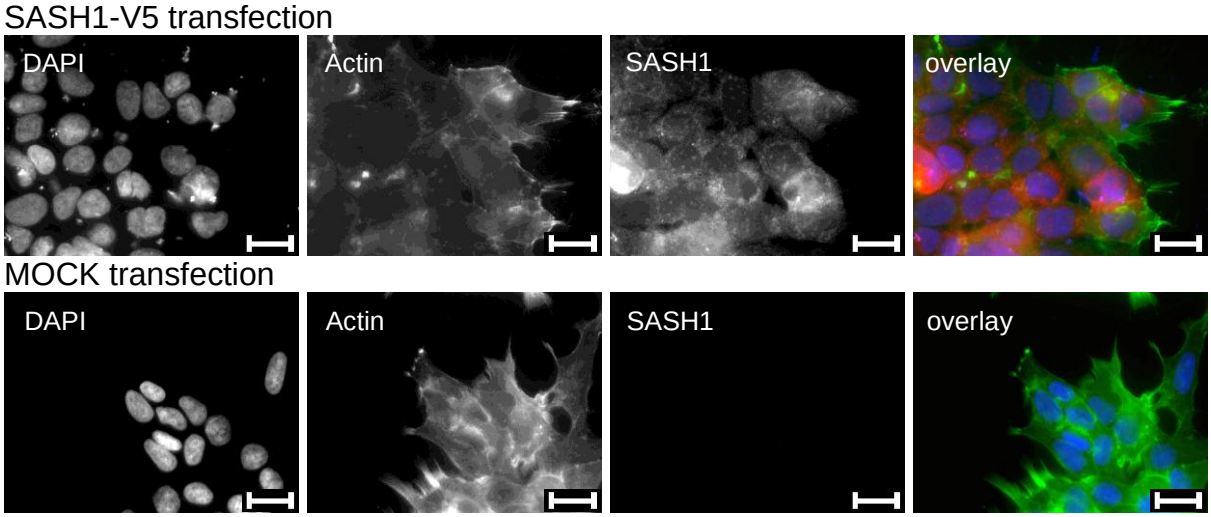

Figure 33: Co-immunoprecipitation of MACC1 and SASH1 revealed no direct protein-protein binding in SW620 cells. The V5 tag does not lead to an apparent change of the molecular weight of SASH1 (170kDa). Incidentally, SASH1 was detectable to a small amount in the MACC1 IP, a finding that has been observed in experiments of our group before and that is thought to be caused by unspecific binding capability of SASH1 to partners, like the actin cytoskeleton.[76] Nonspecific IgG from rabbit serum served as isotype control for SASH1 and IgG from goat serum for MACC1. Five independent experiments were performed without conflicting data despite transient problems of the immunobloting. The displayed results were obtained twice.

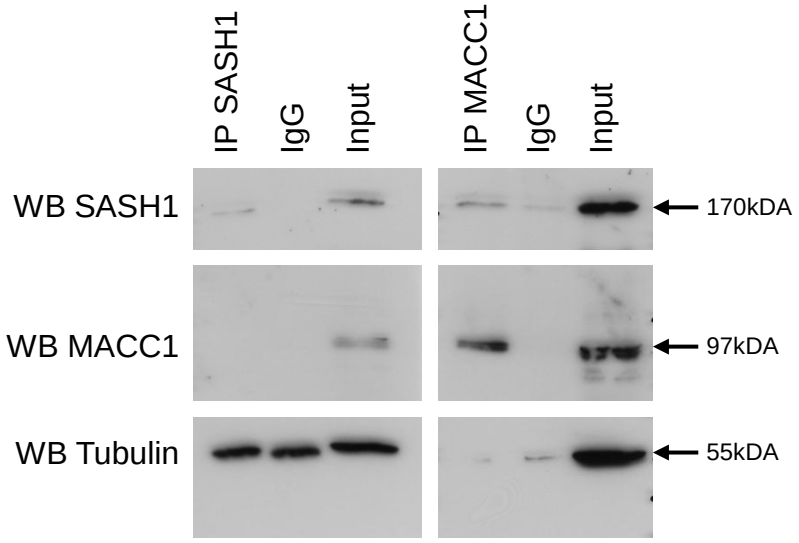

Having detected no direct interactions between the proteins encoded by the candidate tumor suppressor SASH1 and the putative oncogene MACC1, the inverse correlation of transcript levels which we have observed could be caused either by differential promoter activity, or by altered mRNA stability. Both processes could be triggered directly, e.g., by binding of SASH1 to the promoter region of the MACC1 gene, leading to inhibition of transcription, or by binding of SASH1 via its SAM domains to MACC1 transcripts, leading to decreased mRNA stability. Lack of SASH1 expression would in both cases lead to increased MACC1 expression. However, these effects could also be mediated indirectly by other gene products, without direct interactions of both presumed partners. Hence, experiments to analyze mRNA stability were performed. Because SASH1 knockdown led to increased MACC1 transcript levels in SW480 cells, special focus was laid on alterations of MACC1 RNA stability as a function of SASH1 expression. After treatment of cells with the drug Actinomycin D, cell lines cease to produce mRNA. Thus, by monitoring the time dependent decrease of RNA transcripts after Actinomycin D incubation, conclusions regarding the stability and half-life can be drawn. Regardless expression levels of SASH1, mRNA of MACC1 was unstable in SW480 cells (Figure 34 and Figure 35), which were found previously to express low amounts of MACC1, both on protein as well as on mRNA levels under normal growth conditions (Figure 20 and Figure 23). Hence, SW480 cells had a different behavior compared to the other colorectal cancer cell lines HCT116, HT29, and SW620. In those, SASH1 transcripts had the shortest half-life. The time-dependent decay of Hypoxanthine-guanine phosphoribosyl-transferase (HPRT) expression, which was used as control, did not differ significantly between all investigated cell lines (Figure 34; *p*-values of unpaired t test not shown).

Figure 34: Time course experiment on mRNA stability after treatment with Actinomycin D (5µg/ml) up to 24 hours in different cell lines. The curves indicate the interpolated decline of mRNA during 24 hours, starting at 100% without treatment (Non-linear regression, curve interpolation by one phase decay function). HPRT was used as control.[71] Results of at least three independent experiments per cell line are shown. Interpolated curves of nonlinear fit models with mean and standard deviation are indicated.

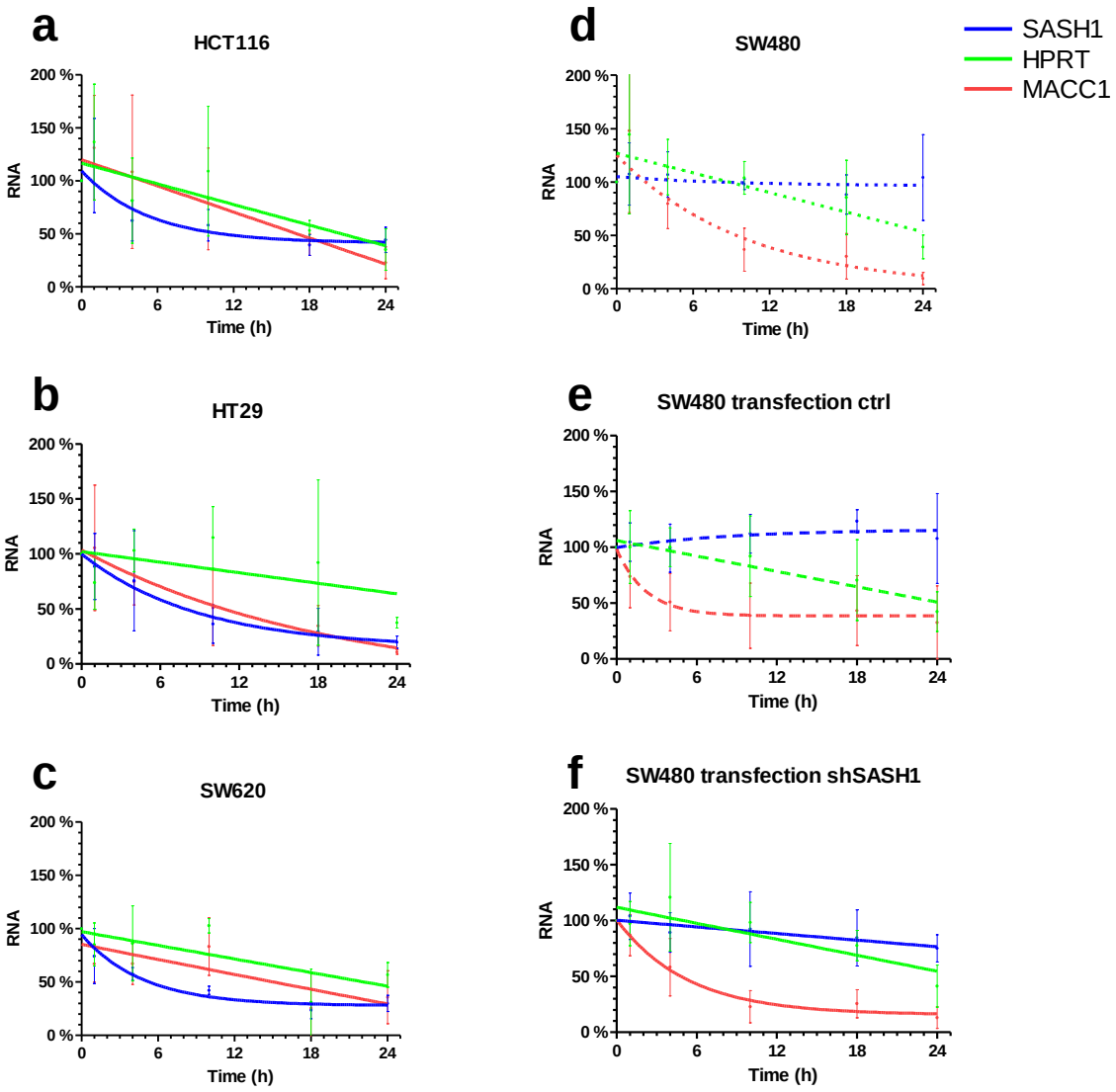

Figure 35: (a) Overlay of the time dependent mRNA decay of MACC1, SASH1 and HPRT in SW480 wild type cells, shRNA transfection control cells, and SASH1 knockdown cells. MACC1 RNA levels did not differ significantly between these three cell lines. (b) The predicted half-life of the intracellular mRNA by one phase decay calculation differed strikingly for SASH1 and MACC1 between the three SW480 clones and the other cell lines. Results of four independent experiments per cell line are shown. Interpolated curves of nonlinear fit models are indicated.

a

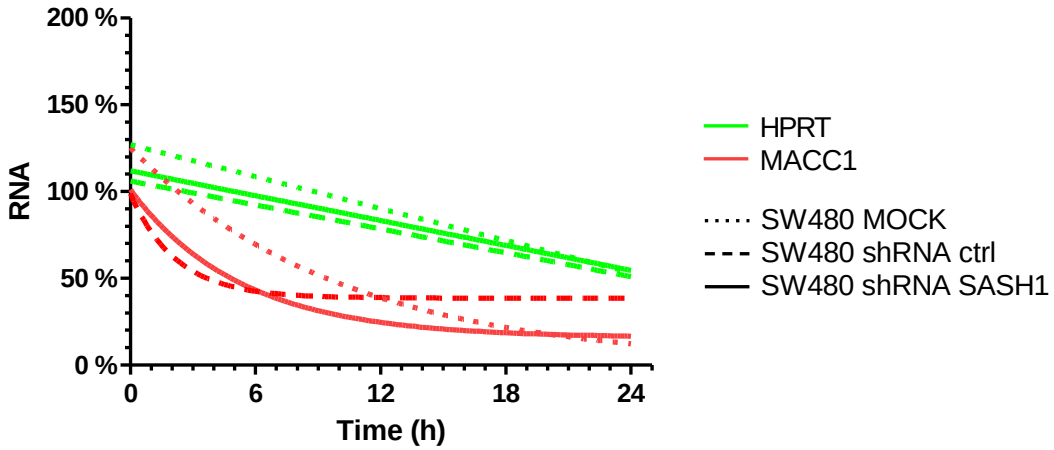

b

	Predicted half-life (h)		
	MACC1	SASH1	HPRT
HCT116	>100	**41.3**	>100
HT29	13.5	**6.2**	>100
SW620	>100	**3.4**	>100
SW480 MOCK	**7.0**	>100	>100
SW480 shRNA ctrl	**1.5**	>100	>100
SW480 shRNA SASH1	**3.7**	>100	>100

MACC1 protein has a short half-life

Our previous experiments have shown strongly cell type dependent differences of MACC1 and SASH1 mRNA stability (see above). Consequently, the stability of the encoded proteins was investigated. For this purpose, SW480 primary colon cancer cells, and SW620 metastatic cancer cells derived from the same patient were treated with the drug cycloheximide, an inhibitor of protein biosynthesis, which interferes with the protein translocation step (Figure 36; experiments performed by Irina Kliewer, student intern).[84] It was not possible to reliably interpret the results for MACC1, due to the weak protein signal intensity on the immunoblots. However, a slightly higher

expression was observable in SW620 cells. Concentrations of SASH1 diminished constantly during 24 hours of treatment, suggesting an intermediate SASH1 protein stability, roughly comparable to the control p53. Wild type p53 undergoes relatively fast degradation, with a half-life of 20min.[49] However, gene mutations of p53 have been shown to prolong the half-life of the protein, depending on the type of mutation. SW480 and SW620 cells both comprise G to A mutation in codon 273 of the p53 gene resulting in an arginine to histidine substitution, leading to a half-life of seven hours.[49] Of note, less SASH1 was detectable in SW620 cells. Moreover, an 110kDa additional band appeared in SW620 cells, with increasing signal strength over time. This signal most likely corresponds to a proteolytic degradation product described earlier.[75, 76] β-Catenin showed a relatively high stability, which can be explained by mutations in the APC gene in both cell lines used, leading to stabilization by reduction of the APC/GSK mediated degradation of β-Catenin protein. Under appropriate conditions, β-Catenin half-life of six hours or longer was reported.[90] Tubulin, which remained stable throughout the course of the experiment, was chosen as another control protein due to its high intracellular protein concentration and stability.[73]

Figure 36: Time dependent decrease of SASH1 and MACC1 protein after treatment with cycloheximide, an inhibitor of protein synthesis (10ng/ml), in SW480 and SW620 cells. In a descending order of protein stability, Tubulin, β-Catenin and p53 were used as controls.

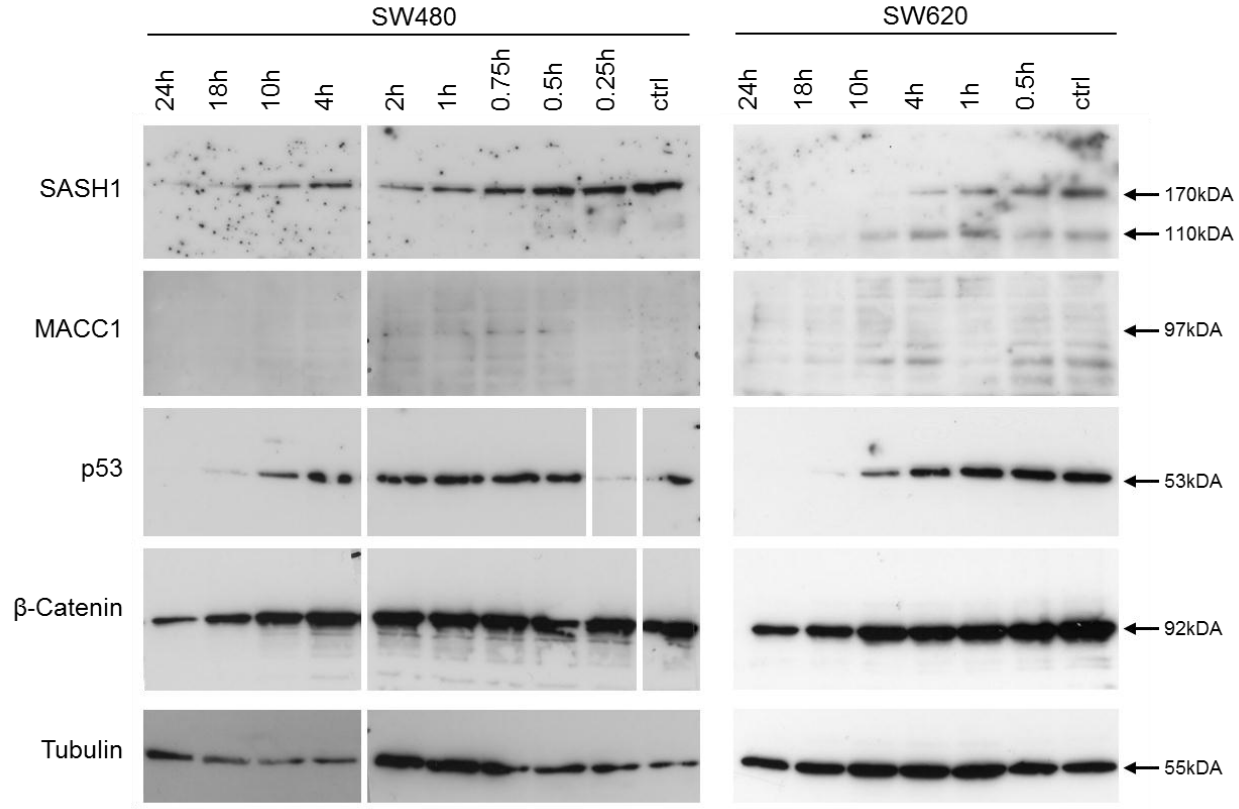

Cell proliferation is independent of MACC1expression

MACC1 has been reported as an activator of the HGF/cMET pathway, suggesting that it plays a major role in cell scattering and invasion, processes important for the formation of metastasis.[117] Additionally however, rising MACC1 expression levels were reported to lead to increased cell proliferation.[117] Here, the spectrophotometric quantification of proliferation by a commercial XTT-assay was performed. Knockdown of MACC1 led to a non-significant trend of reduced proliferation in HCT116, but not in SW620 cells (Figure 37a, b). Stable SASH1 knockdown (Figure 37a), as well as stimulation with HGF (Figure 37c, d), did not lead to changes of the cell growth. Thus, even though HGF treatment leads to upregulation of MACC1 on

mRNA and protein levels (Figure 25), this does not result in increased cell proliferation.

Figure 37: Cell proliferation depending on expression levels of (a, b) MACC1, (a) SASH1, and (c, d) HGF stimulation with 100ng/ml during the whole observational time. Results of at least three independent experiments per cell line are shown.

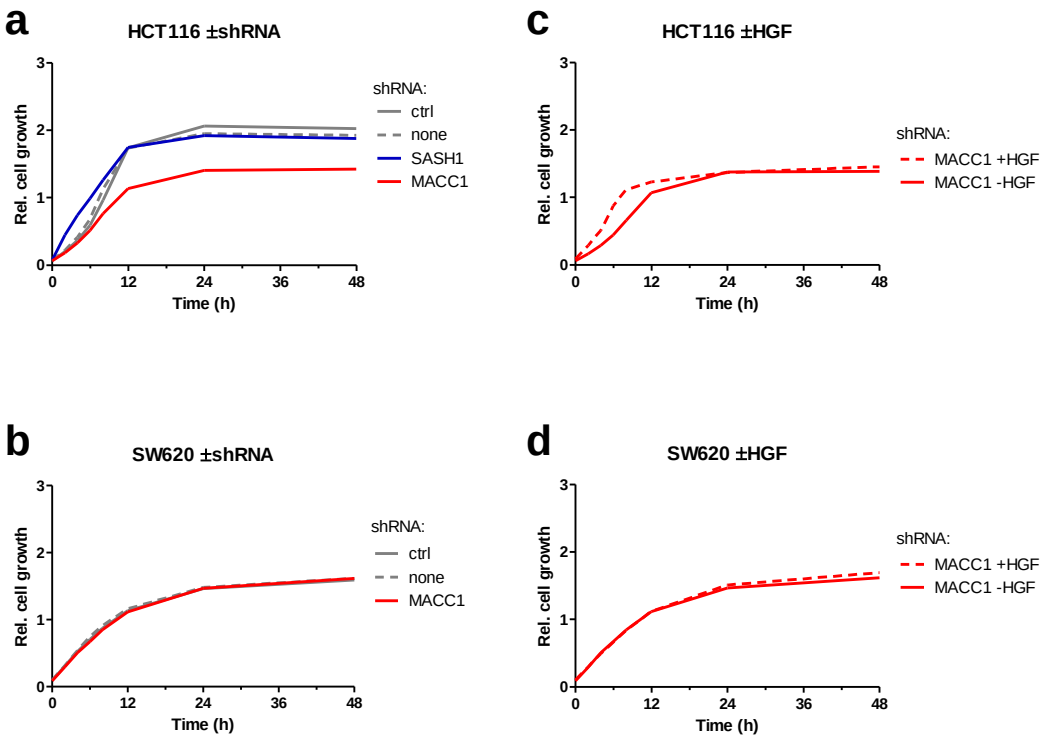

Cell migration depends on MACC1

Hepatocyte growth factor (HGF) is also known as “scatter factor”, and has been reported to induce cell motility. Therefore, signaling downstream of the HGF/cMET axis, as well as MACC1 activation may lead to enhanced cell migration. Different cell lines were seeded on a specialized cell culture plate engineered for two dimensional cell migration assays. At confluency, cell migration was quantified. Prior to analysis, cells were treated with Mitomycin C in order to inhibit cell proliferation, and to only detect migratory effects. Time dependent cell migration into an artificial gap was documented, and the remaining cell-free area of the gap was quantified at different

points of time by external software analysis (www.wimasis.com, Figure 38). HCT116 cells revealed faster migration into the artificial gap than SW620 cells. In the pooled analysis of three experiments, no significant difference regarding cell migration was detected for different HCT116 cell clones. For SW620 cells, there was significantly reduced migration for MACC1 knockdown cells compared to not transfected cells after 72 hours (p=0.016). There was no significant change if untransfected SW620 cells were stimulated by HGF (100ng/ml in medium containing 1% FCS) during the whole experimental setting. However, the trends that were identified in this experiment may not have gained significance due to the relatively low number of repeats.

Figure 38: Representative findings of the migration assay for (a) HCT116 cells after 0 and 15 hours and for (b) SW620 cells after 0 and 50 hours. MACC1 knockdown by shRNA led to a significantly reduced migratory capability in SW620 cells, while (a) SASH1 knockdown or (b) HGF treatment during the whole observation time (100ng/ml in medium containing 1% FCS) did not alter the migratory behavior relevantly. (c) These findings were confirmed in the aggregated assessment of three independent experiments. The interpolated mean gap area and standard deviation of three independent experiments are displayed. HCT116 cells revealed a higher migratory capacity compared to SW620 cells. For SW620 cells, there was significantly reduced cell migration after 72 hours for MACC1 knockdown cells compared to not transfected cells (p=0.016, t test). Scale bar: 100µm (100x magnification).

a) HCT116

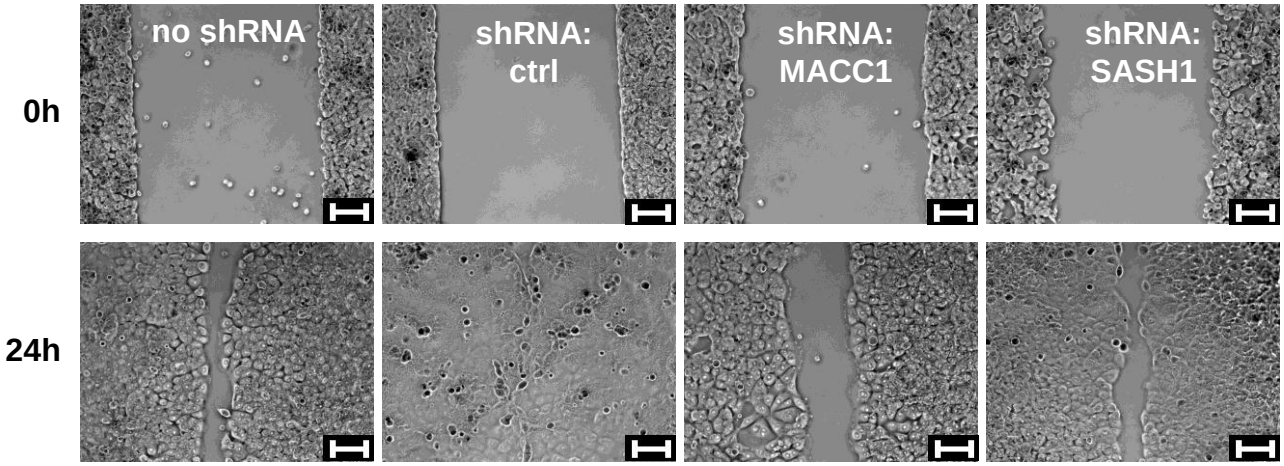

b) SW620

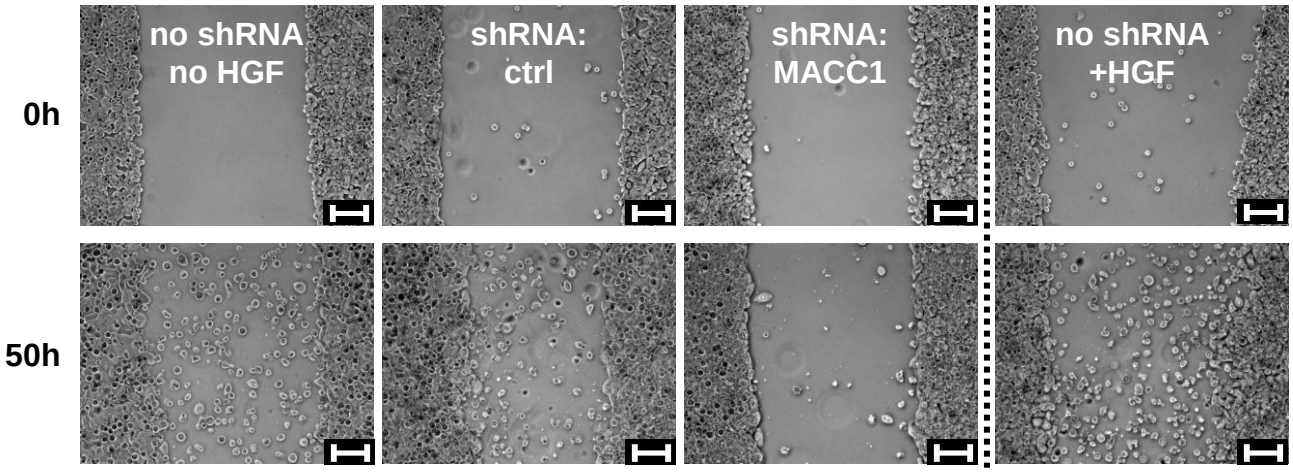

c) Aggregated assessment

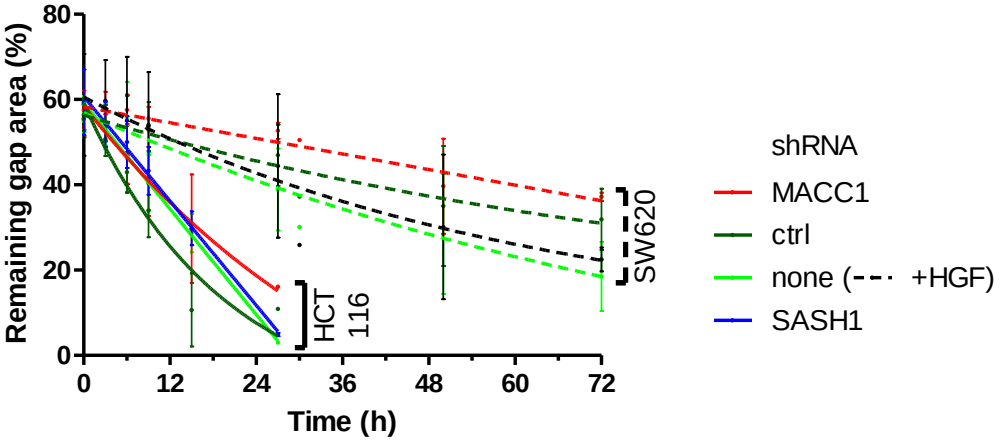

6 Discussion

6.1 Colorectal cancer

Colorectal cancer is the third most frequent cancer worldwide regarding both incidence and mortality.[56] Because of substantial survival differences depending on the cancer spread at diagnosis, current therapy recommendations are mainly tumor stage-dependent.[81, 106, 130] However, there is considerable ambiguity in the clinical stratification between those patients who can be considered cured after surgical tumor resection only, and patients who will benefit from adjuvant treatment.[14, 34, 82] Patients with small tumors and no evidence of tumor cell dissemination (stage I) do not need further treatment after tumor resection, whereas a benefit for systemic chemotherapy has been confirmed repeatedly for advanced stage cancers (stage III and IV).[14, 106] However, the usefulness of prophylactic adjuvant therapy in stage II patients is currently debated extensively.[14, 106] Certainly, not all stage II patients profit from adjuvant treatment, but there is evidence for a subgroup of stage II patients with considerably worse prognosis.[40, 102] The current TNM staging system does not allow the identification of these patients, even in the latest and refined version.[82] Therefore, additional histopathological and molecular genetic biomarkers may provide important information for clinical therapy decisions.[26, 120, 129] Thus, the standard classification into tumor stages I to IV depends mainly on the time of diagnosis, and has proven, but limited prognostic power. However, allocation of patients into evidence-based molecular tumor pathways may allow personalized risk prediction, leading to individualized treatment strategies by predicting the most successful therapy for a specific cancer type.

6.2 Aim of this thesis

Clinically, there is an urgent need for improved metastasis risk prediction in patients with colorectal cancer. Therefore, the basic idea underlying this work was to establish

an “intelligent tumor bank”, which would provide a tissue-based retrospective “library” to study clinical, histopathological and molecular genetic aspects of colorectal cancer. In addition to general clinical parameters like TNM (tumor, lymph node, metastasis), the “intelligent tumor bank” should provide the means for an integrative approach that includes a combination of established and promising novel molecular genetic markers. First, the prognostic power of the investigated biomarkers was thoroughly tested in a cohort of UICC/AJCC stage II colon cancer patients (n=232). Next, the behavior of the markers during the carcinogenic process was tracked in an independent collective of matched tissue samples that recapitulated the progression from normal colon mucosa through development of the primary colorectal cancer to the formation of liver metastasis. Notably, evidence was gathered for a functional interaction between the putative metastasis-associated genes MACC1 and SASH1, which both appeared relevant for prognosis in the patient cohort. Therefore, functional connections between SASH1 and MACC1 were subjected to further in vitro evaluation.

6.3 A new integrative panel of biomarkers for metastasis-risk prediction in colorectal cancer

Currently, mutational status of the oncogene KRAS is the only predictive biomarker[27, 128] routinely applied in the clinical context for colorectal cancer. Mutation of KRAS is a contraindication for treatment with EGFR-inhibitory antibodies in metastasized colorectal cancer. Moreover, microsatellite instability will become the first established prognostic molecular marker for clinical decision making in colon cancer patients.[43, 128] Next to this biomarkers, there is an ever-increasing plethora of further suggested markers today, with the mutation status of the oncogene BRAF emerging as a promising prognostic and predictive tool in clinical practice, especially when joined with microsatellite stability status.[17, 26, 51, 74, 128] Combined (or “integrative”) analysis of several independent markers was performed in some studies so far[59], mainly within the scope of genome-wide expression analyses. Only few independent validations have been reported, and there is a surprisingly large

heterogeneity between reported gene expression signatures in independent studies.[41, 60, 61, 103, 110]

In the present study, six molecular markers were selected and tested for recurrence risk stratification on 232 patients with UICC stage II colon cancer. Individual and combined interpretation was performed: somatic mutation of the oncogenes KRAS (exon 2) and BRAF (exon 15), DNA microsatellite repeat instability, mRNA expression of the canonical Wnt target gene Osteopontin, and expression of the putative metastasis-associated genes SASH1 and MACC1. The panel was based on robust, DNA- or RNA-based tests of molecular alterations that have previously been reported in connection with colorectal carcinogenesis, notably in the context of metastasis formation.[26, 52, 95, 117, 120] Recurrence risk was determined by means of non-microdissected tissue samples. Immanent to the methods, no tolerance for subjective evaluation existed as it may occur in immunohistochemical scoring classifications, thus providing a pragmatic and feasible approach. Microsatellite instability status was measured by the pathological department of the TU München, while High resolution melting (HRM) analysis for the detection of KRAS and BRAF mutations was newly established in our laboratory in the context of this work. Cell line dilution series revealed a detection limit of less than 5% of mutated DNA for HRM. The HRM results were confirmed by cross validation via pyrosequencing on a subset of 118 patients. HRM classified 10 patients wild type for KRAS, respectively six patients for BRAF, who appeared mutated by pyrosequencing, implying an overall discordance of only 7%. No patient was classified mutated by HRM but wild type by pyrosequencing. Thus, pyrosequencing may have a slightly higher sensitivity. It furthermore allows conclusions about the exact type of mutation. This might be relevant e.g. for KRAS, as only the glycine to valine mutation on codon 12 may influence prognosis significantly.[4, 120] However, analyzed DNA fragments for pyrosequencing are small and the exact location of the putative mutation must be known. HRM allows detection of mutations anywhere in a PCR amplicon. With reliable results, HRM screening can be performed on huge sample sizes at one time and provides a robust tool for daily practice.

6.4 Risk prediction for stage II colon cancer patients

Currently, it is not possible to further refine individual prediction of prognosis by relying solely on clinical parameters and TNM subgroups for colorectal cancer, as our own analysis has shown.[82] Therefore, characterization of patients according to their genetic and epigenetic alterations, in addition to the established clinical factors, may improve prognostic models and allow individualized tumor therapy. The present study demonstrates that assessment of molecular markers is feasible for the identification of patients at high risk within a clinically homogeneous collective of stage II colon cancer.

Of note, molecular alterations were detected in expected frequencies (KRAS: 30%; BRAF: 15%; microsatellite instability: 26%), indicating that the collective analyzed here reflects the characteristics of the general population of patients with stage II colon cancer.[26] Moreover, inter-marker correlations confirmed findings described earlier; e.g., mutations in the oncogenes KRAS and BRAF, which belong to the same signaling pathway, were mutually exclusive.[26, 93] BRAF mutations were significantly correlated with microsatellite instability, but were not significantly correlated with prognosis.[66] Expression of the Wnt target gene Osteopontin was repeatedly found to be of prognostic relevance in colon cancer, including metastasized tumor stages, by our group and by others.[55, 96] However, even though Osteopontin was significantly overexpressed in tumors, its expression did not predict outcome. Abnormal Wnt activation due to mutation of APC usually occurs early in colorectal carcinogenesis and possibly does not significantly differ within the subset of stage II patients.[74, 128] In accordance with recent reports[26, 51], patients with KRAS mutant tumors were at slightly higher risk of developing metachronous metastasis. In detail, the number of patients with distant metastasis was significantly higher in the KRAS mutant group (p=0.033) in the Pearson's chi-squared test. However, the time-dependent survival distributions did not differ significantly for KRAS mutant and wild type patients (logrank test, p=0.062, Figure 15). Even though the KRAS mutation status is important for prediction of response to anti-EGFR therapy, its prognostic value is currently a matter of debate.[26] Various reports either encourage or dismiss KRAS

mutations as prognostic biomarker.[26] Microsatellite instability is thought to be the most relevant biomarker for identifying a low-risk group of approximately 20% of all colorectal cancer patients today.[8, 9, 19, 20] Microsatellite instable tumors are specifically associated with female patients, right-side colon localization, and BRAF mutation[17], which is also reflected in the patient collective analyzed here (Table 7). Albeit not exactly known, the favorable prognosis of microsatellite instable patients may be caused by novel peptide epitopes which are created in tumor cells with instable DNA repeats, leading to increased host anti-tumoral immune reactions.[17, 43]

Importantly, at the individual marker level, MACC1 expression was confirmed as a biomarker predicting formation of metastasis, outperforming microsatellite stability status, as well as KRAS and BRAF mutation status. The results suggest that high MACC1 expression and concomitant KRAS mutation indicate high risk, arguing for adjuvant therapy in this group of patients. Whether a high expression of MACC1 is associated with sensitivity or resistance towards a specific form of multimodal therapy remains to be tested. Therefore, further studies are needed in order to proceed from personalized risk stratification to individualized therapy.

6.5 SASH1 and MACC1 in stage II patients

A biomarker which identifies the relatively rare fraction of high-risk stage II patients could have huge clinical impact. The panel employed here comprises the expression of two genes which have specifically been associated with colon cancer metastasis. The candidate tumor suppressor gene SASH1 (SAM- and SH3-domain containing 1) is frequently down regulated at the RNA expression level[95], and MACC1 (Metastasis-associated in colon cancer-1) is often up regulated.[16, 33, 112, 117] In the present study, 20% of the patients had above threshold expression levels of MACC1, which implied a hazard ratio of 6.2 for metachronous metastases. MACC1 was the only prognostic parameter which proved independent of all tested clinical and pathological risk factors (Table 9). In contrast to other reported expression markers, MACC1 has been confirmed repeatedly to be of prognostic relevance for colorectal and other

cancers.[16, 33, 91, 111, 112, 117, 137] Its biological role in the formation of metastases, most likely by enhanced tumor cell scattering induced by its key function as transcriptional coactivator in the prometastastic HGF/cMET pathway, are well documented.[16, 115, 117] Recently, Kennedy et al.[61] developed and independently validated a signature of 634 genes, containing MACC1, to identify high-risk stage II colon cancer patients. Furthermore, in an extensive genome-scale analysis of 276 samples of colorectal cancer by the Cancer Genome Atlas Network, MACC1 was identified to be among the 151 most frequently mutated genes.[22] The present study reports on the largest group of stage II colon cancer patients thus far analyzed, confirming the prognostic value of MACC1, and presents the first validation study with non-microdissected tumor tissue.[33, 112] MACC1 overexpressing tumors were more likely to be microsatellite instable and demonstrated a significant reduction in SASH1 expression, findings that have not been reported previously. The latter, which is in good accordance with earlier in vitro findings, may suggest a functional connection between both genes, which will be discussed further below.

6.6 Established pathways of colorectal cancer

The hypothesis underlying this thesis predicts that patients within one particular tumor stage can be stratified based on the type of molecular alterations, which may fall into several more or less frequent types or classes. The specific combination of mutations and epigenetic or chromosome-level alterations dictates the individual tumor biology, and thus, prognosis and response to therapy. In order to test the collective analyzed here for molecular patterns, patients were allocated into molecular “tumor pathways” according to the results of a two-step cluster analysis, representing the core of the clinical part of this work (Figure 39 and Table 10). Four clusters were predicted by this analysis, based on, e.g., the mutation state of the oncogene KRAS, and expression level of putative metastasis markers. To date, at least three pathways of colorectal cancer are postulated, with clinically, histopathologically, and genetically differing appearances.[55, 59, 66, 74, 86] Molecular determination of colorectal cancer subgroups was repeatedly suggested by different

authors.[55, 59, 74, 86] All proposed classifications thus far are more or less similar to the one by Leggett et al.[66] described in the introduction (Figure 3).

Figure 39: Two-step cluster analysis identified four subgroups of colon cancer in this study, which can be allocated to the Serrated, Traditional, and Alternate pathway previously described by Leggett et al.[66]

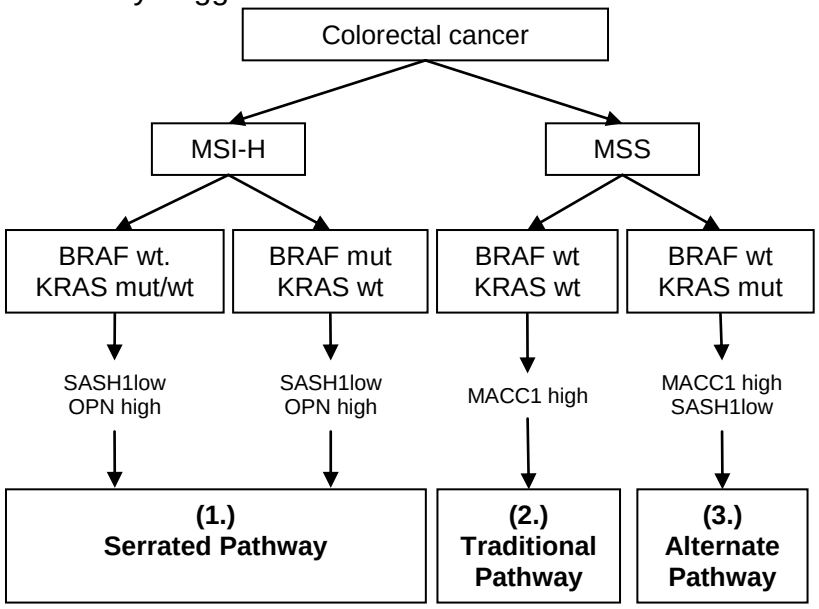

In a review, the late Dr. J. Jass[55] proposed a “speculative” model of five molecular colorectal cancer types (Figure 40): (1.) tumors generally known as “sporadic MSI-high” (methylation of MLH1; 12% of all diagnosed colorectal cancers) that are chromosomally stable, have BRAF mutations, and show a high level of CpG-island methylation (CIMP-high; CIMP: CpG-island methylator phenotype); (2.) tumors that conform to (1.), but are microsatellite-stable (MSS) or have a low level of microsatellite instability (MSI-L) (8%); (3) CIMP-low tumors with KRAS mutation, chromosomal instability and stable microsatellites (MSS or MSI-L; 20%); (4.) sporadic or FAP associated tumors that are CIMP-negative, chromosomally instable and mainly MSS (57%); and, lastly, (5.) lesions attributable to the Lynch syndrome (CIMP-negative, BRAF wild type, chromosomally stable, MSI-H; 3%).

Figure 40: In his review, Jass[55] describes a model of five molecular subtypes of colorectal cancer.

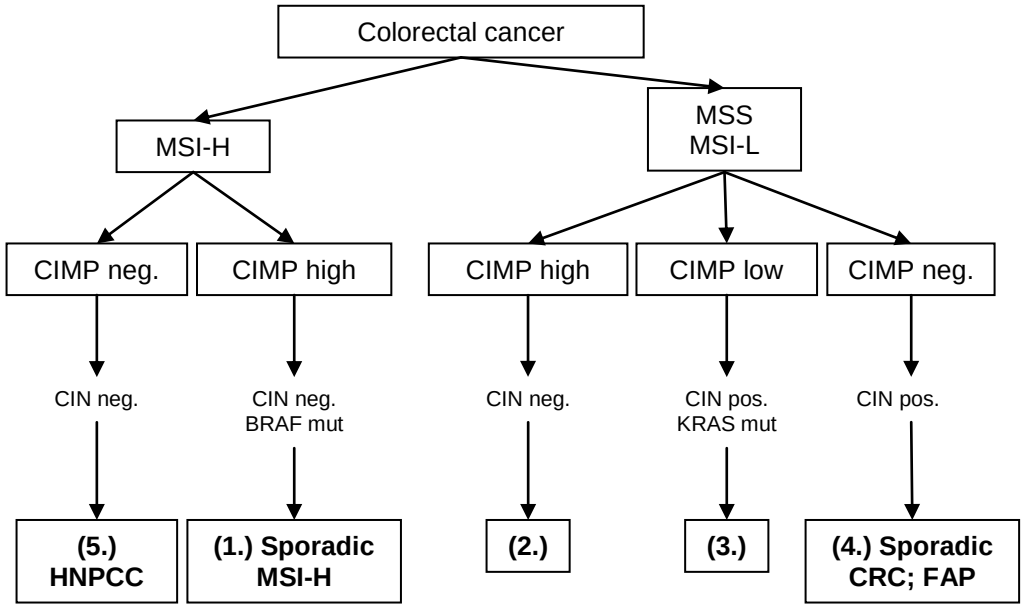

In 2009, a more recent original work by Ostwald et al.[86] confirmed and expanded the classification of Jass[55]. It was based on analysis of DNA content and ploidy by flow cytometry, indicating chromosomal instability (CIN), PCR analysis of the Bethesda marker panel for microsatellite instability (MSI), and bisulfite treatment of genomic DNA followed by quantitative real time PCR to check for the CpG island methylator phenotype (CIMP; Figure 41). Additionally, the mutational status of KRAS, BRAF, TP53 and APC was assessed by a combination of PCR and temperature gradient gel electrophoresis with subsequent sequencing of suspect samples. No survival data are stated, but regarding all possible combinations of CIN, MMR and CIMP, the authors grouped MSI-high patients into the following two groups: (1.) HNPCC if CIMP negative and (2.) sporadic MSI-H if CIMP positive. The remaining majority of MSS/MSI-L patients were divided into the following strata: (3.) CIMP high (only differing from sporadic MSI-H patients due to absence of MLH1 methylation), and CIMP negative (4., “standard” colorectal cancer if chromosomal instable, or 5., triple negative if MSS, CIMP negative and CIN negative). Two further indeterminate groups were described (6., and 7.), with intermediate levels of CIMP or CIN.

Figure 41: The modified flow chart illustrates the approach by Ostwald et al.[86] to classify colorectal carcinomas into subgroups based on microsatellite, CIMP, and CIN status.

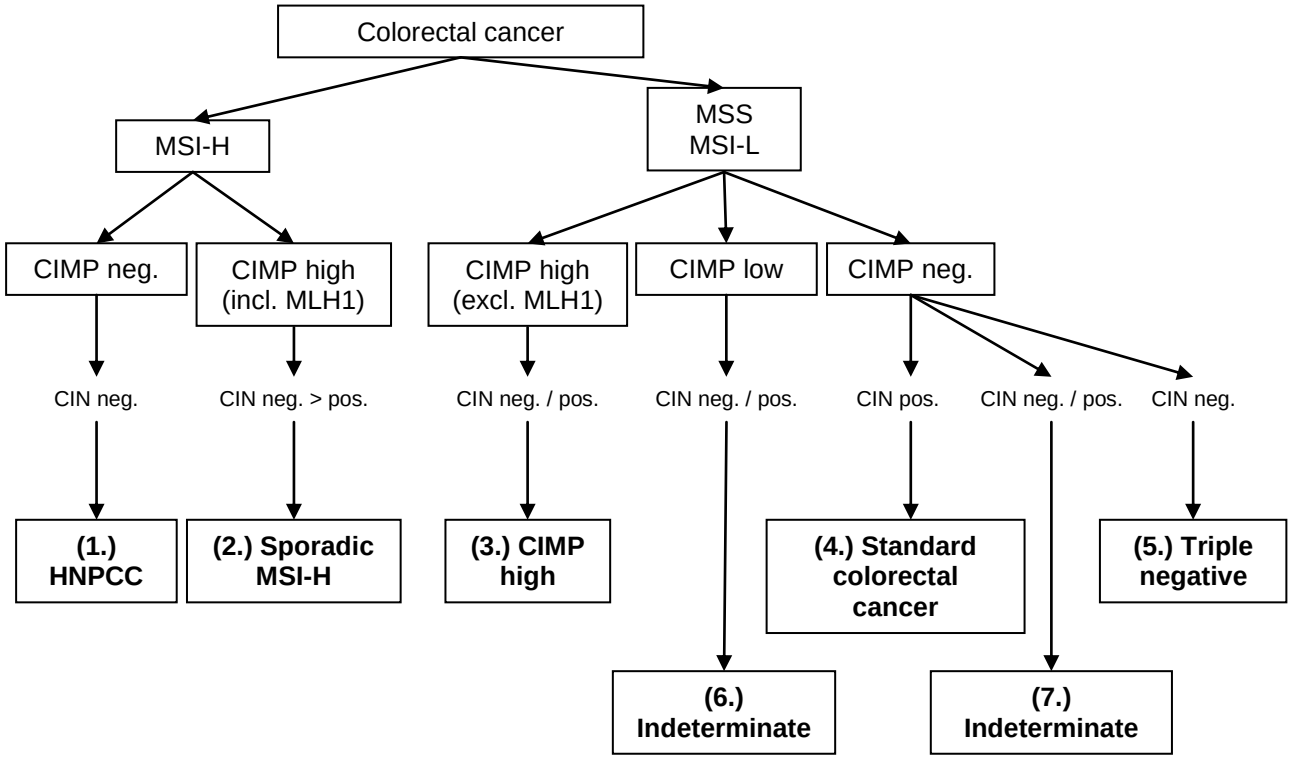

Recently, Kang[59] suggested the basic allocation regarding the two factors microsatellite instability and CpG island methylator phenotype. The author described four possible groups (Figure 42). In this classification, tumors with chromosomal instability (CIN) are reflected by the microsatellite stable and CIMP negative group, whereas the hereditary HNPCC syndrome is incorporated in the microsatellite instable and CIMP negative group. The microsatellite stable and CIMP positive subtype was associated with the worst clinical outcome in this study, especially if associated with KRAS or BRAF mutation.

Figure 42: Kang[59] suggested a classification system for colorectal cancer based on the four possible combinations of microsatellite stable (MSS) or unstable (MSI) and CIMP negative or positive.

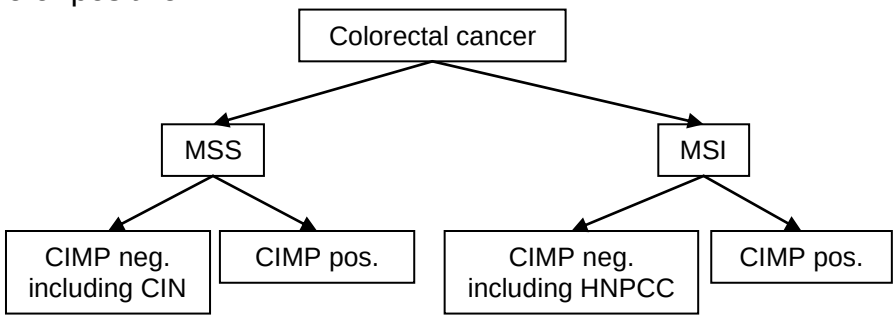

Taken together, allocation of colorectal cancer into molecular subtypes can be carried out in different ways. The model proposed by Leggett et al.[66] maybe provides the most comprehensive classification thus far. The clusters identified here coincide well with the pathways proposed by Leggett and co-workers (Figure 3 and Table 10). Clusters #1 and #2 had the best prognosis; they comprised patients with microsatellite instability and low MACC1 expression levels. Outcome was particularly favorable when associated with BRAF wild type status (only 4% risk of recurrence). These clusters correspond to the “serrated pathway” described by Leggett et al., which is thought to develop initially from so-called “sessile serrated adenomas”, with favorable prognosis and preferred occurrence in the right colon. Cluster #3 comprised tumors of the “traditional pathway”, which are microsatellite stable and have no mutation of KRAS or BRAF. These patients are assumed to have chromosomally instable tumors and aberrant activation of the Wnt pathway by an early occurring loss of function of the β-Catenin destruction complex. In the present study, this group showed an intermediate recurrence risk of 10%. No other obvious aberrations apart from elevated expression of SASH1 were detected. Since SASH1 has been proposed a candidate tumor suppressor, increased expression in the presumed absence of mutations in the coding region might reflect a response to genotoxic or oncogenic stress. Finally, patients allocated to cluster #4 displayed KRAS mutations, microsatellite stable tumors and high MACC1 expression, coinciding with the “alternate pathway”. This group had the most dismal outcome (16% risk of recurrence). Notably, clusters #3 and #4 included the patients with high MACC1 expression levels, suggesting that MACC1/HGF signaling is important in the

traditional and the alternate pathway, and may constitute an additional risk factor for distant metastasis.

6.7 Molecular characteristics of liver metastasis in comparison to the primary colorectal lesions

Liver metastasis can be considered as consequent progression of an initially localized case of colorectal cancer. However, it is not clear whether metastasis really constitutes one of the last molecular steps in the adenoma-carcinoma-sequence as described above, or if genetic tumor characteristics determine the metastatic capability of a tumor already at a very early point of time.[63] Moreover, recent studies indicate a very high and hitherto not anticipated level of intratumoral heterogeneity in solid tumors.[35] Thus, it is likely that metastases share some, but not all of the genetic traits of the primary lesion. To compare genetic alterations of primary tumors and liver metastases, matched samples of both tissue types were analyzed regarding the panel of molecular markers introduced earlier: mutational status of the oncogenes KRAS and BRAF, microsatellite instability, and mRNA expression levels of Osteopontin, SASH1 and MACC1. A high level of consistency between marker status was observed (Figure 19).

Reports in the literature[26, 120] describe lower percentages of microsatellite instability for higher tumor stages (22% in stage II, 12% in stage III, and 2% in stage IV)[24, 116], which was confirmed in this study (26% in stage II, and one out of nine patients with microsatellite instability of the liver metastasis, but not the primary tumor in stage IV). In current studies, more than 90% concordance of markers like KRAS or BRAF was reported, suggesting that diagnosis of mutations is practicable in both, primary tumors and liver metastasis.[64, 125] Surprisingly, MACC1 expression levels in the liver metastases investigated here were lower than in the primary tumors by trend, even though the difference did not attain significance. A possible molecular explanation is that cancer cells, once they have settled in the liver, switch back again from a mesenchymal and migrating phenotype to a more epithelial appearance. In a well-

established liver metastasis, there is obviously no selection pressure to sustain a highly scattering and motile cell phenotype, which would require activated MACC1 signaling. Finally, issues immanent to the experimental setup cannot be excluded at the present stage. The “house-keeping” reference gene HPRT has a similar expression level in primary colorectal cancer and liver metastasis[101], but paracrine stimuli of the surrounding liver parenchyma may influence the regulation of expression levels of other target genes, including MACC1.

6.8 Is there interaction between SASH1 and MACC1, two new metastasis-associated genes, on mRNA or protein level?

Interestingly, in the collective of patients with colon cancer, a significant inverse correlation of SASH1 and MACC1 expression levels was observed (Table 7). Of note, microarray experiments that were performed previously in our laboratory in SW480 cells with a stable knockdown of SASH1 are in line with this results.[75] Reduction of SASH1 expression led to a significant (change more than two fold) de-regulation of 367 gene transcripts. With a 2.98-fold increase and a low false discovery rate (FDR) of 0.01 for MACC1, only six transcripts were more strongly up-regulated. On the other hand, artificial overexpression of SASH1 by transient transfection with V5-tagged SASH1 led to relevant upregulation of only 34 and to downregulation of 12 transcripts, not including MACC1 (1.03-fold increase).[75] Thus, a reduction of SASH1 expression had far greater biological consequences than an increase of its transcription. The earlier microarray results were confirmed in the present work by an independent method (quantitative rtPCR) on the previously established SASH1 knockdown SW480 clones (Figure 27). Thus, the apparent co-regulation of SASH1 and MACC1 led to the working hypothesis that SASH1 is a negative regulator of MACC1 expression. A functional connection of both markers has not been described before. A lack of function of the putative tumor suppressor SASH1 would lead, according to this hypothesis, to an increased expression of the oncogene and metastasis-inducer MACC1. A critical evaluation of this hypothesis

constitutes the second part of this study, which is focused on in vitro experiments in established cell lines.

6.9 Expression pattern of MACC1 and SASH1 in cell lines

A panel of established human colorectal cancer cell lines was analyzed, and found to differ in SASH1 and MACC1 expression levels (Figure 20), which is in good accordance with earlier results.[117, 138] Data by Alexandra Gnann from our laboratory suggest an epigenetic regulation by methylation of CpG-residues in the promoter region for SASH1. Similar but so far preliminary results have been obtained also for MACC1, depending on the specific cell line tested, which could at least in part explain deviations between different cell lines (not shown). To our knowledge, no sequencing analysis to investigate mutations of the coding regions of different cell lines has been described in the literature so far. In a recent large-scale genome wide analysis, MACC1 was identified among the 151 most frequently mutated genes in patients with colorectal cancer.[22] Interestingly, MACC1 expression was not detectable by quantitative rtPCR in Hek293 cells – the only here investigated cell line derived from non-malignant tissue (Human Embryonic Kidney). This is in line with a role of MACC1 for malignant transformation, described previously in the literature.[117]

Differences in mRNA expression were clearly observable in cell lines and human tissue; however, there was no clearly significant correlation between SASH1 and MACC1 mRNA levels in the cell lines analyzed (Figure 20). Detection of protein levels of SASH1 by Western Blot and immunofluorescence using a custom made polyclonal antibody has been described before.[75, 76] After establishment of the immunoblotting protocol, one commercial antibody revealed feasible results for MACC1 in Western Blot analysis (Santa Cruz) and another one in immunofluorescence (ProSci). However, protein levels detected by Western Blot from lysates of cell lines revealed higher accordance with RNA expression than did MACC1 detection by immunofluorescence staining of tissue sections (Figure 21). Next, the intracelluar distribution of the putative transcription factor MACC1 was

analyzed. Detection of MACC1 protein after dividing the cellular compartments into nucleic, cytoplasmatic, and crude membrane fractions (Figure 23) confirmed higher MACC1 concentrations in SW620 cells than in SW480 cells, as expected.[117] Highest concentrations were identified in the nucleus, in line with previously published observations.[117] The reliability of the cell compartments was confirmed by different loading controls, with tubulin serving as control for the cytoplasm. Some contamination in the nucleic and membranous compartments was found, most likely caused by technical issues, like incomplete cell lysis prior to the subcellular fractionation.

Another possible explanation for different MACC1 expression levels in cell lines and tumors was given by Zhang Y. et al.[138], who identified Micro RNA 143 as putative inhibitor of MACC1. Non-coding small RNAs (miRNAs) inhibit translation or directly induce degradation of a variety of expressed genes by integrating into an RNA-inducing silencing complex (RISC) and binding to specific complementary sites within 3' untranslated regions of their target gene mRNAs.[138] They can function as tumor suppressors or oncogenes; miRNA 143 has been shown to be reduced in colorectal cancer. Interestingly, Zhang Y. et al.[138] found lower miRNA 143 levels in SW620 than in SW480 cells, and a negative correlation to MACC1 expression levels. Using the online miRNA target prediction databases *miRNA.org* and *Targetscan*, a predicted miRNA 143 binding site within the MACC1 3' UTR was identified. By luciferase reporter study, the authors verified that miRNA 143 directly targets MACC1 through binding to a specific complementary site within its 3' untranslated region. Furthermore, tumorigenic characteristics of SW620 cells were repressed after transfecting miRNA 143 into SW620 cells. On the other side, tumorigenic characteristics of SW480 cells were increased after transfecting miRNA 143 inhibitors. Synergistic effects on MACC1 expression were observed when treating SW620 cells with siRNA against MACC1 in combination with miRNA 143 mimetics.[138]

6.10 The role of MACC1 in the context of altered signaling pathways in colorectal cancer

As discussed earlier, colon cancer can be grouped in at least three distinct "pathways", based on the nature of the specific alterations. In the following, the newly described metastasis marker MACC1 will be discussed, with regards to its interactions and functional connections with well-established signaling cascades, such as growth factor receptor/KRAS signaling, or the Wnt pathway. The hepatocyte growth factor/scatter factor (HGF) has been described to lead to activation of cMET signaling in vitro, forming a positive feedback loop.[118] The resulting increased amounts of cMET protein, the membrane bound receptor of HGF, might then lead to even more binding of HGF molecules, further enhancing HGF/cMET signaling, which has been described to be connected to increased cell motility, proliferation, and finally metastasis formation.[5] A MACC1-driven positive feedback activation of this pathway has been described, which is capable of increasing the metastatic process.[5, 116]

Furthermore, MACC1 may be a downstream target gene of the growth factor receptor / MAPK signaling pathway.[5, 117] Proliferation of colon cancer cells is regulated in large parts by the Epidermal growth factor receptor (EGFR), which activates a cascade of downstream components, including the GTPase KRAS, and finally a kinase cascade composed of BRAF, and the MAPKs.[117] It has been shown that HGF stimulation also leads to downstream activation of the EGFR/KRAS pathway (via MAPK and PI3K).[69] Upregulation of cMET and activating KRAS mutations may support and even require each other for the formation of tumorigenicity[69], possibly enabling cross-pathway reactions consecutive to MACC1/HGF stimulation. From the cell lines investigated here, only HT29 are KRAS wild type.[18, 109] However, no systematic association of MACC1 expression with KRAS mutation status was observable in our analysis.

cMET can also contribute to activation of the Wnt pathway, another central driver of colon carcinogenesis, by transcriptional activation of Wnt ligands, such as Wnt7B.[37] Further, cMET dependent induction of target genes of β-Catenin, TCF, and Lymphoid enhancer-binding factor (LEF) has been reported;[32, 44] e.g., through tyrosine phosphorylation and nuclear targeting of β-Catenin, or by inhibition of the β-Catenin degradation complex by Akt-mediated phosphorylation of the glycogen synthase kinase-3β (GSK).[37]

As expected, HGF stimulation led to ERK1/2 phosphorylation in our experiments (Figure 24)[69], to upregulation of MACC1 (Figure 25), but not to increased cell proliferation (Figure 26). Of note, SW620 cells did respond to HGF treatment by downregulation of the proposed MACC1 antagonist SASH1, even though this effect did not attain significance, and was not observed in other cell types, like DLD1 (Figure 25).[69] The finding that DLD1 cells act differently after interfering with MACC1/HGF signaling was also observed after siRNA treatment against MACC1 (MACC1 knockdown, Figure 27). DLD1 cells, in contrast to the cell lines SW480 and SW620, responded by SASH1 downregulation. SW480 cells are lacking cMET expression, the cellular HGF receptor.[136] This finding may explain the minimal ERK phosphorylation after HGF treatment (Figure 24) and the lacking response of MACC1 gene expression (Figure 25). In contrast, SW620 cells do express cMET, and consequently respond to HGF stimulation by upregulation of MACC1, as expected.

6.11 Knockdown of SASH1 and MACC1 reveals cell-type specific evidence for mutual regulation

For transient knockdown of SASH1 and MACC1, cell lines with low (SW480), intermediate (DLD1) and high (SW620) transcript levels of the genes were chosen (Figure 27). A significant reduction of gene expression levels after SASH1 knockdown was obtained in SW480 and DLD1, but not in SW620 cells. A significant reduction of gene expression after MACC1 knockdown was obtained in SW620 and

DLD1, but not in SW480 cells, presumably due to low endogenous MACC1 levels in SW480. After exploratory transient siRNA transfection experiments, stable expressing clones were obtained based on SW620 and HCT116 cells, which both demonstrated promising transfection efficiency (Figure 30). However, in contrast to the earlier findings in other cell lines, neither SASH1 nor MACC1 knockdown did influence gene expression levels of the other gene, respectively. Thus, a negative association of the transcription of both genes could not be formally confirmed, similar to the results found in DLD1 cells before (Figure 27). Yet, no conclusive explanation for these differing effects upon stable gene knockdown is available, apart from the long process of clonal selection and sub-passaging required for both cell lines, which may render the approach quite sensitive to aberrations. Based on the assumption that SASH1 and MACC1 indeed interfere with each other, cell line specific differences may occur due to mutations or epigenetic silencing of different genes. Cell line specific effects and possible differences even between individual clones of the same parental cell line could also explain, at least in part, the difficulties encountered during the unsuccessful attempts of establishing stable knockdown clones in the cell line HT29, or SW620 cells with clearly reduced SASH1 levels. Analysis of changes of protein levels of SASH1 and MACC1 could have provided further clarity.

6.12 SASH1/MACC1: no evidence for mutual protein-protein interactions

Since the proteins encoded by SASH1 and MACC1 have been found to be co-expressed in some of the colon cancer cell lines in this work, and are localized to the same intracellular compartment, i.e., the nucleus, it is tempting to speculate that there is a direct or indirect interaction on the protein level. Moreover, MACC1 has been reported as transcription cofactor for the cMET gene, and previous results from our laboratory indicate that SASH1 may regulate the transcription level of a number of genes. Therefore, the proteins encoded by both genes may play a common role in gene transcription control, or counteract each other’s activity. Unbalancing of this

interaction may be a causative factor in carcinogenesis. To confirm or exclude interactions between SASH1 and MACC1 proteins, each was precipitated with specific antibody-labeled Sepharose beads (Immunoprecipitation or “pull-down” approach). Consecutive Western Blot analysis revealed no presence of the respective other protein (Figure 33), suggesting there is no direct or indirect binding under the circumstances tested. Thus, other regulatory mechanisms may be involved in the putative co-regulation of these two factors. This result is in line with previous findings from our laboratory group, where MACC1 protein was not identified among binding partners of SASH1 in a mass-spectrometry approach of putative SASH1-interaction partners (A. Gnann, K.-P. Janssen, unpublished observations).[75]

Of note, the functional and prognostic role of MACC1 surpasses the activation of its hitherto only identified transcriptional target cMET upon direct comparison.[33, 117] To identify additional putative gene promoter regions that may be regulated by MACC1, Galimi et al.[33] performed sophisticated *in silico* enrichment analyses on published gene sets. They identified 129 transcripts as putative MACC1 targets, including cMET, interaction partners of RAP1A and KRAS (ral guanine nucleotide dissociation stimulator RALGDS), factors of the Wnt signaling pathway (frizzled homolog drosophila FZD10), negative regulators of the MAPK superfamily (dual specificity phosphatase DUSP18), ring finger protein RNF170, which plays a role in the ubiquitination pathway, and factors with putative structural similarity to SASH1 (sterile alpha motif domain containing SAMD12, and coiled-coil domain containing CCDC92). However, SASH1 itself was not included.[33]

6.13 Stability and half-life of MACC1 transcript is not influenced by SASH1 expression

As described above, upregulation of MACC1 transcripts after SASH1 knockdown was observed in SW480 cells (Figure 20). However, overexpression of SASH1 did not lead to relevant changes of MACC1 expression.[75] These findings led to the

working hypothesis that SASH1 may negatively regulate MACC1 transcription. Two alternative, but not mutually exclusive mechanisms are feasible to explain our observations: (1.) reduced stability of MACC1 mRNA resulting from direct or indirect SASH1 effects, or (2.) inhibition of de novo MACC1 transcription by SASH1. Mechanism (1.) may be mediated by direct action of SASH1 protein on the transcript of MACC1, since the SAM-domains, which are present in SASH1, have been described in homologous proteins to bind directly to RNA. Mechanism (2.) could be mediated by a transcriptional silencing effect of SASH1 at the MACC1 gene locus. However, both proposed mechanisms could also be of indirect nature, and involve further yet unknown interaction partners. To investigate whether SASH1 has an influence on MACC1 mRNA stability, the half-life and stability of transcripts was recorded in cells with physiological SASH1 levels and after SASH1 knockdown (Figure 34 and Figure 35).

The physiological importance of mRNA stability lies in the need for the cell to quickly adjust mRNA levels in response to intrinsic or extrinsic stimuli, even in the absence of altered transcription.[133] Aberrations of this regulatory mechanism during carcinogenesis are possible, albeit they remain largely uncharacterized. The 3' untranslated region [35] of MACC1 contains several AU-rich elements (AREs, e.g., UUUUU, AUUUA, AUUUUA, $(U)_{5-7}$). These short "instability elements" can facilitate RNA stabilization or destabilization by altered nuclease activity through ARE binding proteins like Tristetraprolin (TTP) or Heterogeneous nuclear ribonucleoprotein D0 (HNRNPD), also known as AU-rich element RNA-binding protein 1 (AUF1).[19, 107, 133] AREs are found in proto-oncogenes (for example, cFOS), inflammatory mediators (for example, TNFα), Interleukin 1/2/3, and Granulocyte macrophage colony-stimulating factor (GM-CSF).[107] In a recent review, Wu et al.[133] describe a possible role of the SASH1 interacting protein 14-3-3σ[75] for the nucleocytoplasmatic transport of AUF1 isoforms, which accelerates mRNA decay through AREs.

Additionally, several alternative polyadenylation sites in the 3' UTR of MACC1 (hexameric polyadenylation signals, e.g., AAUAAA) could lead to mature transcripts with 3' ends of variable length by cleavage at different sites.[10] As UTRs often contain

regulatory elements affecting mRNA stability or translation efficiency, the choice of alternate polyadenylation sites could be influenced by SASH1 and may affect final MACC1 expression levels, as well.[10] According to this hypothesis, MACC1 transcripts would be less stable in cells with high SASH1 levels. However, no significant differences were observed for SW480 cells with different SASH1 mRNA expression levels (Figure 35). A further aspect arguing against the putative role for SASH1 in RNA degradation is that MACC1 transcript reduction was most distinct in SW480 cells, as compared to HCT116, HT29 and SW620 (Figure 34). While MACC1 expression levels vary strongly between these four cell lines, SW480 are the only cells with clearly lower SASH1 expression levels (Figure 20).

Since the mRNA stability of MACC1 has not been described previously, we describe here for the first time a generally reduced stability of MACC1 mRNA in SW480 cells as compared to other transcripts. This suggests that regulation of mRNA stability may be a major axis for the co-regulation of SASH1 and MACC1. Finally, since a Micro RNA dependent silencing of MACC1 transcripts has been reported, an interaction between SASH1 and MACC1 mediated by miRNAs is feasible.[133]

6.14 Protein stability of MACC1 and SASH1

Similar to the mRNA level, few data are available on the protein stability of SASH1 and MACC1.[75, 117] To gather evidence of protein stability and of possible regulatory mechanisms, concentrations were analyzed at different points of time after inhibition of new protein biosynthesis (Figure 36). Despite technical difficulties of MACC1 detection related to insufficient specificities of commercial antibodies, SASH1 protein revealed a relatively high time dependent stability.

Lang et al.[65] described recently a SNP variant in an intronic region of MACC1 (rs1990172), which does not affect any splice site of a coding exon, but may correlate with patient survival. Another work by Schmid et al.[105] from Prof. U. Stein's

group also investigated the clinical role of MACC1 single nucleotide polymorphisms (SNPs) and was published only some months later. Here, the authors confirmed three SNPs for MACC1 in a cohort of 154 patients with colorectal cancer stages I to III. In detail, the variant L41V was observed in 13% of cases; the variant S515L in 48% of cases; and finally, the SNP R804T in 48% of cases (aga/aga to aga/aca, respectively in 36%: aga/aga to aca/aca).[105] However, no association of these SNPs with MACC1 expression, formation of metastasis, age, gender, or clinicopathological parameters was identified in this study. In accordance with these findings, induced expression of MACC1 SNPs in cell line experiments did not affect cell motility or proliferation.[105] Thus, common SNPs do not seem to play a relevant role for the functional activity of MACC1, further suggesting that they do not influence RNA or protein stability, as well.

6.15 MACC1 activates cell migration, but not cell proliferation

In accordance to previous observations[117], MACC1 signaling was found to be relevant for the cell-scattering associated with an activation of the HGF/cMET pathway in this work. Thus, we could confirm a more pronounced effect of MACC1 signaling in cell migration than in proliferation. In a wound healing assay, a clearly reduced migratory rate was observed for SW620 cells with reduced expression of MACC1 when compared to corresponding controls (Figure 38). An XTT based cell proliferation assay did not reveal any significant differences in the growth rate of SW620 cells, with respect to MACC1 expression levels or HGF stimulation (Figure 37). Whether the reduced growth of HCT116 cells with MACC1 knockdown can indeed be attributed to reduced MACC1 expression, needs to be confirmed by further testing.

Our findings regarding MACC1 dependent migration are in line with data reported by Stein et al.[117] However, Prof. Stein described significantly higher growth rates of SW480 cells transfected with MACC1 under HGF stimulation, when compared to unstimulated cells. Similar to these experiments, Zhang RT. et al.[137] generated

ovarian cancer cells (OVCAR-3) with RNA interference against MACC1. The starting point for this work was the authors' observation of elevated MACC1 levels in ovarian cancer compared to normal ovary or benign tumors. From three specific shRNAs against MACC1, Zhang and co-workers selected the one with the most promising results upon quantitative rtPCR-based expression analysis. MACC1 knockdown by the selected shRNA led to significant inhibition of growth in an MTT assay. Further, the migration ability in a transwell migration assay and monolayer cell migration wound healing assay was suppressed. Finally, after MACC1 knockdown, Zhang RT. et al. report reduced invasion in a Matrigel invasion assay.[137] Thus, the invasion behavior of the stable MACC1 knock-down clones generated in this work should be studied in future experiments, in order to find out whether the previously described effects for MACC1 on invasion can be confirmed as generalized observation, or have to be considered as cell-type specific, similar to the effects on cell proliferation described here.

6.16 Outlook

Further experiments could clarify possible functions and interactions of SASH1 and MACC1 in more detail. SASH1 may bind to the MACC1 promoter region as a negative regulator of transcription. A chromatin immune precipitation (ChIP) assay may identify putative transcription factors of MACC1. Furthermore, the effects of MACC1 upregulation – in addition to the inhibition of endogenous MACC1 expression reported here – would be needed to investigate the phenotypical consequences of high versus low expression rates of SASH1 and MACC1. Next, invasion assay experiments should be performed (Boyden chamber, with the extracellular matrix surrogate Matrigel), which more closely resemble the clinical phenomenon of invasion than 2D cell migration assays. To promote the encouraging retrospective results of MACC1 for prediction of prognosis in patients with colon cancer, the next step would be a prospective clinical observational trial. Besides the usefulness of MACC1 for diagnostic purposes, further studies may also identify whether it constitutes a target for therapeutic interventions. Inhibition of MACC1, which has no reported enzyme acitivity, may prove to be difficult. However, inhibitors of the

cMET/HGF pathway are currently tested in phase I clinical trials.[80] The effects of cMET pathway inhibition on MACC1 should be studied in detail.

7 Synopsis

7.1 English

This work describes signaling pathways and their interactions relevant for metastasis formation in colorectal cancer. Stable DNA microsatellites, low expression levels of the candidate tumor suppressor gene SASH1 and high expression levels of the metastasis associated gene MACC1 were associated with poor prognosis for stage II colorectal cancer patients (n=232). Despite currently being considered as potential risk indicators, neither established clinical factors, nor mutation status of the oncogenes KRAS and BRAF, nor the activity level of the Wnt pathway, allowed a reliable prognostic stratification. Expression of MACC1 was the only independent prognostic marker predicting the risk of distant metastasis (HR 6.2; 95% CI 2.4-16; p<0.001). By integrative marker analysis, individual tumors could be assigned into previously described molecular genetic pathways of colorectal cancer. Importantly, distinct risk profiles could be confirmed for these molecular cancer subtypes. Tracking of the marker status in matched samples of primary colorectal tumors and corresponding liver metastasis confirmed molecular consistency between both entities. Moreover, an inverse correlation of SASH1 and MACC1 expression was detected in patients, indicating that SASH1 may inhibit MACC1 expression. This causal dependency was probed, and could be confirmed in colorectal cancer cell lines by siRNA-mediated gene knockdown. However, no direct or indirect interactions could be identified on the protein level for MACC1 and SASH1. Aberrant cell type-specific regulatory processes may play a role, which affect mRNA stability and provoke reduced stability of MACC1 mRNA, as compared to SASH1. Finally, cells with a stable reduction of MACC1 expression had a less aggressive phenotype, in line with its presumed role as metastasis-enhancing factor.

7.2 Deutsch

Diese Arbeit befasst sich mit molekulargenetischen Signalwegen und ihren Interaktionen, die beim kolorektalen Karzinom relevant für das Entstehen von Metastasen sind. In einem Patientenkollektiv des Tumorstadiums II (n=232) zeigten sich Mikrosatellitenstabilität, niedrige Expressionswerte des Tumorsuppressorgens SASH1 und hohe Expression des „Metastasierungsgens“ MACC1 als prognostisch ungünstig. Die derzeit diskutierten Prognosemarker KRAS, BRAF, eine aberrante Aktivierung des Wnt Signalwegs, sowie etablierte klinische Parameter erlaubten dagegen keine zuverlässige Risikoabschätzung. MACC1 war der einzige unabhängige Prognosefaktor für die postoperative Entwicklung von Fernmetastasen (HR 6,2; 95% CI 2.4-16; p<0,001). Im Rahmen einer integrativen Markeranalyse gelang es, individuelle Kolonkarzinome zuvor postulierten molekular definierten Gruppen zuzuordnen. Es konnte nachgewiesen werden, dass die molekulargenetisch basierte Stratifizierung mit unterschiedlichen Risikoprofilen verbunden war. Um die Entwicklung der Biomarker während des Metastasierungsprozesses zu überprüfen, wurde ein weiteres Patientenkollektiv untersucht, das aus Primärtumoren mit zugehörigen Normalgeweben und Lebermetastasen bestand. Hier zeigte sich eine hohe Übereinstimmung der molekularen Marker zwischen beiden Entitäten. Darüber hinaus ließ sich in den Kolonkarzinomen eine inverse Korrelation der Genexpression von SASH1 und MACC1 beobachten. Spezifische siRNA-vermittelte Hemmversuche in Darmkrebszelllinien bestätigten einen kausalen Zusammenhang, der auf eine Inhibition der MACC1 Expression durch SASH1 hinweist. Es konnten jedoch keine direkten oder indirekten Proteininteraktionen zwischen SASH1 und MACC1 nachgewiesen werden. Der Zusammenhang scheint daher durch andere Mechanismen bedingt zu sein, möglicherweise durch Zelltyp-spezifische Regulationsprozesse, welche die RNA Stabilität beeinflussen und für die kurze Lebensdauer der MACC1 RNA im Vergleich zu SASH1 RNA verantwortlich sind, die in Versuchen ermittelt wurde. Schließlich führte die stabile Reduktion der MACC1 Expression in Darmkrebszelllinien zu einem weniger aggressiven Zellwachstum, was in guter Übereinstimmung mit der vermuteten Rolle von MACC1 als Metastasierungsfaktor steht.

8 References

1. Abal M., Obrador-Hevia A., Janssen K.P., Casadome L., Menendez M., Carpentier S., Barillot E., Wagner M., Ansorge W., Moeslein G., Fsihi H., Bezrookove V., Reventos J., Louvard D., Capella G., Robine S., *APC inactivation associates with abnormal mitosis completion and concomitant BUB1B/MAD2L1 up-regulation.* Gastroenterology, 2007. **132**(7): p. 2448-58.
2. Al-Haj L., Blackshear P.J., Khabar K.S., *Regulation of p21/CIP1/WAF-1 mediated cell-cycle arrest by RNase L and tristetraprolin, and involvement of AU-rich elements.* Nucleic Acids Res, 2012. **40**(16): p. 7739-52.
3. Altekruse S.F., Kosary C.L., Krapcho M., al. e. *SEER Cancer Statistics Review, 1975-2007 [SEER web site].* 2010 October 8, 2010 [cited 2012 September 01]; Available from: http://seer.cancer.gov/csr/1975_2007/.
4. Andreyev H.J., Norman A.R., Cunningham D., Oates J., Dix B.R., Iacopetta B.J., Young J., Walsh T., Ward R., Hawkins N., Beranek M., Jandik P., Benamouzig R., Jullian E., Laurent-Puig P., Olschwang S., Muller O., Hoffmann I., Rabes H.M., Zietz C., Troungos C., Valavanis C., Yuen S.T., Ho J.W., Croke C.T., O'Donoghue D.P., Giaretti W., Rapallo A., Russo A., Bazan V., Tanaka M., Omura K., Azuma T., Ohkusa T., Fujimori T., Ono Y., Pauly M., Faber C., Glaesener R., de Goeij A.F., Arends J.W., Andersen S.N., Lovig T., Breivik J., Gaudernack G., Clausen O.P., De Angelis P.D., Meling G.I., Rognum T.O., Smith R., Goh H.S., Font A., Rosell R., Sun X.F., Zhang H., Benhattar J., Losi L., Lee J.Q., Wang S.T., Clarke P.A., Bell S., Quirke P., Bubb V.J., Piris J., Cruickshank N.R., Morton D., Fox J.C., Al-Mulla F., Lees N., Hall C.N., Snary D., Wilkinson K., Dillon D., Costa J., Pricolo V.E., Finkelstein S.D., Thebo J.S., Senagore A.J., Halter S.A., Wadler S., Malik S., Krtolica K., Urosevic N., *Kirsten ras mutations in patients with colorectal cancer: the 'RASCAL II' study.* Br J Cancer, 2001. **85**(5): p. 692-6.
5. Arlt F., Stein U., *Colon cancer metastasis: MACC1 and Met as metastatic pacemakers.* Int J Biochem Cell Biol, 2009. **41**(12): p. 2356-9.
6. ATTC. *[ATTC web site].* 2012 [cited 2012 September 01]; Available from: http://www.atcc.org.

7. Balmert A., *Molekulargenetische Faktoren zur Prognose und Prädiktion des Krankheitsverlaufes beim Kolorektalkarzinom*. 2011, Master's Thesis, Technische Universität München.
8. Bamford. *The COSMIC (Catalogue of Somatic Mutations in Cancer) database and website*. 2012 [cited 2012 September 01]; Available from: http://www.sanger.ac.uk/genetics/CGP/cosmic, Br J Cancer, 91,355-358.
9. Bardelli A., Siena S., *Molecular mechanisms of resistance to cetuximab and panitumumab in colorectal cancer.* J Clin Oncol, 2010. **28**(7): p. 1254-61.
10. Beaudoing E., Gautheret D., *Identification of alternate polyadenylation sites and analysis of their tissue distribution using EST data.* Genome Res, 2001. **11**(9): p. 1520-6.
11. Beer S., Simins A.B., Schuster A., Holzmann B., *Molecular cloning and characterization of a novel SH3 protein (SLY) preferentially expressed in lymphoid cells.* Biochim Biophys Acta, 2001. **1520**(1): p. 89-93.
12. Behrens J., *The role of the Wnt signalling pathway in colorectal tumorigenesis.* Biochem Soc Trans, 2005. **33**(Pt 4): p. 672-5.
13. Benson A.B., 3rd, *New approaches to assessing and treating early-stage colon and rectal cancers: cooperative group strategies for assessing optimal approaches in early-stage disease.* Clin Cancer Res, 2007. **13**(22 Pt 2): p. 6913s-20s.
14. Benson A.B., 3rd, Schrag D., Somerfield M.R., Cohen A.M., Figueredo A.T., Flynn P.J., Krzyzanowska M.K., Maroun J., McAllister P., Van Cutsem E., Brouwers M., Charette M., Haller D.G., *American Society of Clinical Oncology recommendations on adjuvant chemotherapy for stage II colon cancer.* J Clin Oncol, 2004. **22**(16): p. 3408-19.
15. Benzinger A., Muster N., Koch H.B., Yates J.R., 3rd, Hermeking H., *Targeted proteomic analysis of 14-3-3 sigma, a p53 effector commonly silenced in cancer.* Mol Cell Proteomics, 2005. **4**(6): p. 785-95.
16. Boardman L.A., *Overexpression of MACC1 leads to downstream activation of HGF/MET and potentiates metastasis and recurrence of colorectal cancer.* Genome Med, 2009. **1**(4): p. 36.
17. Boland C.R., Goel A., *Microsatellite instability in colorectal cancer.* Gastroenterology, 2010. **138**(6): p. 2073-2087 e3.

18. Buck E., Eyzaguirre A., Barr S., Thompson S., Sennello R., Young D., Iwata K.K., Gibson N.W., Cagnoni P., Haley J.D., *Loss of homotypic cell adhesion by epithelial-mesenchymal transition or mutation limits sensitivity to epidermal growth factor receptor inhibition.* Mol Cancer Ther, 2007. **6**(2): p. 532-41.
19. Chamboredon S., Ciais D., Desroches-Castan A., Savi P., Bono F., Feige J.J., Cherradi N., *Hypoxia-inducible factor-1alpha mRNA: a new target for destabilization by tristetraprolin in endothelial cells.* Mol Biol Cell, 2011. **22**(18): p. 3366-78.
20. Chen E.G., Chen Y., Dong L.L., Zhang J.S., *Effects of SASH1 on lung cancer cell proliferation, apoptosis, and invasion in vitro.* Tumour Biol, 2012. **33**(5): p. 1393-401.
21. Claudio J.O., Zhu Y.X., Benn S.J., Shukla A.H., McGlade C.J., Falcioni N., Stewart A.K., *HACS1 encodes a novel SH3-SAM adaptor protein differentially expressed in normal and malignant hematopoietic cells.* Oncogene, 2001. **20**(38): p. 5373-7.
22. *Comprehensive molecular characterization of human colon and rectal cancer.* Nature, 2012. **487**(7407): p. 330-7.
23. Cunningham D., Atkin W., Lenz H.J., Lynch H.T., Minsky B., Nordlinger B., Starling N., *Colorectal cancer.* Lancet, 2010. **375**(9719): p. 1030-47.
24. de Lau W., Barker N., Low T.Y., Koo B.K., Li V.S., Teunissen H., Kujala P., Haegebarth A., Peters P.J., van de Wetering M., Stange D.E., van Es J.E., Guardavaccaro D., Schasfoort R.B., Mohri Y., Nishimori K., Mohammed S., Heck A.J., Clevers H., *Lgr5 homologues associate with Wnt receptors and mediate R-spondin signalling.* Nature, 2011. **476**(7360): p. 293-7.
25. De Roock W., Biesmans B., De Schutter J., Tejpar S., *Clinical biomarkers in oncology: focus on colorectal cancer.* Mol Diagn Ther, 2009. **13**(2): p. 103-14.
26. Deschoolmeester V., Baay M., Specenier P., Lardon F., Vermorken J.B., *A review of the most promising biomarkers in colorectal cancer: one step closer to targeted therapy.* Oncologist, 2010. **15**(7): p. 699-731.
27. Di Nicolantonio F., Martini M., Molinari F., Sartore-Bianchi A., Arena S., Saletti P., De Dosso S., Mazzucchelli L., Frattini M., Siena S., Bardelli A., *Wild-type BRAF is required for response to panitumumab or cetuximab in metastatic colorectal cancer.* J Clin Oncol, 2008. **26**(35): p. 5705-12.

28. Downward J., *Targeting RAS signalling pathways in cancer therapy.* Nat Rev Cancer, 2003. **3**(1): p. 11-22.
29. Dubois F., Vandermoere F., Gernez A., Murphy J., Toth R., Chen S., Geraghty K.M., Morrice N.A., MacKintosh C., *Differential 14-3-3 affinity capture reveals new downstream targets of phosphatidylinositol 3-kinase signaling.* Mol Cell Proteomics, 2009. **8**(11): p. 2487-99.
30. Dunlevy J.R., Berryhill B.L., Vergnes J.P., SundarRaj N., Hassell J.R., *Cloning, chromosomal localization, and characterization of cDNA from a novel gene, SH3BP4, expressed by human corneal fibroblasts.* Genomics, 1999. **62**(3): p. 519-24.
31. Edge S., Byrd D., Compton C., *AJCC Cancer Staging Manual (ed 7)*. 2010, New York: Springer.
32. Fearon E.R., Vogelstein B., *A genetic model for colorectal tumorigenesis.* Cell, 1990. **61**(5): p. 759-67.
33. Galimi F., Torti D., Sassi F., Isella C., Cora D., Gastaldi S., Ribero D., Muratore A., Massucco P., Siatis D., Paraluppi G., Gonella F., Maione F., Pisacane A., David E., Torchio B., Risio M., Salizzoni M., Capussotti L., Perera T., Medico E., Di Renzo M.F., Comoglio P.M., Trusolino L., Bertotti A., *Genetic and expression analysis of MET, MACC1, and HGF in metastatic colorectal cancer: response to met inhibition in patient xenografts and pathologic correlations.* Clin Cancer Res, 2011. **17**(10): p. 3146-56.
34. Gangadhar T., Schilsky R.L., *Molecular markers to individualize adjuvant therapy for colon cancer.* Nat Rev Clin Oncol, 2010. **7**(6): p. 318-25.
35. Gerlinger M., Rowan A.J., Horswell S., Larkin J., Endesfelder D., Gronroos E., Martinez P., Matthews N., Stewart A., Tarpey P., Varela I., Phillimore B., Begum S., McDonald N.Q., Butler A., Jones D., Raine K., Latimer C., Santos C.R., Nohadani M., Eklund A.C., Spencer-Dene B., Clark G., Pickering L., Stamp G., Gore M., Szallasi Z., Downward J., Futreal P.A., Swanton C., *Intratumor heterogeneity and branched evolution revealed by multiregion sequencing.* N Engl J Med, 2012. **366**(10): p. 883-92.
36. Gertler R., Rosenberg R., Schuster T., Friess H., *Defining a high-risk subgroup with colon cancer stages I and II for possible adjuvant therapy.* Eur J Cancer, 2009. **45**(17): p. 2992-9.

37. Gherardi E., Birchmeier W., Birchmeier C., Vande Woude G., *Targeting MET in cancer: rationale and progress.* Nat Rev Cancer, 2012. **12**(2): p. 89-103.
38. Gillingham A.K., Munro S., *Long coiled-coil proteins and membrane traffic.* Biochim Biophys Acta, 2003. **1641**(2-3): p. 71-85.
39. Grady W.M., *Genomic instability and colon cancer.* Cancer Metastasis Rev, 2004. **23**(1-2): p. 11-27.
40. Gray R., Barnwell J., McConkey C., Hills R.K., Williams N.S., Kerr D.J., *Adjuvant chemotherapy versus observation in patients with colorectal cancer: a randomised study.* Lancet, 2007. **370**(9604): p. 2020-9.
41. Gray R.G., Quirke P., Handley K., Lopatin M., Magill L., Baehner F.L., Beaumont C., Clark-Langone K.M., Yoshizawa C.N., Lee M., Watson D., Shak S., Kerr D.J., *Validation Study of a Quantitative Multigene Reverse Transcriptase-Polymerase Chain Reaction Assay for Assessment of Recurrence Risk in Patients With Stage II Colon Cancer.* J Clin Oncol, 2011. **29**(35): p. 4611-9.
42. Greene F.L., *Current TNM staging of colorectal cancer.* Lancet Oncol, 2007. **8**(7): p. 572-3.
43. Guastadisegni C., Colafranceschi M., Ottini L., Dogliotti E., *Microsatellite instability as a marker of prognosis and response to therapy: a meta-analysis of colorectal cancer survival data.* Eur J Cancer, 2010. **46**(15): p. 2788-98.
44. Gunderson L.L., Jessup J.M., Sargent D.J., Greene F.L., Stewart A.K., *Revised TN categorization for colon cancer based on national survival outcomes data.* J Clin Oncol, 2010. **28**(2): p. 264-71.
45. Guo A., Villen J., Kornhauser J., Lee K.A., Stokes M.P., Rikova K., Possemato A., Nardone J., Innocenti G., Wetzel R., Wang Y., MacNeill J., Mitchell J., Gygi S.P., Rush J., Polakiewicz R.D., Comb M.J., *Signaling networks assembled by oncogenic EGFR and c-Met.* Proc Natl Acad Sci U S A, 2008. **105**(2): p. 692-7.
46. Half E., Bercovich D., Rozen P., *Familial adenomatous polyposis.* Orphanet J Rare Dis, 2009. **4**: p. 22.
47. Hanahan D., Weinberg R.A., *Hallmarks of cancer: the next generation.* Cell, 2011. **144**(5): p. 646-74.
48. Harrell Jr F. *Design: Design Package. R package version 2.3-0*. , 2009 [cited 2009 January 01]; Available from: http://CRAN.R-project.org/package=Design.

49. Hinds P.W., Finlay C.A., Quartin R.S., Baker S.J., Fearon E.R., Vogelstein B., Levine A.J., *Mutant p53 DNA clones from human colon carcinomas cooperate with ras in transforming primary rat cells: a comparison of the "hot spot" mutant phenotypes.* Cell Growth Differ, 1990. **1**(12): p. 571-80.
50. Hothorn T., Zeileis A., *Generalized maximally selected statistics.* Biometrics, 2008. **64**(4): p. 1263-9.
51. Hutchins G., Southward K., Handley K., Magill L., Beaumont C., Stahlschmidt J., Richman S., Chambers P., Seymour M., Kerr D., Gray R., Quirke P., *Value of Mismatch Repair, KRAS, and BRAF Mutations in Predicting Recurrence and Benefits From Chemotherapy in Colorectal Cancer.* J Clin Oncol, 2011. **29**(10): p. 1261-70.
52. Ikenoue T., Hikiba Y., Kanai F., Tanaka Y., Imamura J., Imamura T., Ohta M., Ijichi H., Tateishi K., Kawakami T., Aragaki J., Matsumura M., Kawabe T., Omata M., *Functional analysis of mutations within the kinase activation segment of B-Raf in human colorectal tumors.* Cancer Res, 2003. **63**(23): p. 8132-7.
53. Ionov Y., Peinado M.A., Malkhosyan S., Shibata D., Perucho M., *Ubiquitous somatic mutations in simple repeated sequences reveal a new mechanism for colonic carcinogenesis.* Nature, 1993. **363**(6429): p. 558-61.
54. Janssen K.P., Alberici P., Fsihi H., Gaspar C., Breukel C., Franken P., Rosty C., Abal M., El Marjou F., Smits R., Louvard D., Fodde R., Robine S., *APC and oncogenic KRAS are synergistic in enhancing Wnt signaling in intestinal tumor formation and progression.* Gastroenterology, 2006. **131**(4): p. 1096-109.
55. Jass J.R., *Classification of colorectal cancer based on correlation of clinical, morphological and molecular features.* Histopathology, 2007. **50**(1): p. 113-30.
56. Jemal A., Bray F., Center M.M., Ferlay J., Ward E., Forman D., *Global cancer statistics.* CA Cancer J Clin, 2011. **61**(2): p. 69-90.
57. Jo W.S., Carethers J.M., *Chemotherapeutic implications in microsatellite unstable colorectal cancer.* Cancer Biomark, 2006. **2**(1-2): p. 51-60.
58. Jones S., Chen W.D., Parmigiani G., Diehl F., Beerenwinkel N., Antal T., Traulsen A., Nowak M.A., Siegel C., Velculescu V.E., Kinzler K.W., Vogelstein B., Willis J., Markowitz S.D., *Comparative lesion sequencing provides insights into tumor evolution.* Proc Natl Acad Sci U S A, 2008. **105**(11): p. 4283-8.

59. Kang G.H., *Four molecular subtypes of colorectal cancer and their precursor lesions.* Arch Pathol Lab Med, 2011. **135**(6): p. 698-703.
60. Kelley R.K., Venook A.P., *Prognostic and predictive markers in stage II colon cancer: is there a role for gene expression profiling?* Clin Colorectal Cancer, 2011. **10**(2): p. 73-80.
61. Kennedy R.D., Bylesjo M., Kerr P., Davison T., Black J.M., Kay E.W., Holt R.J., Proutski V., Ahdesmaki M., Farztdinov V., Goffard N., Hey P., McDyer F., Mulligan K., Mussen J., O'Brien E., Oliver G., Walker S.M., Mulligan J.M., Wilson C., Winter A., O'Donoghue D., Mulcahy H., O'Sullivan J., Sheahan K., Hyland J., Dhir R., Bathe O.F., Winqvist O., Manne U., Shanmugam C., Ramaswamy S., Leon E.J., Smith W.I., Jr., McDermott U., Wilson R.H., Longley D., Marshall J., Cummins R., Sargent D.J., Johnston P.G., Harkin D.P., *Development and Independent Validation of a Prognostic Assay for Stage II Colon Cancer Using Formalin-Fixed Paraffin-Embedded Tissue.* J Clin Oncol, 2011. **29**(35): p. 4620-6.
62. Kim C.A., Gingery M., Pilpa R.M., Bowie J.U., *The SAM domain of polyhomeotic forms a helical polymer.* Nat Struct Biol, 2002. **9**(6): p. 453-7.
63. Klein C.A., *The systemic progression of human cancer: a focus on the individual disseminated cancer cell--the unit of selection.* Adv Cancer Res, 2003. **89**: p. 35-67.
64. Knijn N., Mekenkamp L.J., Klomp M., Vink-Borger M.E., Tol J., Teerenstra S., Meijer J.W., Tebar M., Riemersma S., van Krieken J.H., Punt C.J., Nagtegaal I.D., *KRAS mutation analysis: a comparison between primary tumours and matched liver metastases in 305 colorectal cancer patients.* Br J Cancer, 2011. **104**(6): p. 1020-6.
65. Lang A.H., Geller-Rhomberg S., Winder T., Stark N., Gasser K., Hartmann B., Kohler B., Grizelj I., Drexel H., Muendlein A., *A common variant of the MACC1 gene is significantly associated with overall survival in colorectal cancer patients.* BMC Cancer, 2012. **12**: p. 20.
66. Leggett B., Whitehall V., *Role of the serrated pathway in colorectal cancer pathogenesis.* Gastroenterology, 2010. **138**(6): p. 2088-100.
67. Lengauer C., Kinzler K.W., Vogelstein B., *Genetic instabilities in human cancers.* Nature, 1998. **396**(6712): p. 643-9.

68. Locker G.Y., Hamilton S., Harris J., Jessup J.M., Kemeny N., Macdonald J.S., Somerfield M.R., Hayes D.F., Bast R.C., Jr., *ASCO 2006 update of recommendations for the use of tumor markers in gastrointestinal cancer.* J Clin Oncol, 2006. **24**(33): p. 5313-27.
69. Long I.S., Han K., Li M., Shirasawa S., Sasazuki T., Johnston M., Tsao M.S., *Met receptor overexpression and oncogenic Ki-ras mutation cooperate to enhance tumorigenicity of colon cancer cells in vivo.* Mol Cancer Res, 2003. **1**(5): p. 393-401.
70. Lynch H.T., de la Chapelle A., *Hereditary colorectal cancer.* N Engl J Med, 2003. **348**(10): p. 919-32.
71. Ma Y., Dai H., Kong X., Wang L., *Impact of thawing on reference gene expression stability in renal cell carcinoma samples.* Diagn Mol Pathol, 2012. **21**(3): p. 157-63.
72. Maak M., *Development and copyright of marked drawings*. 2012: Journal/Volume/Issue/Pages do not apply.
73. Mackinnon J.C., Huether P., Kalisch B.E., *Effects of nerve growth factor and nitric oxide synthase inhibitors on amyloid precursor protein mRNA levels and protein stability.* Open Biochem J, 2012. **6**: p. 31-9.
74. Markowitz S.D., Bertagnolli M.M., *Molecular origins of cancer: Molecular basis of colorectal cancer.* N Engl J Med, 2009. **361**(25): p. 2449-60.
75. Martini M., *Charakterisierung der physiologischen Funktion des neuartigen Tumorsuppressors SASH1 und seiner Rolle in der Tumorgenese*. 2011, Doctoral Thesis, Technische Universität München. Available from: http://nbn-resolving.de/urn/resolver.pl?urn:nbn:de:bvb:91-diss-20100712-982903-1-9.
76. Martini M., Gnann A., Scheikl D., Holzmann B., Janssen K.P., *The candidate tumor suppressor SASH1 interacts with the actin cytoskeleton and stimulates cell-matrix adhesion.* Int J Biochem Cell Biol, 2011. **43**(11): p. 1630-40.
77. Meyerhardt J.A., Mayer R.J., *Systemic therapy for colorectal cancer.* N Engl J Med, 2005. **352**(5): p. 476-87.
78. Migliore C., Martin V., Leoni V.P., Restivo A., Atzori L., Petrelli A., Isella C., Zorcolo L., Sarotto I., Casula G., Comoglio P.M., Columbano A., Giordano S., *MiR-1 downregulation cooperates with MACC1 in promoting MET overexpression in human colon cancer.* Clin Cancer Res, 2012. **18**(3): p. 737-47.

79. Nardon E., Glavac D., Benhattar J., Groenen P.J., Hofler G., Hofler H., Jung A., Keller G., Kirchner T., Lessi F., Ligtenberg M.J., Mazzanti C.M., Winter G., Stanta G., *A multicenter study to validate the reproducibility of MSI testing with a panel of 5 quasimonomorphic mononucleotide repeats.* Diagn Mol Pathol, 2010. **19**(4): p. 236-42.
80. NCT00651365. *A Safety and Dose-finding Study of JNJ-38877605 in Patients With Advanced or Refractory Solid Tumors*. 2012 [cited 2012 September 01]; Available from: http://clinicaltrials.gov/ct2/show/NCT00651365.
81. Nitsche U., Maak M., Künzli B., Schuster T., Friess H., Rosenberg R., *Prognostic factors and survival improvements in stage IV colorectal cancer.* Eur Surg, 2012. **44/1**: p. 47-53.
82. Nitsche U., Maak M., Schuster T., Kunzli B., Langer R., Slotta-Huspenina J., Janssen K.P., Friess H., Rosenberg R., *Prediction of prognosis is not improved by the seventh and latest edition of the TNM classification for colorectal cancer in a single-center collective.* Ann Surg, 2011. **254**(5): p. 793-800; discussion 800-1.
83. Nowaczyk M.J., Carter M.T., Xu J., Huggins M., Raca G., Das S., Martin C.L., Schwartz S., Rosenfield R., Waggoner D.J., *Paternal deletion 6q24.3: a new congenital anomaly syndrome associated with intrauterine growth failure, early developmental delay and characteristic facial appearance.* Am J Med Genet A, 2008. **146**(3): p. 354-60.
84. Obrig T.G., Culp W.J., McKeehan W.L., Hardesty B., *The mechanism by which cycloheximide and related glutarimide antibiotics inhibit peptide synthesis on reticulocyte ribosomes.* J Biol Chem, 1971. **246**(1): p. 174-81.
85. Ogino S., Nosho K., Kirkner G.J., Kawasaki T., Meyerhardt J.A., Loda M., Giovannucci E.L., Fuchs C.S., *CpG island methylator phenotype, microsatellite instability, BRAF mutation and clinical outcome in colon cancer.* Gut, 2009. **58**(1): p. 90-6.
86. Ostwald C., Linnebacher M., Weirich V., Prall F., *Chromosomally and microsatellite stable colorectal carcinomas without the CpG island methylator phenotype in a molecular classification.* Int J Oncol, 2009. **35**(2): p. 321-7.
87. Pacheco T.R., Oreskovich N., Fain P., *Genetic heterogeneity in the multiple lentigines/LEOPARD/Noonan syndromes.* Am J Med Genet A, 2004. **127A**(3): p. 324-6.

88. Pawson T., *Protein modules and signalling networks.* Nature, 1995. **373**(6515): p. 573-80.
89. Pichorner A., Sack U., Kobelt D., Kelch I., Arlt F., Smith J., Walther W., Schlag P.M., Stein U., *In vivo imaging of colorectal cancer growth and metastasis by targeting MACC1 with shRNA in xenografted mice.* Clin Exp Metastasis, 2012. **29**(6): p. 573-83.
90. Playford M.P., Bicknell D., Bodmer W.F., Macaulay V.M., *Insulin-like growth factor 1 regulates the location, stability, and transcriptional activity of beta-catenin.* Proc Natl Acad Sci U S A, 2000. **97**(22): p. 12103-8.
91. Qiu J., Huang P., Liu Q., Hong J., Li B., Lu C., Wang L., Wang J., Yuan Y., *Identification of MACC1 as a novel prognostic marker in hepatocellular carcinoma.* J Transl Med, 2011. **9**: p. 166.
92. Quirke P., Williams G.T., Ectors N., Ensari A., Piard F., Nagtegaal I., *The future of the TNM staging system in colorectal cancer: time for a debate?* Lancet Oncol, 2007. **8**(7): p. 651-7.
93. Rajagopalan H., Bardelli A., Lengauer C., Kinzler K.W., Vogelstein B., Velculescu V.E., *Tumorigenesis: RAF/RAS oncogenes and mismatch-repair status.* Nature, 2002. **418**(6901): p. 934.
94. Rimkus C., Friederichs J., Rosenberg R., Holzmann B., Siewert J.R., Janssen K.P., *Expression of the mitotic checkpoint gene MAD2L2 has prognostic significance in colon cancer.* Int J Cancer, 2007. **120**(1): p. 207-11.
95. Rimkus C., Martini M., Friederichs J., Rosenberg R., Doll D., Siewert J.R., Holzmann B., Janssen K.P., *Prognostic significance of downregulated expression of the candidate tumour suppressor gene SASH1 in colon cancer.* Br J Cancer, 2006. **95**(10): p. 1419-23.
96. Rohde F., Rimkus C., Friederichs J., Rosenberg R., Marthen C., Doll D., Holzmann B., Siewert J.R., Janssen K.P., *Expression of osteopontin, a target gene of de-regulated Wnt signaling, predicts survival in colon cancer.* Int J Cancer, 2007. **121**(8): p. 1717-23.
97. Romanus D., Weiser M.R., Skibber J.M., Ter Veer A., Niland J.C., Wilson J.L., Rajput A., Wong Y.N., Benson A.B., 3rd, Shibata S., Schrag D., *Concordance with NCCN Colorectal Cancer Guidelines and ASCO/NCCN Quality Measures: an NCCN institutional analysis.* J Natl Compr Canc Netw, 2009. **7**(8): p. 895-904.

98. Rosenberg R., Engel J., Bruns C., Heitland W., Hermes N., Jauch K.W., Kopp R., Putterich E., Ruppert R., Schuster T., Friess H., Holzel D., *The prognostic value of lymph node ratio in a population-based collective of colorectal cancer patients.* Ann Surg, 2010. **251**(6): p. 1070-8.
99. Rosenberg R., Friederichs J., Schuster T., Gertler R., Maak M., Becker K., Grebner A., Ulm K., Hofler H., Nekarda H., Siewert J.R., *Prognosis of patients with colorectal cancer is associated with lymph node ratio: a single-center analysis of 3,026 patients over a 25-year time period.* Ann Surg, 2008. **248**(6): p. 968-78.
100. Rosenberg R., Hoos A., Mueller J., Baier P., Stricker D., Werner M., Nekarda H., Siewert J.R., *Prognostic significance of cytokeratin-20 reverse transcriptase polymerase chain reaction in lymph nodes of node-negative colorectal cancer patients.* J Clin Oncol, 2002. **20**(4): p. 1049-55.
101. Rubie C., Kempf K., Hans J., Su T., Tilton B., Georg T., Brittner B., Ludwig B., Schilling M., *Housekeeping gene variability in normal and cancerous colorectal, pancreatic, esophageal, gastric and hepatic tissues.* Mol Cell Probes, 2005. **19**(2): p. 101-9.
102. Salazar R., Roepman P., Capella G., Moreno V., Simon I., Dreezen C., Lopez-Doriga A., Santos C., Marijnen C., Westerga J., Bruin S., Kerr D., Kuppen P., van de Velde C., Morreau H., Van Velthuysen L., Glas A.M., Van't Veer L.J., Tollenaar R., *Gene expression signature to improve prognosis prediction of stage II and III colorectal cancer.* J Clin Oncol, 2010. **29**(1): p. 17-24.
103. Salazar R., Roepman P., Capella G., Moreno V., Simon I., Dreezen C., Lopez-Doriga A., Santos C., Marijnen C., Westerga J., Bruin S., Kerr D., Kuppen P., van de Velde C., Morreau H., Van Velthuysen L., Glas A.M., Van't Veer L.J., Tollenaar R., *Gene expression signature to improve prognosis prediction of stage II and III colorectal cancer.* J Clin Oncol, 2011. **29**(1): p. 17-24.
104. Saville D.J., *Multiple Comparison Procedures - the Practical Solution.* American Statistician, 1990. **44**(2): p. 174-180.
105. Schmid F., Burock S., Klockmeier K., Schlag P.M., Stein U., *SNPs in the coding region of the metastasis-inducing gene MACC1 and clinical outcome in colorectal cancer.* Mol Cancer, 2012. **11**(1): p. 49.
106. Schmiegel W., Reinacher-Schick A., Arnold D., Graeven U., Heinemann V., Porschen R., Riemann J., Rodel C., Sauer R., Wieser M., Schmitt W., Schmoll

H.J., Seufferlein T., Kopp I., Pox C., *[Update S3-guideline "colorectal cancer" 2008].* Z Gastroenterol, 2008. **46**(8): p. 799-840.

107. Schoenberg D.R., Maquat L.E., *Regulation of cytoplasmic mRNA decay.* Nat Rev Genet, 2012. **13**(4): p. 246-59.
108. Segditsas S., Tomlinson I., *Colorectal cancer and genetic alterations in the Wnt pathway.* Oncogene, 2006. **25**(57): p. 7531-7.
109. Seth R., Crook S., Ibrahem S., Fadhil W., Jackson D., Ilyas M., *Concomitant mutations and splice variants in KRAS and BRAF demonstrate complex perturbation of the Ras/Raf signalling pathway in advanced colorectal cancer.* Gut, 2009. **58**(9): p. 1234-41.
110. Shibayama M., Maak M., Nitsche U., Gotoh K., Rosenberg R., Janssen K., *Prediction of Metastasis and Recurrence in Colorectal Cancer Based on Gene Expression Analysis: Ready for the Clinic?* Cancers, 2011(3): p. 2858-2869.
111. Shimokawa H., Uramoto H., Onitsuka T., Chundong G., Hanagiri T., Oyama T., Yasumoto K., *Overexpression of MACC1 mRNA in lung adenocarcinoma is associated with postoperative recurrence.* J Thorac Cardiovasc Surg, 2011. **141**(4): p. 895-8.
112. Shirahata A., Shinmura K., Kitamura Y., Sakuraba K., Yokomizo K., Goto T., Mizukami H., Saito M., Ishibashi K., Kigawa G., Nemoto H., Hibi K., *MACC1 as a marker for advanced colorectal carcinoma.* Anticancer Res, 2010. **30**(7): p. 2689-92.
113. Sobin L.H., Gospodarowicz M.K., Wittekind C., *TNM classification of Malignant Tumours, 7th Edition*. 2009, West Sussex: John Wiley & Sons.
114. Stein U., Arlt F., Smith J., Sack U., Herrmann P., Walther W., Lemm M., Fichtner I., Shoemaker R.H., Schlag P.M., *Intervening in beta-catenin signaling by sulindac inhibits S100A4-dependent colon cancer metastasis.* Neoplasia, 2011. **13**(2): p. 131-44.
115. Stein U., Dahlmann M., Walther W., *MACC1 - more than metastasis? Facts and predictions about a novel gene.* J Mol Med (Berl), 2010. **88**(1): p. 11-8.
116. Stein U., Smith J., Walther W., Arlt F., *MACC1 controls Met: what a difference an Sp1 site makes.* Cell Cycle, 2009. **8**(15): p. 2467-9.
117. Stein U., Walther W., Arlt F., Schwabe H., Smith J., Fichtner I., Birchmeier W., Schlag P.M., *MACC1, a newly identified key regulator of HGF-MET signaling, predicts colon cancer metastasis.* Nat Med, 2009. **15**(1): p. 59-67.

118. Stella M.C., Comoglio P.M., *HGF: a multifunctional growth factor controlling cell scattering.* Int J Biochem Cell Biol, 1999. **31**(12): p. 1357-62.
119. Stites E.C., Trampont P.C., Ma Z., Ravichandran K.S., *Network analysis of oncogenic Ras activation in cancer.* Science, 2007. **318**(5849): p. 463-7.
120. Tejpar S., Bertagnolli M., Bosman F., Lenz H.J., Garraway L., Waldman F., Warren R., Bild A., Collins-Brennan D., Hahn H., Harkin D.P., Kennedy R., Ilyas M., Morreau H., Proutski V., Swanton C., Tomlinson I., Delorenzi M., Fiocca R., Van Cutsem E., Roth A., *Prognostic and predictive biomarkers in resected colon cancer: current status and future perspectives for integrating genomics into biomarker discovery.* Oncologist, 2010. **15**(4): p. 390-404.
121. Tessema M., Willink R., Do K., Yu Y.Y., Yu W., Machida E.O., Brock M., Van Neste L., Stidley C.A., Baylin S.B., Belinsky S.A., *Promoter methylation of genes in and around the candidate lung cancer susceptibility locus 6q23-25.* Cancer Res, 2008. **68**(6): p. 1707-14.
122. Toyota M., Ahuja N., Ohe-Toyota M., Herman J.G., Baylin S.B., Issa J.P., *CpG island methylator phenotype in colorectal cancer.* Proc Natl Acad Sci U S A, 1999. **96**(15): p. 8681-6.
123. Umar A., Boland C.R., Terdiman J.P., Syngal S., de la Chapelle A., Ruschoff J., Fishel R., Lindor N.M., Burgart L.J., Hamelin R., Hamilton S.R., Hiatt R.A., Jass J., Lindblom A., Lynch H.T., Peltomaki P., Ramsey S.D., Rodriguez-Bigas M.A., Vasen H.F., Hawk E.T., Barrett J.C., Freedman A.N., Srivastava S., *Revised Bethesda Guidelines for hereditary nonpolyposis colorectal cancer (Lynch syndrome) and microsatellite instability.* J Natl Cancer Inst, 2004. **96**(4): p. 261-8.
124. Umar A., Risinger J.I., Hawk E.T., Barrett J.C., *Testing guidelines for hereditary non-polyposis colorectal cancer.* Nat Rev Cancer, 2004. **4**(2): p. 153-8.
125. Vakiani E., Janakiraman M., Shen R., Sinha R., Zeng Z., Shia J., Cercek A., Kemeny N., D'Angelica M., Viale A., Heguy A., Paty P., Chan T.A., Saltz L.B., Weiser M., Solit D.B., *Comparative Genomic Analysis of Primary Versus Metastatic Colorectal Carcinomas.* J Clin Oncol, 2012. **30**(24): p. 2956-62.
126. Vasen H.F., Watson P., Mecklin J.P., Lynch H.T., *New clinical criteria for hereditary nonpolyposis colorectal cancer (HNPCC, Lynch syndrome) proposed by the International Collaborative group on HNPCC.* Gastroenterology, 1999. **116**(6): p. 1453-6.

127. Vossen R.H., Aten E., Roos A., den Dunnen J.T., *High-resolution melting analysis (HRMA): more than just sequence variant screening.* Hum Mutat, 2009. **30**(6): p. 860-6.
128. Walther A., Johnstone E., Swanton C., Midgley R., Tomlinson I., Kerr D., *Genetic prognostic and predictive markers in colorectal cancer.* Nat Rev Cancer, 2009. **9**(7): p. 489-99.
129. Washington M.K., *Colorectal carcinoma: selected issues in pathologic examination and staging and determination of prognostic factors.* Arch Pathol Lab Med, 2008. **132**(10): p. 1600-7.
130. Weitz J., Koch M., Debus J., Hohler T., Galle P.R., Buchler M.W., *Colorectal cancer.* Lancet, 2005. **365**(9454): p. 153-65.
131. WHO. *World Health Organisation [WHO web site]*. 2012 [cited 2012 September 01]; Available from: http://www.who.int.
132. Worthley D.L., Whitehall V.L., Spring K.J., Leggett B.A., *Colorectal carcinogenesis: road maps to cancer.* World J Gastroenterol, 2007. **13**(28): p. 3784-91.
133. Wu X., Brewer G., *The regulation of mRNA stability in mammalian cells: 2.0.* Gene, 2012. **500**(1): p. 10-21.
134. Zeestraten E.C., Maak M., Shibayama M., Schuster T., Nitsche U., Matsushima T., Nakayama S., Gohda K., Friess H., van de Velde C.J., Ishihara H., Rosenberg R., Kuppen P.J., Janssen K.P., *Specific activity of cyclin-dependent kinase I is a new potential predictor of tumour recurrence in stage II colon cancer.* Br J Cancer, 2012. **106**(1): p. 133-40.
135. Zeller C., Hinzmann B., Seitz S., Prokoph H., Burkhard-Goettges E., Fischer J., Jandrig B., Schwarz L.E., Rosenthal A., Scherneck S., *SASH1: a candidate tumor suppressor gene on chromosome 6q24.3 is downregulated in breast cancer.* Oncogene, 2003. **22**(19): p. 2972-83.
136. Zeng Z., Weiser M.R., D'Alessio M., Grace A., Shia J., Paty P.B., *Immunoblot analysis of c-Met expression in human colorectal cancer: overexpression is associated with advanced stage cancer.* Clin Exp Metastasis, 2004. **21**(5): p. 409-17.
137. Zhang R.T., Shi H.R., Huang H.L., Chen Z.M., Liu H.N., Yuan Z.F., *[Expressions of MACC1, HGF, and C-met protein in epithelial ovarian cancer*

and their significance]. Nan Fang Yi Ke Da Xue Xue Bao, 2011. **31**(9): p. 1551-5.

138. Zhang Y., Wang Z., Chen M., Peng L., Wang X., Ma Q., Ma F., Jiang B., *MicroRNA-143 Targets MACC1 to Inhibit Cell Invasion and Migration in Colorectal cancer.* Mol Cancer, 2012. **11**: p. 23.

9 List of Tables and Figures

9.1 Tables

9.2 Figures

10 Publications

Integrative marker analysis allows risk assessment for metastasis in stage II colon cancer

Nitsche U, Rosenberg R, Balmert A, Schuster T, Slotta-Huspenina J, Herrmann P, Bader FG, Friess H, Schlag PM, Stein U, Janssen KP

Accepted for publication in the Annals of Surgery (November Issue 2012), subsequent to presentation at the 19th Annual Meeting of the European Surgical Association (ESA) on May 5th 2012 in Hamburg.

Acknowledgements

The greatest compliment without any doubt belongs to Priv.-Doz. Dr. rer. nat. Klaus-Peter Janßen. His widespread knowledge, availability for any questions, together with incomparable kindness and de-escalation skills made this work finally possible. Exceptionally to mention are his dedicated engagement and mentoring during the whole last three years.

I like to thank my further Ph.D. mentors, Univ.-Prof. Dr. med. Bernhard Holzmann and apl. Prof. Dr. med. Robert Rosenberg. Robert's thoroughly support reached far beyond my employment, including free food and beverages in many cases. Bernhard's broad view of matter and ideas led to repeated beneficial changes in the concept of this thesis. Priv.-Doz. Dr. med. Franz G. Bader deserves many thanks for his brilliant clinical support. Universitätsprofessor Dr. med. Helmut Friess has to be acknowledged for making it possible for me to conduct this work at his clinic. He arranged an excellent environment, allowing basic research together with clinical training, and provides great support for my scientific, surgical and occupational career.

I have to thank Prof. Dr. rer. nat. Ulrike Stein and Pia Herrmann for performing the MACC1 rtPCR on the stage II patient cohort. Prof. Dr. med. Andreas Jung deserves many thanks for the possibility of performing the pyrosequencing analysis in his laboratory and for his consulting, Prof. Dr. rer. nat. Gisela Keller for the microsatellite analysis, Lynette Henkel from the Schiemann laboratory for the FACS analysis, and Dr. rer. nat. Tibor Schuster for the outlandish statistical support.

Further appreciation goes to all not yet mentioned colleagues and friends in the laboratory, including the Holzmanns and Laschingers and (nearly all) transient members. Every single person contributed to an environment of pleasure, which I am very proud to have been received and integrated in. You all gave me a delightful

place which I unfortunately was not always able to experience as much as I would have been supposed to during my past three years. Special appreciations go to Widya, Alex G., Larissa, Tanja, Matze, Christoph, and Alex B.! And now the time has come! Sabine and Anne, who kindly share everything including me: You are the best, and even better, there are two of you! We are like that, like that! Doubtless, without Bibi's excellent and continuous commitment, this work would have never been possible.

And, finally, I would like to thank you, valued reader, for keenly working through this whole thesis and not only reading the acknowledgements.